ERROR SOURCES AND ERROR CORRECTION FOR FLOW MEASUREMENT IN OPEN CHANNEL BY ULTRASONIC TRANSIT TIME FLOW METER AND PROPELLER CURRENT METERS

A DISSERTATION

Submitted in partial fulfillment of the
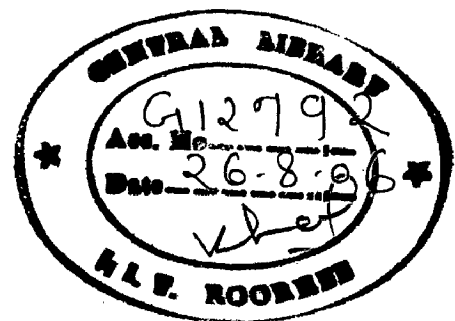*requirements for the award of the degree*
of

MASTER OF TECHNOLOGY

in

ELECTRICAL ENGINEERING

(With Specialization in Measurement and Instrumentation)

By

BOBY ABRAHAM Y

DEPARTMENT OF ELECTRICAL ENGINEERING
INDIAN INSTITUTE OF TECHNOLOGY ROORKEE
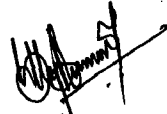## ROORKEE -247 667 (INDIA)
JUNE, 2006

CANDIDATE'S DECLARATION

I hereby declare that the work that is being presented in this dissertation report entitled "ERROR SOURCES AND ERROR CORRECTION FOR FLOW MEASUREMENT IN OPEN CHANNEL BY ULTRASONIC TRANSIT TIME FLOW METER AND PROPELLER CURRENT METERS" submitted in partial fulfillment of the requirements for the award of the degree of **Master of Technology** in **Electrical Engineering** with specialization in MEASUREMENT AND INSTRUMENTATION, to the **Department of Electrical Engineering, Indian Institute of Technology, Roorkee,** is an authentic record of my own work carried out, under the guidance of **Dr. H. K. VERMA**, Professor, Department of Electrical Engineering and **Dr. B. K. GANDHI**, Assoc. Professor, Department of Mechanical and Industrial Engineering.

The matter embodied in this dissertation report has not been submitted by me for the award of any other degree or diploma.

Date: 27-06-'06
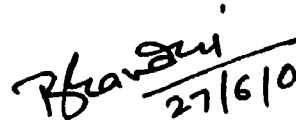
Place: Roorkee

(BOBY ABRAHAM .Y)

This is to certify that the above statement made by the candidate is correct to the best of my knowledge.

Dr. H. K. VERMA

Professor,

Department of Electrical Engineering,

Indian Institute of Technology Roorkee,

Uttaranchal - 247 667, INDIA.

DR. B. K. GANDHI

Assoc. Professor,

Mechanical and Industrial Engg. Dept.

Indian Institute of Technology Roorkee

Uttaranchal - 247 667, INDIA.

i

ACKNOWLEDGEMENT

I am very indebted to my institution, **Indian Institute of Technology, Roorkee** for providing me opportunity to pursue my Masters. The lessons that this campus has taught are of immense value to me and I hope to cherish over the memories of this stay in the years to come.

Thanks to Head, Department of Electrical Engineering, Group leader and the team of **MEASUREMENT AND INSTRUMENTATION** for extending their co-operation in the academic proceedings.

Dr. H. K. VERMA, Professor, Department of Electrical Engineering, IIT Roorkee, my guide is the first person behind the success of this dissertation. *"Great men are as gentle as flowers and as strong as trees"*, that is my guide. I frankly admit that this work evolved through substantial discussions with him. He was my motivation all through the work and had been a great encouragement at times when I stuck up. Man of his own kind, I salute to his perfection. For sure, learning under him is a unique experience.

I should be grateful to **Dr. B. K. GANDHI**, Assoc. Professor, Dept. of Mechanical and Industrial Engg., IIT Roorkee, my co-guide, for his timely advices and support he has given to me through out the work. I am very much an admirer of his enthusiasm and mingling nature. He has been a knowledge resource to me through out the work.

I thank **SASANK, RESEARCH SCHOLAR, AHEC** for his valuable support and help he has given to me.

I am left indebted to all my friends, for letting their lives run beside mine for a while. They had always been a cheerful company to me. My gratitude to them cannot be expressed in words, i thank all my friends for rendering a ready help whenever I needed.

In the first place, I thank my God and my family, Papa, mummy and my sister for all that they are to me.

Dedicated

to

My Parents

ABSTRACT

Discharge (flow rate) measurement in hydro-power stations is quite complex and demands very accurate methods. For years together the accuracy of flow measurement remained unsatisfying, until the high speed digital age took over the analog methods. The complexity of fluid dynamics with respect to open channel flow influences the measurement of discharge in such channels. The velocity profiles developed in various geometries of open channel are found to be very complex, such that the accurate measurement of these profiles is a tedious and challenging job. Though various correction methods have been tried over the past 20 years, yet the accuracy demands have not been met.

The focus of this dissertation work is to investigate the velocity profiles in open channels of various geometries and to develop a mathematical model for these profiles. Flow for various geometries have been modeled and simulated by Computational Fluid Dynamics (CFD) analysis. The flow thus developed is being mimicked by using mathematical expressions (two major expressions- one for horizontal and other for vertical) with 10 control parameters. These parameters accounts for various factors in real situations such as side wall, bed friction, air friction and the geometry of the channel. Prior to the modeling, validation of CFD has been done by comparing the modeling results with site data (measurement done by Acoustic Doppler Current Profiler). Thus in this work an effort has been made to reveal the complex profiles of open channel flow for various conditions, the complexity of which is a major source of error for discharge measurement. An attempt has also been made to generalize these profiles using mathematical models.

Subsequently, various error sources involved in the discharge measurement using propeller current meters and Ultrasonic Transit Time Flow meters (UTTF) have been identified. Later part of the work is dedicated to uncertainty analysis. The numerical integration error, which is a major source of error in discharge calculation, is analytically investigated for the simulated profiles, for both propeller current meters and UTTF.

LIST OF FIGURES

LIST OF TABLES

ABBREVATIONS AND ACRONYMS

UTTF	Ultrasonic Transit Time Flow meters
CM	Current meters
CFD	Computational Fluid Dynamics
VOF	Volume Of Fluid Model
ISO	International Standards Organization
IEC	International Electrotechnical Commission
ADCP	Acoustic Doppler Current Profiler
PC	Personal Computer
CSI	Cubic Spline Interpolation
MATLAB	Matrix Laboratory
GJ	Gauss – Jacobi Numerical Integration
GL	Gauss- Legendre Numerical Integration
OWICS	Optimal Weighted Integration for Circular Section

CONTENTS

CHAPTER 1

INTRODUCTION

The flow measurement in open channels is a complex phenomenon. The complexity of fluid dynamics with respect to open channel influences the measurement of flow rate. A detailed analysis of the flow profiles in various open channel conditions and the uncertainties involved in measurement of these profiles has been the subject of this study.

1.1 FLOW MEASUREMENT IN HYDRO POWER STATIONS

Measuring flow rate (discharge rate) is one of the vital parameters in determining efficiency of hydroelectric turbines. The other parameters appearing in the efficiency measurement are the water head and the electric output of the hydroelectric generating unit, both of which can be determined with good accuracy without much difficulty. Therefore the accuracy of efficiency measurement is largely decided by the accuracy of flow measurement.

There are several methods being employed for measuring the discharge in open channels like current meter, electromagnetic, ultrasonic transit time, tracer methods and thermodynamic. Due to higher accuracy and versatility for discharge measurement, UTTF and Propeller current meter has been extensively used in the field .

The main issue that needs attention when Current meters or UTTF is employed for discharge measurement in hydro-power stations is the solution of 'measurement section'. Not all hydro-power stations have measurement section as specified by IEC 60041, which in turn suggests us that the accuracy is affected by deviations from the requirements specified in IEC 60041 [1]. Effect of such deviations of measurement section in the velocity profile is also addressed in the dissertation work through CFD analysis.

1

1.2   INTRODUCTION TO CFD

Computational Fluid Dynamics (CFD) analysis can be used to model the channel and simulate the flow in it [2]. In Computational Fluid Dynamics (CFD), general equations of fluid flow are used to model the physical world. In doing so, a number of assumptions are made to simplify the problem. This allows a wide range of complex problems to be simulated on a computer. However, it is important to realise that CFD results can be subject to errors. In addition, there are situations in which a CFD analysis will fail to produce results. With such cases, negative fluid densities may be encountered [impossible!]. So prior to CFD analysis validation of the software for the particular problem is an inevitable part to confirm the reliability of the software.

The main feature of CFD is discretisation. This means that the volume being analysed is sub-divided into numerous smaller parts. These parts are known as *cells* and they join together to form a *mesh*. When CFD was first developed, these cells were usually had the shape of a rectangular block. However, modern CFD techniques allow cells of different shapes to be mixed and used. Even rhombic or tetrahedral shaped cells are possible.

Broadly, the strategy of CFD is to replace the continuous problem domain with a discrete domain using a grid. In the continuous domain, each flow variable is defined at every point in the domain. For instance, the pressure p in the continuous 1D domain shown in the figure below would be given as

$$p = p(x), \ 0 < x < 1$$

In the discrete domain, each flow variable is defined only at the grid points. So, in the discrete domain shown below, the pressure would be defined only at the N grid points.

$$p_i = p(x_i), \ i = 1, 2, \ldots, N$$

Continuous Domain
$0 \leq x \leq 1$

Discrete Domain
$x = x_1, x_2, \ldots, x_N$
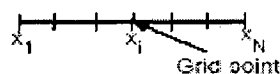
Grid point

Coupled PDEs + boundary
conditions in continuous
variables

Coupled algebraic eqs. in
discrete variables

2

In a CFD solution, one would directly solve for the relevant flow variables only at the grid points. The values at other locations are determined by interpolating the values at the grid points. The governing partial differential equations and boundary conditions are defined in terms of the continuous variables p, $\vec{V}$ etc. One can approximate these in the discrete domain in terms of the discrete variables p_i, $\vec{V_i}$ etc. The discrete system is a large set of coupled, algebraic equations in the discrete variables. Setting up the discrete system and solving it (which is a matrix inversion problem) involves a very large number of repetitive calculations and is done by the digital computer. This idea can be extended to any general problem domain.

1.3   OBJECTIVES OF DISSERTATION

Briefly stated, following are the objectives of dissertation work:
- Modeling and simulation of velocity profiles for various open channel geometries by CFD analysis.
- Development of mathematical model for above created profiles and correlation of equation parameters with field conditions
- Identification of error sources in UTTF and Current meter measurements and experimental verification of measurement errors by comparison with generated profiles.
- Suggesting methods of correcting the results of flow measurements made with current meters/ UTTF

1.4   ORGANIZATION OF DISSERTATION REPORT

The dissertation report is organized as follows:
Chapters 1 and 2 introduce the dissertation work and open channel discharge measurement with UTTF and Current meters respectively.
Chapter 3 is introduces the basic steps involved in CFD analysis for Open channel modeling .

Chapter 4 is devoted to real time time data acquisition by the profiler (ADCP) and for the discussion of validation procedure.

Chapter 5 discusses the development of mathematical model and the physical significances of the parameters involved in the horizontal and vertical profile.

Chapter 6 presents the results of CFD simulations for various open channel geometries and the development of an equivalent mathematical model for all the simulated profiles..

Chapter 7 describes various error sources in measurement using propeller current meters and suggests methods for the accuracy improvement. Second half of the chapter is dedicated to experimental verification of measurement errors and uncertainty analysis.

Chapter 8 introduces the various sources of error in flow measurement using UTTF, with a perspective toward the correction of the errors. Second half of the chapter describes two numerical integration methods namely Gauss-Jacobi and Gauss-Legendre for open channels, and presents the results of the integration error for each of the simulated profiles.

Finally, *chapter 9* concludes the report and puts forth the scope of further work that can be done as an extension of this dissertation work.

FLOW-VELOCITY MEASUREMENT IN OPEN CHANNELS

2.1 BASIC CONCEPT OF OPEN-CHANNEL FLOW

Flow can be classified into open channel flow and closed conduit flow. Open channel flow conditions occurs whenever the flowing stream has a free or an unconstrained surface that is open to the atmosphere. The presence of the free water surface prevents transmission of pressure from one end of the conveyance channel to another as in fully flowing pipelines. Thus, in open channels, the only force that can cause flow is the force of gravity on the fluid. As a result, with steady uniform flow under free discharge conditions, a progressive fall or decrease in the water surface elevation always occurs as the flow moves downstream.

The actual distribution of flow velocity is generally quite complex. Open channel flow is often laminar or near-laminar, with the different layers moving at different velocities. Flow velocity at the contact point with the channel boundary is low. Typically, the highest velocity flow is located in the center of the flow channel and slightly below the water surface. Fig. 2.1 shows typical velocity profile or vertical velocity distribution under open channel flow conditions.
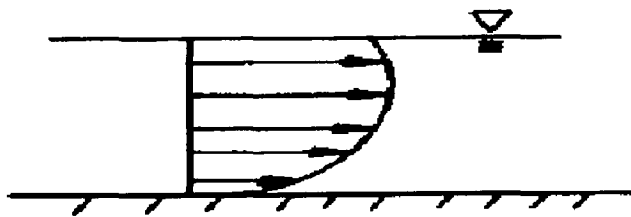
Fig.2.1 Typical Velocity Profile in Open Channel, (Source: www.usgs.com, [25])

A general knowledge of velocity distributions is extremely important in evaluating and selecting a method of flow measurement. Sites with irregular or complicated channel geometries, such as meanders or riffle areas, can cause a decrease in measurement accuracy when using methods that rely on velocity measurements to calculate discharge.

5

2.2 APPLICATION OF CURRENT METERS TO OPEN CHANNEL FLOW

2.2.1 PRINCIPLE OF OPERATION

A current meter consists of a rotor or propeller mounted on a bearing and shaft. The fluid to be measured in passed through the housing, causing the propeller to spin with the rotational speed proportional to the velocity of the flowing fluid within the meter. A device to measure the speed of the rotor is employed to make the actual flow measurement. The sensor is generally an electronic type sensor that detects the passage of each rotor blade generating a pulse. The principle of the operation is based on the proportionality between the velocity of the water and the resulting angular velocity of the meter rotor.

By placing a current meter at a point in a stream and counting the number of revolutions of the rotor during the measured interval of time, the velocity of water at that point is determined. The number of revolutions of the rotor is obtained by an electrical circuit through the contact chamber. The current meter is put in the flow with the propeller axis parallel to the flow direction and the propeller peak against the flow. The rotational speed N, (Hz) of the propeller is a linear function of the flow velocity V, m/s in the measuring point;

$$V = (K) * N + B; \qquad (2.1)$$

Where;

N: It is the number of pulses counted for a given preset time, Hz

K: Hydraulic Pitch of Propeller, m

B: Characteristics of Current Meter, m/s

The K and B are constants of the current meter and have to be determined by calibration.

2.2.2 METHODS OF DETERMINATION OF CHANNEL MEAN VELOCITIES

The mean velocity of the water in each vertical can be determined by any of the following methods, depending on the time available and having regard to the width and depth of the water, to the bed conditions. The following methods are used to determine mean velocities in a vertical section from the current meters:

➤ Two-Point Method

Velocity observations shall be made at each vertical by exposing the current-meter at 0.2 and 0.8 of the depth below the surface. The average of the two values shall be taken as the mean velocity in the vertical.

➤ Vertical Velocity-Curve Method

The measurement of velocity by this method shall consist of velocity observations made at a number of points along the vertical between the surface and the bed of the channel. The spacing of the measuring points shall be so chosen that the difference of velocities between two adjacent points shall be not more than 20 percent w. r. t higher value of the two. The mean velocity of that vertical and its position shall then be determined from the graph. The method is very accurate, depending upon the number of data points measured for profile, but is time consuming and costly. When the turbulent flow condition exists, the velocity curve can be extrapolated from the last measuring point to the bed or wall by calculating v_x from the equation;(m varies from 2 to 10)

$$v_x = v_a \left(\frac{x}{a} \right)^{\frac{1}{m}}$$ (2.2)

where;

v_x is the open point velocity in the extrapolated zone at a distance x from the bed or wall.

v_a is the velocity at the last measuring point at a distance a, from the bed or wall.

➤ Subsurface Method

The subsurface method involves measuring the velocity near the water surface and then multiplying it by a coefficient ranging from 0.85 to 0.95, depending on the depth of water, the velocity, and the nature of the stream or canal bed. The difficulty of determining the exact coefficient limits the usefulness and accuracy of this method.

➤ Six-Tenths Depth Method

Mean velocity is measured at each vertical by exposing the current meter at 0.6 of the depth below the surface. The value observed should be taken as the mean velocity in the vertical.

7

> **Three-Point Method, Five-Point method, etc.**

In this methods velocities are measured on each vertical at various depth below the surface and as near as possible to the surface and the bottom. The mean velocity may be determined from the below eq;

Three-point method - $V_{(mean)} = 0.25 * (V_{0.2} + 2 * V_{0.6} + V_{0.8})$

Five-point method - $V_{(mean)} = 0.1 * (V_{sur} + 3 * V_{0.2} + 3 * V_{0.6} + 2 * V_{0.8} + V_{bed})$

> **Integration Method**

In this method, the current-meter is lowered and raised through the entire depth on each vertical at a uniform rate. The speed at which the meter is lowered or raised should not be more than 5 % of the mean water velocity and should not in any event exceed 0.04 m/s. Two complete cycles should be made on each vertical and if the results differ by more than 10 %, the operation (two complete cycles) should be repeated until results within this limit are obtained. This method is suitable for propeller-type current-meters and cup-type current meters and for electromagnetic current-meters, provided the vertical movement is less than 5 % of the mean velocity. The integration method gives good results if the time of measurement allowed is sufficiently long (60 s to 100 s) [1].

2.2.3 AREA-VELOCITY INTEGRATION

The velocity-area principle is used to compute discharge/flow-rate from current-meter data. In this method, the channel is divided into finite number of sub-sections [3]. The partial discharge in each sub-section is computed by multiplication of mean velocity of flow to the area of cross-section. A partial discharge is the product of an average point or vertical line velocity and its meaningfully associated partial area, expressed as:

$$q_n = \overline{V}_n a_n \tag{2.3}$$

Total discharge is determined by summation of partial discharges in the cross-sections and is described as:

$$Q = \sum_1^n (\overline{V}_n a_n) \tag{2.4}$$

8

Represents the computation, where Q is the total discharge, a_n is the individual subsection area, and the V_n is the corresponding mean velocity of the flow normal to the subsection. The cross-sections are defined by depths at verticals 1, 2..., n, where n is the number of verticals in the channel. At each vertical the velocities are sampled by current meter to obtain the mean velocity for each sub-section. The velocity readings recorded for each vertical are plotted against depth as shown in Fig. 2.2. The area contained by the velocity curve produced for each vertical gives the discharge for unit width or known as *unit-width discharge* of the corresponding section.
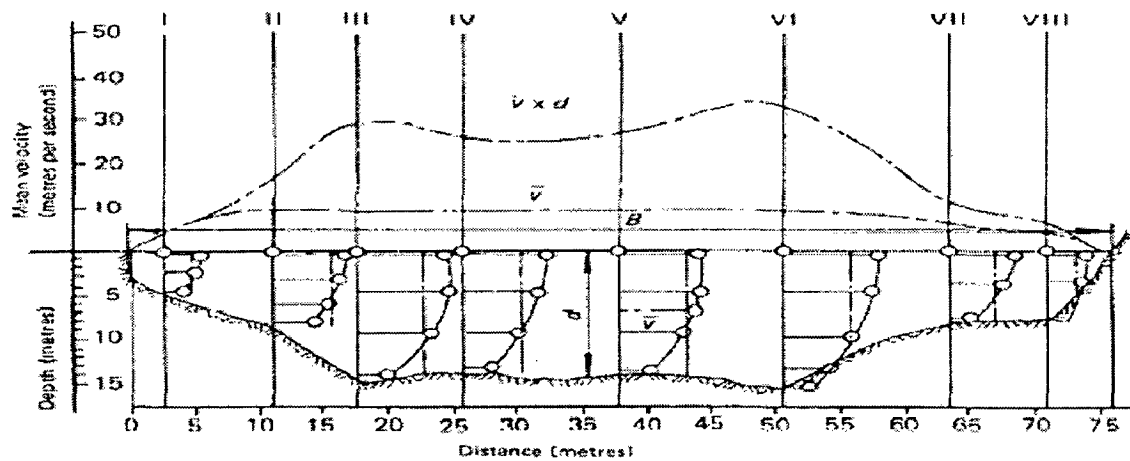
Fig. 2.2: Computation of Discharge from Current-Meter Measurements (Area-Velocity Integration method), [Source: ISO: 748]

The values of unit-width discharges (v. d) are then plotted for each vertical cross-section and joined to form a continuous curve. The area enclosed between this curve and the line representing the water surface gives the total discharge through the section.

2.3 APPLICATION OF UTTF TO OPEN CHANNEL FLOW

2.3.1 THEORY AND BACKGROUND

Primitive single path UTTF consists of two transceivers, which are mounted on either side of the flow conduit, and at an angle to the flow direction. An ultrasonic wave is exchanged between the two transducers. The time difference between the upstream time and downstream time is called the transit time. Transit time is directly proportional to the flow rate in the conduit [4]. The circuit on which the UTTF works is illustrated in Fig.2.3

9
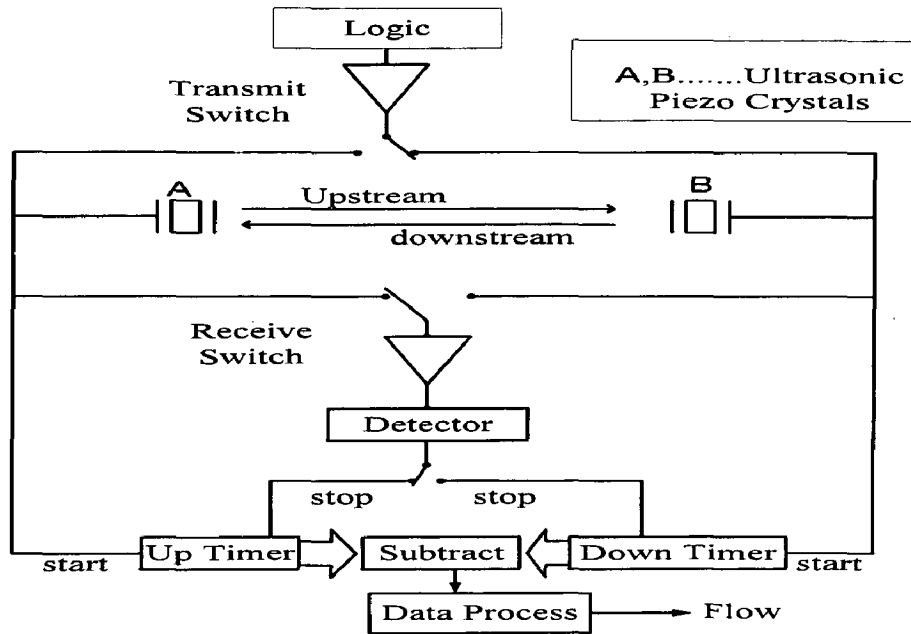
Fig.2.3 Basic circuit of single path UTTF.

The governing equation for mean flow calculation using single path UTTF is as follows:

$$\overline{V}_{ax} = K \frac{L}{2.\cos\alpha} \left(\frac{1}{t_d} - \frac{1}{t_u} \right)$$ (2.5)

where

t_u is the upstream time,

t_u is the downstream time,

L is the length of the ultrasonic path,

α is the angle made by the ultrasonic path with the flow direction,

$\overline{V}_{ax}$ is the average flow velocity measured along the ultrasonic path and

K is the shape factor.

Flow rate in the conduit is not uniform but is subject to the shape of the conduit, Reynolds number, conduit roughness and transducer protrusion etc. The mean flow rate of flow conduit is the average value of the flow velocity sampled over the cross section of the flow conduit. The accuracy of flow rate calculation is proportional to the area of interrogation of the flow conduit. Reynolds number for the flow in hydro-power stations is a high (typically 4×10^5 to 3×10^6), which implies that it is a turbulent flow. Thus the flow distribution is not only non-uniform but also contains the transverse component in it.

10

A single path UTTF measures average flow velocity along the ultrasonic path. With the intension of making a better interrogation of the flow conduit, the number of ultrasonic paths was increased to two. Individual path velocities are integrated by numerical integration techniques. A four path UTTF was observed to perform better than the two path flowmeter. Fig. 2.5 illustrates the four-path UTTF. The mounting angle varies from 45° to 65°.
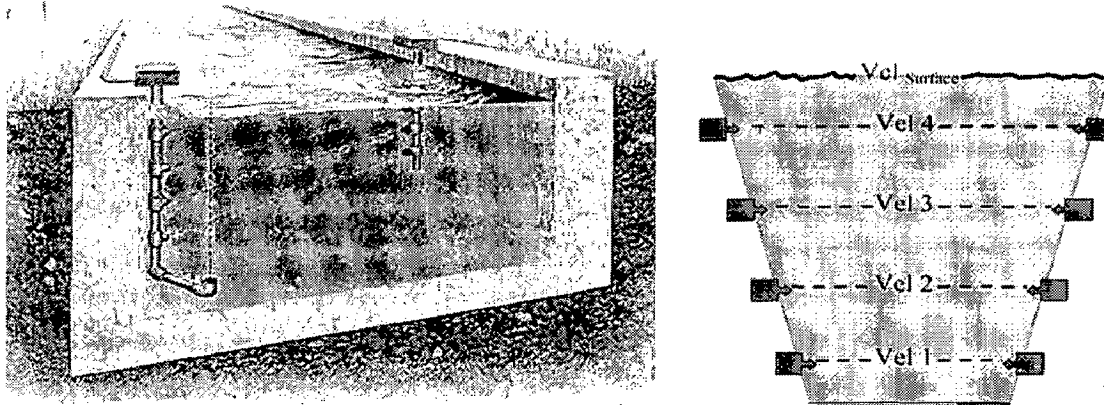
Fig. 2.4   4-Path UTTF arrangement for Open-Channel

The accuracy of flow rate measurement increases with the increase in the number of paths. But on adding an ultrasonic path, the cost of the transducers and the installation cost are to be added. IEC 60041 proposes an eight path UTTF for discharge measurement as a tradeoff between accuracy and cost. IEC 60041 promises accuracy of 2 % in discharge measurement but only under certain conditions that must be satisfied by the field situation. The eight path ultrasonic flowmeter cancels out the transverse component in the flow, but accounts least for asymmetric nature of flow distribution [19].

2.3.2 EIGHT PATH UTTF: A CRITICAL EXAMINATION

The eight path UTTF suggested by IEC 60041 is such an application for flow measurement, which involves many instructions that has to be strictly followed. The section where the ultrasonic transducers are installed is called the measurement section. One important rule is that the 'measuring section' should have a straight conduit of 10 times the width upstream and 3 times the width downstream. It is difficult to fulfill this condition due to topology of the hydro-power station, and especially in small hydro-power stations.

11

An eight-path UTTF has two ultrasonic paths in a plane and four such planes distributed over the whole cross section of the conduit. The transverse component of the flow is compensated by the axis-symmetric path in a plane. But still the measurement can be made by the four horizontal paths installed in vertical pane, provided that the flow is free from transverse components. The discharge measurements made this way are found to be satisfactory in many instances. So not necessarily eight-path UTTF be used to make the discharge measurement if the knowledge of how intense is the influence of the transverse component is available. Transverse flow component is influenced by the disturbances such as valves and obstacles in the upstream conduit in the proximity of measuring section.

The Gaussian numerical integration methods are suggested for the eight-path UTTF. But both of the Gaussian quadrature techniques namely, Gauss-Lacobi and Gauss-Legendre are very well suited for smooth flow distribution in the channel [1]. The methods doesn't account for steep variations in the flow profile, which results in error typically less than 0.5 to 1 %. A typical setup of an 8- path UTTF is shown in following figure 2.5:
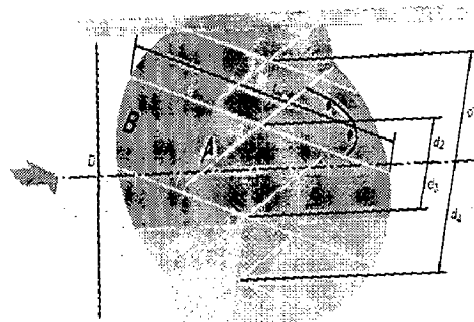
Fig. 2.5 An eight path UTTF (Source: technical data sheets of Risonic 2000, Rittmeyer) [20]

IEC 60041 suggests weighting factors for the two Gaussian quadrature techniques and the correction factors depending on the shape of the conduit. The weighting factors and the parameters that are used in the discharge calculation of the discharge by an eight-path UTTF are reproduced in Table 2.1.

		Gauss-Legendre method		Gauss-Jacobi method	
		Paths 1 and 4	Paths 2 and 3	Paths 1 and 4	Paths 2 and 3
d/(D/2)		± 0.861136	± 0. 339981	± 0.809017	± 0.309017
W		0.347855	0.652145	0.369317	0.597667
k	Circular section	0.994		1	
	Rectangular section	1		1.034	

Table 2.1. Weighting coefficients for discharge measurement using eight-path UTTF

The error due to installation and the complexity of near wall flow are not much accounted by IEC 60041. Further improvement in the promised accuracy (2 %) of the UTTF is possible if the two above mentioned problems are dealt with appropriating. The expression used for discharge calculation using multi-path UTTF is given below.

$$Q = k\frac{D}{2}\sum_{1}^{n} W_i \overline{v}_{ai} L_{wi} \sin \varphi \qquad (2.6)$$

where

φ is the angle made by the ith path with flow direction,

L_{wi} is the distance from left wall to right wall along the ith ultrasonic path,

$L_{wi} \sin \varphi = B$, i.e, is the distance from left wall to right wall (breadth),

$\overline{v}_{ai}$ is the flow velocity averaged along i^{th} path,

W_i is the weighting factor of ith path depending on the numerical integration method used,

n is the number of UTTF paths,

D is the depth of the channel,

k is the correction factor depending on the numerical integration method and the shape of the conduit and

Q is the discharge measured.

OPEN- CHANNEL MODELING BY CFD

3.1 NEED FOR FLOW SIMULATION

The velocity profile developed in various open channel field conditions is found to be different from each other depending on the size and shape of the cross-section of the channel. Accurate measurement of discharge in these conditions is a challenging and tedious job. Accuracy of measurement is very much affected by the placement and also the number of flow meters in the channel to obtain these profiles. So for minimizing the measurement errors and uncertainty in discharge measurement, placement of the flow meters across the cross-section of the channel should be precise.

The placement of flow meters should be such that by using the prescribed number of flow meter, it should be possible to trace out the variation in velocity profiles to the maximum. The placement and number of flow meters used will be varying as the cross-section of the channel changes. IEC-41 provides the guidelines for the number and also the placement of flow meters.

In such a situation the flow meters can be efficiently placed by the knowledge of expected velocity profile. Therefore a general awareness about the expected profiles in various channel geometries is desirable for reducing the uncertainty in measurement. Modeling the effect of channel geometries in the profiles can be done by CFD analysis.

3.2 CFD: THE SCIENCE OF PREDICTING THE FLUID FLOW

3.2.1 GOVERNING EQUATIONS

Computational Fluid Dynamics (CFD) is the science of predicting fluid flow, heat transfer, mass transfer, chemical reactions, and related phenomena by solving mathematical equations that represent physical laws, using a numerical process.

Applying the fundamental laws of mechanics to a fluid gives the governing equations for a fluid. The conservation of mass equation is

$$\frac{\partial \rho}{\partial t} + \nabla \cdot (\rho \vec{V}) = 0$$

and the conservation of momentum equation is

$$\rho \frac{\partial \vec{V}}{\partial t} + \rho(\vec{V} \cdot \nabla)\vec{V} = -\nabla p + \rho \vec{g} + \nabla \cdot \tau_{ij}$$

These equations along with the conservation of energy equation form a set of coupled, nonlinear partial differential equations. It is not possible to solve these equations analytically for most engineering problems. However, it is possible to obtain approximate computer-based solutions to the governing equations for a variety of engineering problems. This is the subject matter of Computational Fluid Dynamics (CFD). Fluent is a Finite Volume based code for fluid flow simulations [5].

3.2.2 STAGES OF CFD ANALYSIS
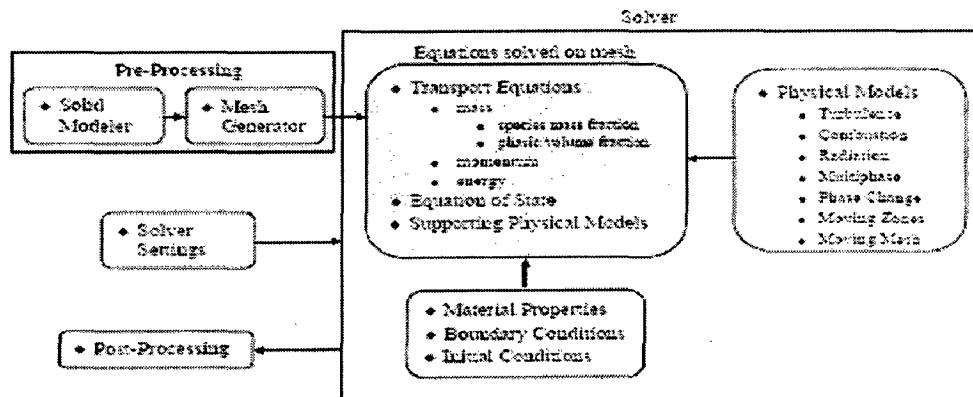
Fig. 3.1 Overview of CFD modeling

Stage 1 Modeling Geometry: The first step in performing a CFD analysis is to create the shape of the fluid that needs to be analysed. This can usually be done with the help of a standard CAD program or GAMBIT etc. It is easily possible to import data generated by such programs into a CFD package.

Stage 2 Meshing: In the second stage the fluid is then sub-divided into numerous cells. This can be thought of as being similar to the way in which a Rubics Cube is divided into smaller bits. In many CFD packages, meshing can be done while the shape is being

15

defined. For such cases, it is not uncommon to have the first two stages performed simultaneously.

Stage 3 Preprocessing: Once meshing has been completed, boundary conditions are then applied to the fluid. This generally means specifying known velocities or pressures at specific points of the fluid. These initial conditions are what the computer uses to calculate the velocities and pressures in other parts of the fluid volume.

Stage 4 CFD Analysis: This step involves using a computer to solve mathematical equations of fluid motion. It is very intensive and usually requires the computer to solve many thousands of equations. In each case, the equations are integrated and boundary conditions are applied to it. This is known as equation discretisation and is applied to each individual cell of the mesh. The process is repeated in an iterative fashion until a required accuracy is achieved.

Stage 5 Post Processing: Post processing is done to make sense of the data generated by the CFD analysis. In solving the equations, a computer would have generated a fair amount of data for each cell. Since there are typically several thousand cells in a mesh, the total amount of data we are looking at here is enormous - definitely not something an engineer would like to browse through! Using the post processor, the results are easily sorted by a computer. It may then be displayed to the engineer as a graph. This usually has little arrows and contours that are much easier to understand. In such graphs, colours are used to differentiate between the different size of the values.

CFD package used in this work is FLUENT and the geometry creation is done using GAMBIT

3.2.3 SOLUTION PROCEDURE USING FLUENT

As in every CFD-package, the solution procedure of

Fluent can be divided into three parts:

1. Pre-processing
2. Calculation
3. Post processing

16

The most important part of a CFD analysis is the preprocessing of the problem. This is not simply done by setting up a geometry and activating some toggle switches in the GUI (Graphical User Interface) of the program. Before turning on the workstation, one should be concerned about the physics of the problem. This determines the models (turbulent/ laminar flow, compressible/incompressible flow, transient/stationary flow, inclusion of energy balance, etc.) as well – and this cannot be emphasized sufficiently – the boundary conditions at the borders of the calculation domain. In this stage of the analysis also the decision whether a specific solver – like for instance Fluent 5.5 – is capable of the requirements resulting from this previous assessment has to be made [2].

3.2.4   PRE-PROCESSING WITH FLUENT

The steps of setting up a simulation in Fluent are roughly given by:

- Defining geometry
- Creating the grid
- Importing and checking the grid
- Selection of solver formulation and equations to be solved (laminar/turbulent, heat transfer, multiple species, etc.)
- Specification of operation conditions (material properties)
- Specification of boundary conditions
- Specification of numerical properties (under relaxation factors, etc.)
- Initialization of variables

The first two steps of the pre-processing part require additional software for geometry and/or grid generation. Fluent can handle grid topologies provided by the following packages: Gambit, TGrid, Geo-Mesh, preBFC, ICEMCFD, I-DEAS, NASTRAN, PATRAN, ARIES, and ANSYS. Since Gambit and TGrid also are products provided by Fluent Inc., the communication between these two packages and Fluent is quite uncomplicated. In fact you are even able to define boundary types already in Gambit, a task that normally has to be done in the Fluent preprocessor. Fluent can use unstructured as well as body fitted structured meshes with all types of mesh elements, such as triangular and quadrilateral elements (or combination of the two) in 2-D, and tetrahedral, hexahedral, pyramid, and wedge elements (or a combination of these) in 3-D analysis.

As mentioned earlier, one can choose between different solvers for two and three dimensional analysis (referred to as solver version) and different precisions (single as well as double). It is also possible to perform parallel simulations. However, there can be restrictions what comes to the application of certain physical models. The formulation of the solver can be either segregated (i.e. sequential solution of the equations) or coupled. The linearization of the equations can either be chosen to be explicit or implicit in time. Also different time-discretization schemes (first and second order) are implemented. The choice of the physical models as well as the solver really depends on the specific problem that is examined and thus should be part of the previous assessment. Unfortunately there exists no simple strategy and some basic knowledge of the applied models and numerical techniques is required.

3.2.5 PERFORMING CALCULATIONS WITH FLUENT

After the pre-processing part being finished the simulation setup can be stored in a so called case-file (files with extension *.CAS). This file includes information on the grid file, the boundary conditions and the physical as well as computational models of the run.

Modelling of the geometry & meshing is done in Gambit while simulation of this model by specifying the boundary condition is done by Fluent in this work.

3.3 GEOMETRY MODELING IN GAMBIT

Steps involved in GAMBIT:

3.3.1 CREATING THE GEOMETRY

When you click the **Geometry** command button on the **Operation** toolpad, GAMBIT opens the **Geometry** subpad. The **Geometry** subpad contains command buttons that allow you to create, move, copy, modify, summarize, and delete vertices, edges, faces, and volumes. The **Geometry** subpad also contains a command button that allows you to perform operations involving groups of topological entities.

3.3.2 MESHING THE MODEL

The **Mesh Volumes** command allows you to create a mesh for one or more volumes in the model. When you mesh a volume, GAMBIT creates mesh nodes throughout the volume according to the currently specified meshing parameters. To mesh a volume, you must specify the following parameters:

- Volume(s) to be meshed
- Meshing scheme
- Mesh node spacing
- Meshing options

The meshing scheme used for this study is hexahedral and the mesh node spacing is set to be 5 mm after the mesh independency test.

3.3.3 SPECIFYING ZONE TYPES

Zone-type specifications define the physical and operational characteristics of the model at its boundaries and within specific regions of its domain. There are two classes of zone-type specifications: 1. Boundary types   2. Continuum types

Boundary-type specifications, such as WALL or VENT, define the characteristics of the model at its external or internal boundaries. Continuum-type specifications, such as FLUID or SOLID, define the characteristics of the model within specified regions of its domain.

3.4   SIMULATING OPEN CHANNEL FLOWS BY FLUENT:

3.4.1 SETTING THE PARAMETERS

FLUENT can model the effects of open channel flow (e.g., rivers, dams, and surface-piercing structures in unbounded stream) using the VOF formulation and the open channel boundary condition. These flows involve the existence of a free surface between the flowing fluid and fluid above it (generally the atmosphere).

In such cases, the wave propagation and free surface behavior becomes important. Flow is generally governed by the forces of gravity and inertia. This feature is mostly applicable to marine applications and the analysis of flows through drainage systems. Using the VOF formulation, open channel flows can be modeled in **FLUENT**. To start using the open channel flow boundary condition, perform the following:

1. Turn on gravity.

    (a) Open the **Operating Conditions** panel.

        Define →**Operating Conditions...**

    (b) Turn on **Gravity** and set the gravitational acceleration fields.

2. Enable the volume of fluid model.

    (a) Open the **Multiphase Model** panel.

        Define →**Models** →**Multiphase...**

    (b) Under **Model**, turn on **Volume of Fluid**.

    (c) Under **VOF Scheme**, select either **Implicit**, **Explicit**, or **Geo-Reconstruct**.

3. Under **VOF Parameters**, select **Open Channel Flow**.

Table 3.1: Open Channel Boundary Parameters for the VOF Model

Boundary Type	Parameter
pressure inlet	Inlet Group ID; Secondary Phase for Inlet; Flow Specification Method; Free Surface Level, Bottom Level; Velocity Magnitude
pressure outlet	Outlet Group ID: Pressure Specification Method; Free Surface Level; Bottom Level
mass flow inlet	Inlet Group ID; Secondary Phase for Inlet; Free Surface Level; Bottom Level

20

3.4.2 DEFINING THE BOUNDARY CONDITIONS

In order to set specific parameters for a particular boundary for open channel flows, turn on the **Open Channel Flow** option in the corresponding boundary condition panel. Table 1 summarizes the types of boundaries available to the open channel flow boundary condition, and the additional parameters needed to model open channel flow.

Defining Inlet Groups: Open channel systems involve the flowing fluid (the secondary phase) and the fluid above it (the primary phase).

If both phases enter through the separate inlets (e.g., inlet-phase2 and inlet-phase1), these two inlets form an inlet group. This inlet group is recognized by the parameter **Inlet Group ID**, which will be same for both the inlets that make up the inlet group. On the other hand, if both the phases enter through the same inlet (e.g., inlet-combined), then the inlet itself represents the inlet group.

Defining Outlet Groups: Outlet-groups can be defined in the same manner as the inlet groups.

Setting the Inlet Group: For pressure inlets and mass flow inlets, the **Inlet Group ID** is used to identify the different inlets that are part of the same inlet group. For instance, when both phases enter through the same inlet (single face zone), then those phases are part of one inlet group and you would set the **Inlet Group ID** to 1 for that inlet (or inlet group).

In the case where the same inlet group has separate inlets (different face zones) for each phase, then the **Inlet Group ID** will be the same for each inlet of that group.

When specifying the inlet group, use the following guidelines:

- Since the **Inlet Group ID** is used to identify the inlets of the same inlet group, general information such as **Free Surface Level, Bottom Level,** or the mass flow rate for each phase should be the same for each inlet of the same inlet group.
- You should specify a different **Inlet Group ID** for each distinct inlet group.

21

For example, consider the case of two inlet groups for a particular problem. The first inlet group consists of water and air entering through the same inlet (a single face zone). In this case, you would specify an inlet group ID of 1 for that inlet (or inlet group). The second inlet group consists of oil and air entering through the same inlet group, but each uses a different inlet (oil-inlet and air-inlet) for each phase. In this case, you would specify the same **Inlet Group ID** of 2 for both of the inlets that belong to the inlet group.

Setting the Outlet Group: For pressure outlet boundaries, the **Outlet Group ID** is used to identify the different outlets that are part of the same outlet group. For instance, when both phases enter through the same outlet (single face zone), then those phases are part of one outlet group and you would set the **Outlet Group ID** to 1 for that outlet (or outlet group).

In the case where the same outlet group has separate outlets (different face zones) for each phase, then the **Outlet Group ID** will be the same for each outlet of that group.

When specifying the outlet group, use the following guidelines:

- Since the **Outlet Group ID** is used to identify the outlets of the same outlet group, general information such as **Free Surface Level** or **Bottom Level** should be the same for each outlet of the same outlet group.
- You should specify a different **Outlet Group ID** for each distinct outlet group.

For example, consider the case of two outlet groups for a particular problem. the first inlet group consists of water and air exiting from the same outlet (a single face zone). In this case, you would specify an outlet number of 1 for that outlet (or outlet group). The second outlet group consists of oil and air exiting through the same outlet group, but each uses a different outlet (oil-outlet and air-outlet) for each phase. In this case, you would specify the same **Outlet Group ID** of 2 for both of the outlets that belong to the outlet group.

REAL TIME DATA ACQUISITION AND VALIDATION

Validation of the simulation techniques used is an important part of the work to determine the reliability of the analysis done. Acoustic Doppler Current Profiler (ADCP) is the instrument used in this work for obtaining the velocity profile from the measurement site. This chapter discusses the basic working of ADCP and the associated software for real time data acquisition. Later in the chapter the validation procedure and its results are discussed

4.1   WORKING OF THE PROFILER

4.1.1   BASIC THEORY

The ADCP uses sound to measure water velocity. The sound transmitted by the ADCP is in the ultrasonic range. The lowest frequency used by commercial ADCPs is around 30 kHz, and the common range used by the for open channel measurements is between 300–3,000 kHz. The ADCP measures water velocity using a principle of physics discovered by Johann Doppler known as Doppler shift. Doppler's principle relates the change in frequency of a source to the relative velocities of the source and the observer [6, 7]. Doppler shift can be defined as the apparent change in the frequency of a wave as sensed by an observer, due to the relative motion of the source and the observer. If the exact source frequency is known and the observed frequency can be calculated, eqn 4.1 can be used to calculate Doppler shift due to the relative velocities of the source and observer

$$F_D = F_S \left(\frac{V}{C} \right)$$

(4.1)

F_D = the Doppler shift frequency, in hertz; C = the speed of sound, in m/s;

F_S = the transmitted frequency of the sound from a stationary source, in hertz;

V = relative velocity between the sound source and sound wave receiver in m/s;

If the observer walks faster (V increases), the Doppler shift (F_D) increases. If the observer walks away from the sound (V is negative), the F_D is negative. If the frequency of the sound (F_S) increases, the F_D increases. As speed of sound (C) increases, the F_D decreases.

4.1.2 MEASURING DOPPLER SHIFTS USING ACOUSTIC BACKSCATTER

An ADCP applies the Doppler principle by bouncing an ultrasonic sound pulse off small particles of sediment and other material (collectively referred to as backscatterers) that are present, to some extent, even in optically clear water. A magnified view of the water column and the backscatterers "illuminated" by the sound pulse are shown in figure 4.1.
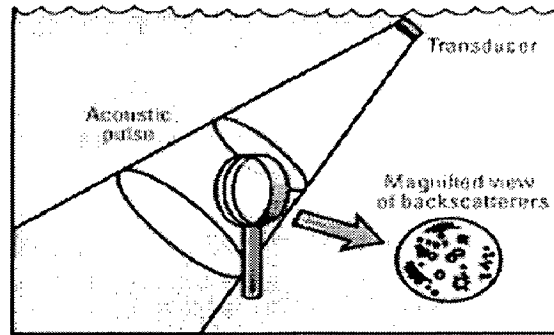
Fig 4.1. Magnified view of backscatterers.

The ADCP transmits an acoustic "ping," or pulse into the water column and then listens for the return echo from the acoustic backscatterers in the water column. Upon receiving the return echo, the ADCP's onboard signal-processing unit calculates the Doppler shift using a form of autocorrelation (the signal is compared with itself later). A schematic diagram of a transmitted acoustic pulse (ping) and the resulting reflected acoustic energy are shown in figure 4.2.
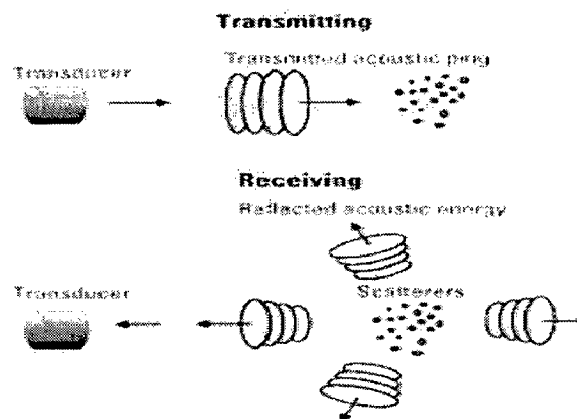
Fig 4.2. An acoustic pulse being backscattered.

Very little reflected acoustic energy is reflected back towards the transducer in fig. 4.2; most of the acoustic energy is absorbed or reflected in other directions.

4.1.3 MEASURING DOPPLER SHIFTS FROM A MOVING PLATFORM

When the scatterers are moving away from the ADCP, the sound (if it could be perceived by the scatterers) shifts to a lower frequency. This shift is proportional to the relative velocity between the ADCP and the scatterers (fig. 4.2). Part of this Doppler-shifted sound is backscattered towards the ADCP, as if the scatterers were the sound source (fig. 4.3). The sound is shifted one time (as perceived by the backscatterer) and a second time (as perceived by the ADCP transducer) [6]
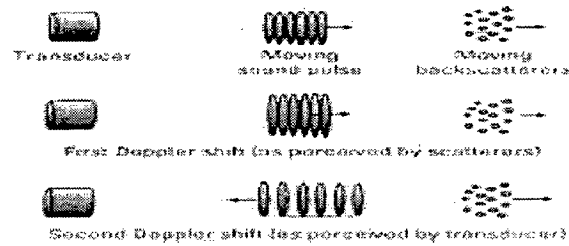
Fig 4.3. Reflected pulse showing two Doppler shifts.

Because there are two Doppler shifts, Equation 4.1 becomes:

$$F_D = 2 F_0 \left(\frac{V}{C} \right)$$

(4.2)

Only radial motion, which is a change in distance between the source and receiver, will cause a Doppler shift. Mathematically, this means the Doppler shift results from the velocity component in the direction of the line between the source and receiver as shown:

$$F_D = 2 F_s \left(\frac{V}{C} \right) \cos(\theta)$$

(4.3)

θ, the angle between the relative-velocity vector and the line of the ADCP beam.
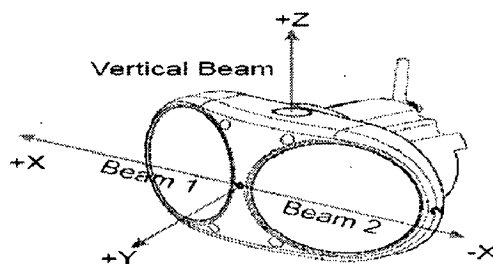
Fig 4.4 ADCP with beam orientations

Normally the ADCP will be mounted in one side wall of the channel normal to the flow. The ADCP will transmit two acoustic waves to the channel at angle of 10-15° at both sides of the normal(fig 4.4). By comparing the reflected and the parent wave frequencies of the two acoustic beam both the magnitude and the direction of flow can be estimated.

25

4.2   DATA ACQUSITION WITH THE PROFILER

For data acquisition the communication between ADCP and PC has to be established through RS-232 serial port. This is done with the help of BBTalk (provided by ADCP manufacturers). After communication is established successfully, proper mounting of the ADCP is done and real time data is monitored and acquired using Win-HADCP [8, 9].

4.2.1   COMMUNICATION PARAMETERS

Before establishing communications with the ADCP, *BBTalk* must be configured [9].

a. At the Connect To screen, select the ADCP type (WorkHorse, Broad-Band, NarrowBand, Channel Master, or NEMO) from the list.

b. Select the COM Port the ADCP is connected to. Click Next.
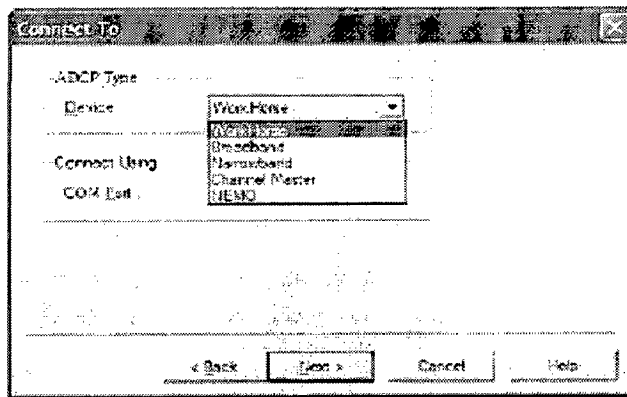
Fig 4.5. BBTalk - Connect To Screen

c. On the Port Settings screen, select the baud rate, parity, stop bits, and flow control. Click Next.
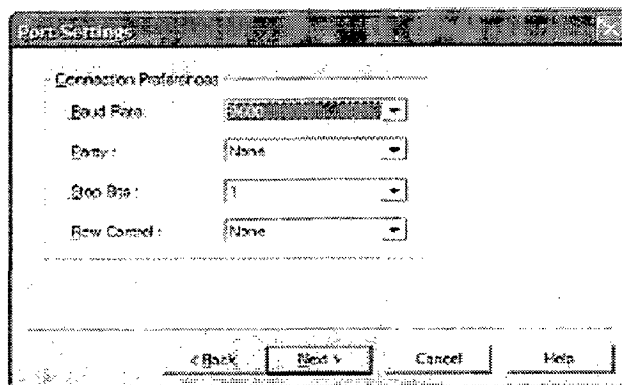
Fig 4.6. BBTalk - Port Settings Screen

26

d. On the Options screen, select the desired settings.
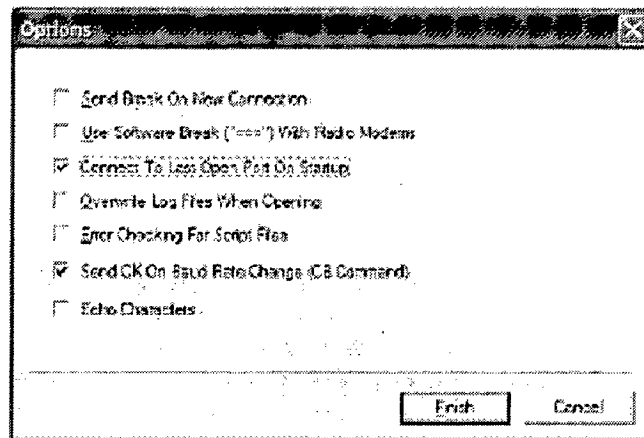
Fig 4.7. BBTalk - Options Screen

e. Click Finish.

f. On the File menu, click Break. The following wakeup message appears on the log file window.

xxxxxx ADCP
RD INSTRUMENTS (c) 1997-2002
ALL RIGHTS RESERVED
Firmware Version xx.xx
>
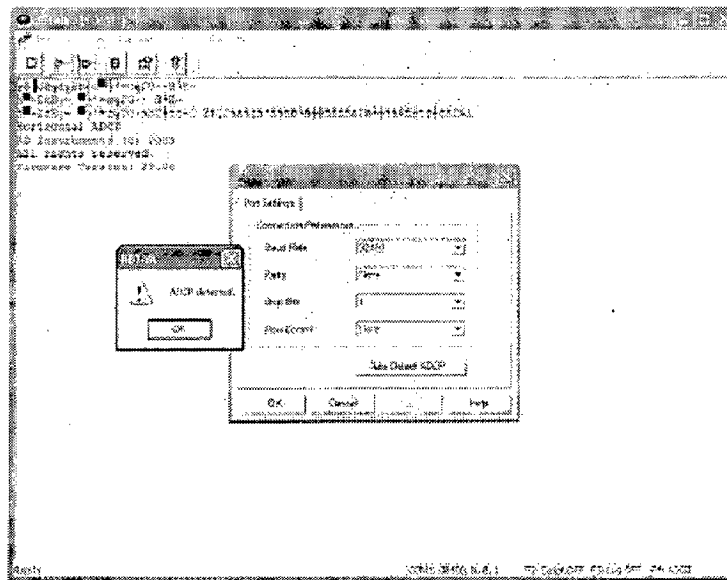
Fig 4.8. BBTalk - Auto Detect

g. Click OK when the ADCP is detected. Try to wakeup the WorkHorse again.

27

4.2.2   ADCP MOUNTING

WinH-ADCP can help with the physical mounting of an H-ADCP by causing it to ping and displaying real time orientation, depth, and temperature data in a large font

a. Start *WinH-ADCP*.

b. On the **Start** Screen, click **Mount ADCP**.

c. On the **Communications Settings** screen (see Figure 4.9), enter the communications settings for the H-ADCP. If you are unsure of the setting, use the **Auto Detect** button.
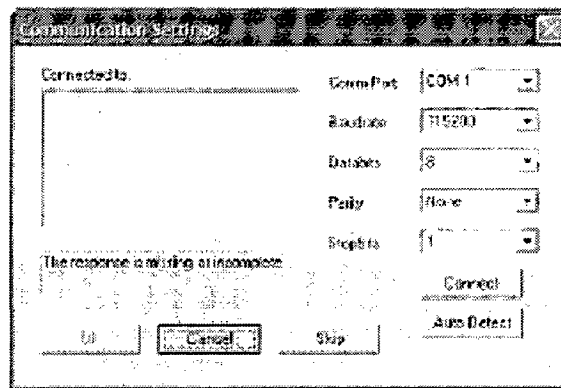
Fig 4.9 Communications Setting Screen

d. The Sensors screen of the *WinH-ADCP* software indicates the pitch and roll angles of the H-ADCP. Adjust the mount until the roll is zero. The H-ADCP rolls about the Y-axis. The roll must be zero. Adjust the mount until the pitch is zero. The H-ADCP pitches about the X-axis.
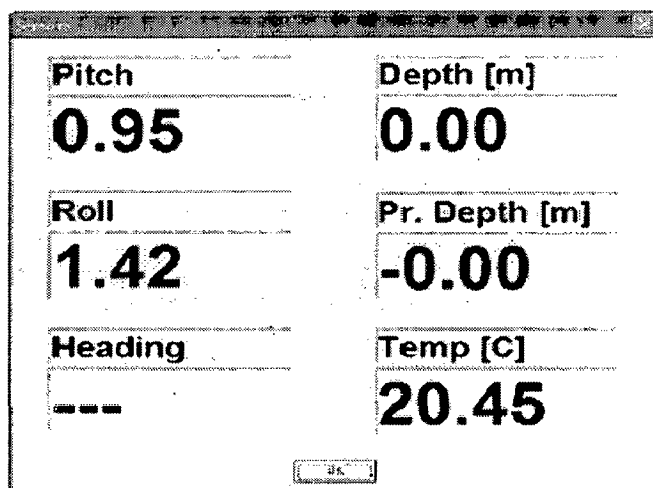
Fig 4.10. Sensors Screen

4.2.3 REAL TIME DATA ACQUISITION

When *WinH-ADCP* is first started in the Data Acquisition mode, communications with the H-ADCP must be set up [8, 9].

a. Connect and power up the H-ADCP using 12V DC.

b. Start *WinH-ADCP*. If *WinH-ADCP* is already running, on the Configure menu, click Setup Wizard. On the Start dialog, click Real-Time Data Acquisition.

c. On the Communications Settings dialog box, select the COM Port, Baudrate, Databits, and Stopbits that the H-ADCP is connected to. If you are unsure of the setting, use Auto Detect. Once setup, *WinH-ADCP* will remember these setting and automatically connect the ADCP the next time the program is started. To skip connecting to the ADCP, click the Skip button.

d. *WinH-ADCP* will connect to the H-ADCP and confirm the communication setting. On the **Connected to** box, the H-ADCP wakeup message is seen.

e. Click **OK** to continue to the **Real-Time Data Acquisition** screen
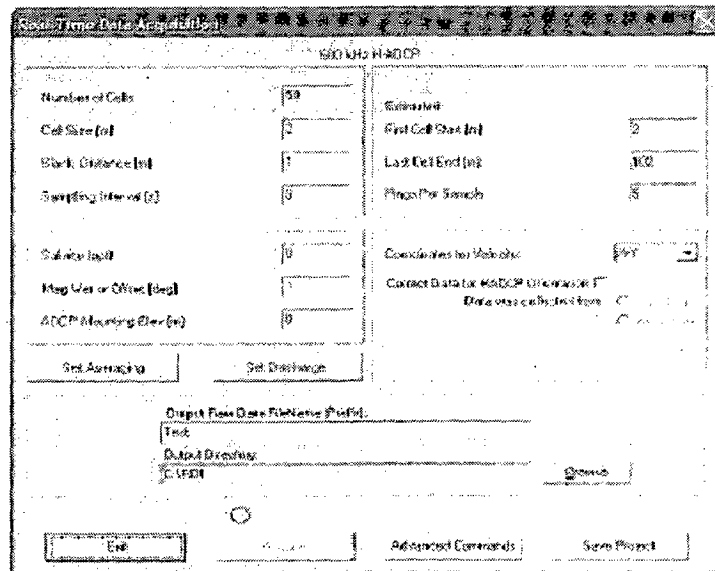
Fig 4.11. Real-Time Data Acquisition Screen

f. Once the **Real-Time Data Acquisition** screen is setup, click the **Save Workspace** button to save the discharge and averaging settings.

g. Click **Acquire** to begin data collection.

4.3   VALIDATION

Validation is done by comparing the measured data from the site with simulated data. For this purpose, a well defined, lined and simple section of an open channel has been identified and measurement has been done in this site using ADCP. Later these site conditions have been modeled and the flow is been simulated by CFD analysis. Comparison of these results is discussed in the following sections.

4.3.1   WHY VALIDATION ?

CFD analysis for this particular work is done in Fluent software. In CFD analysis prediction of the flow is done by solving the governing flow equations for each mesh. The exactness of this procedure with real data depends on the software used, size of the mesh used and also the conditions specified in the solver. It is evident that the prediction may be prone to error. Therefore closeness of these simulated profiles with the real situation has to be verified so that the accuracy of the simulated results can be trusted.

4.3.2   SITE SELECTION

Validation has to be done in a simple and well defined geometry. The selected channel should be long enough to have a fully developed flow at the measuring section. A lined open-channel in Roorkee, with steady flow has been selected for measurements. It is a straight channel, with left wall vertical and the right wall tapered and both sides lined. The depth of the channel is 2meters. The width at the top is 5.2 meters and at the bottom is 4 meters with a tapering angle of 30.96°. The conditions of the channel was very favorable to carry out a steady measurement with ADCP.

4.3.3   MODELING OF SITE IN CFD

An exact model of the site with the above mentioned geometry has been created and the meshing is done in Gambit. For meshing the volume in Gambit, the following parameters should be specified:1) *Meshing Scheme* specified by 3 parameters (**Elements**- defines the shape of elements used to mesh the volume, **Type**- defines the meshing algorithms used and **Smoother**- describes the smoothing algorithm used, if any) 2) *Mesh node spacing.*

Since the geometry which has to be meshed here is simple, lined and regular, simple meshing schemes are used to obtain good results.

Meshing Element used: Hex – specifies that mesh includes only hexahedral elements.

Meshing Type used   : Map- creates a regular structural grid of hexahedral elements.

Mesh node spacing   : 0.005 m. i.e. the whole volume will be divided into hexahedral elements with face length equals to 0.005 m. The volume is initially checked with three different mesh spacing of 0.01 m, 0.005 m and 0.0025 m and it was found that there is no further improvement in the simulation results as the grid size reduces beyond 0.005 m. Therefore mesh spacing is selected to be 0.005 m in this work.

After meshing the volume grid check, has been conducted to ensure the regularity of the cells formed. The meshing is considered good if volume passes grid check.
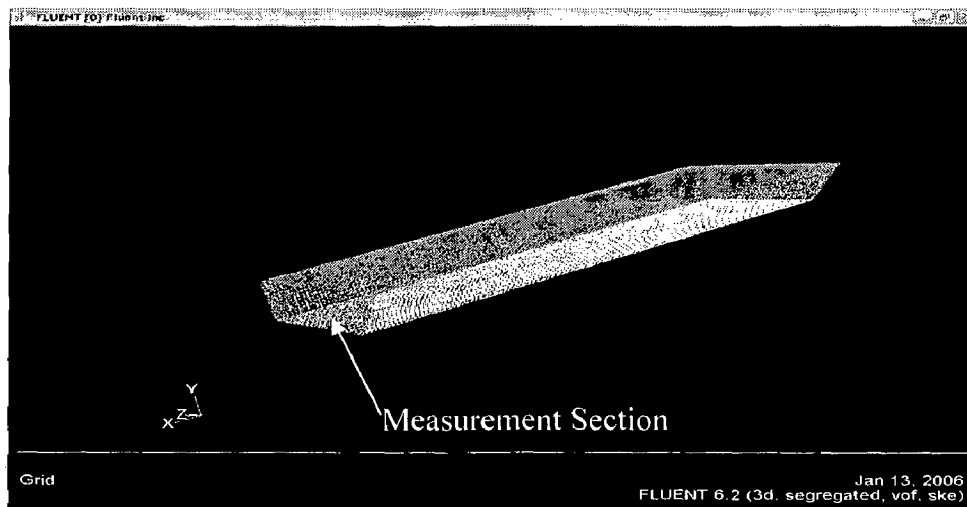
Figure 4.12   Site for validation modeled in Gambit

Specifying zone types: Zone-type specifications define the physical and operational characteristics of the model at its boundaries and within specific regions of its domain. There are two classes of zone-type specifications:

- Boundary types – WALL type for side walls and bed, PRESSURE_INLET for inflow and free surface, PRESSURE_OUTLET for outlet

- Continuum types – FLUID, whose specifications define the physical characteristics of the model within specified regions of its domain. Here it is water flow.

4.3.4 PROFILE SIMULATION IN CFD

The open channel flow is modeled as a multi phase flow which includes two phases: water and air. Three general multi phase models are available, Mixture model, Eulerian model and Volume Of Fluid (VOF) model. The VOF model is appropriate for stratified or free-surface flows, and the mixture and Eulerian models are appropriate for flows in which the phases mix or separate. The solver used is the Segregated solver. In this solution algorithm the governing equations are solved sequentially.

The operating conditions have to be specified such as the direction of flow, the direction of gravity and the density of lightest phase, i.e. air. The lightest phase air is set as primary phase and water as secondary phase in open channel flows. The boundary conditions specified for each of the boundary types are as follows:

1) INLET and FREE SURFACE – Type (PRESSURE INLET)

        Open channel inlet Group ID -1

        Secondary phase for flow – Water

        Flow direction – X

        Velocity magnitude – 0.35 m/s (average)

        Bottom level – 0m

        Free surface level – 2m

        Turbulence specification method – k-ε

Volume fraction at free surface is zero indicating only air exists at the free surface.

2) SIDE WALLS and BED – Type (WALL)

        Wall motion –Stationary wall

        Wall Roughness: Roughness height – 0m (Lined wall)

                Roughness constant – 0.5 (default)

3) OUTLET – Type (PRESSURE_OUTLET)

        Open channel outlet Group ID – 1

        Free Surface level – 1.8 m

        Bottom level - -0.2 m

        Back flow direction specification method – From neighboring cell

        Turbulence specification method – k-ε

After the parameters are set, the solver is initialized with inlet conditions and the iteration is done. 500 iterations where given inside which the solution has converged. The simulation result of the flow in the channel is shown in fig. 4.13

Contours of Velocity Magnitude (mixture) (m/s)   Jan 13, 2006
                                                     FLUENT 6.2 (3d, segregated, vof, ske)
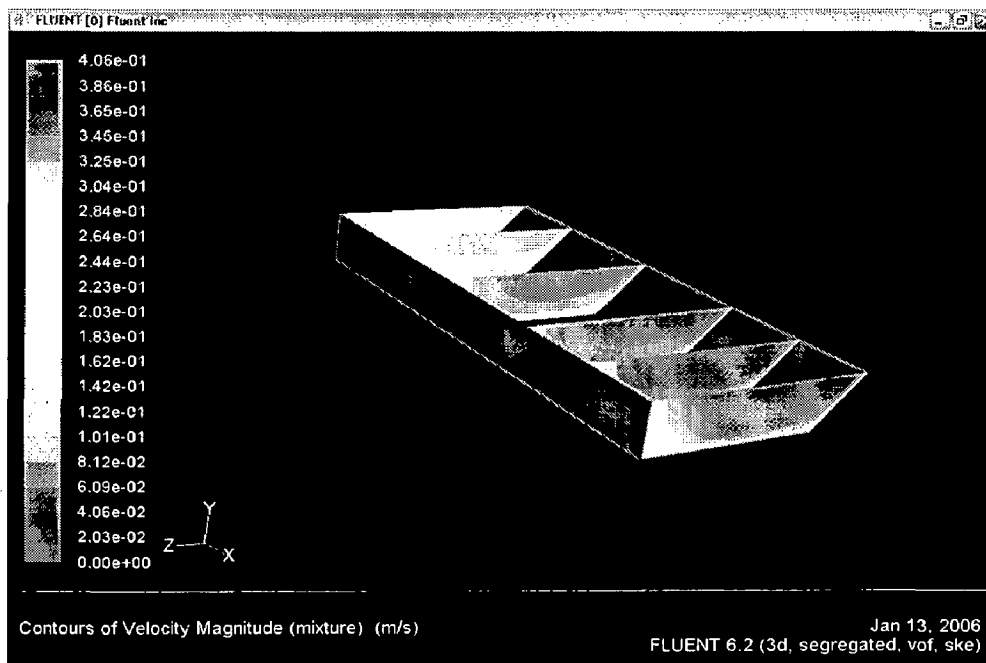
Fig. 4.13 Simulation of flow in CFD
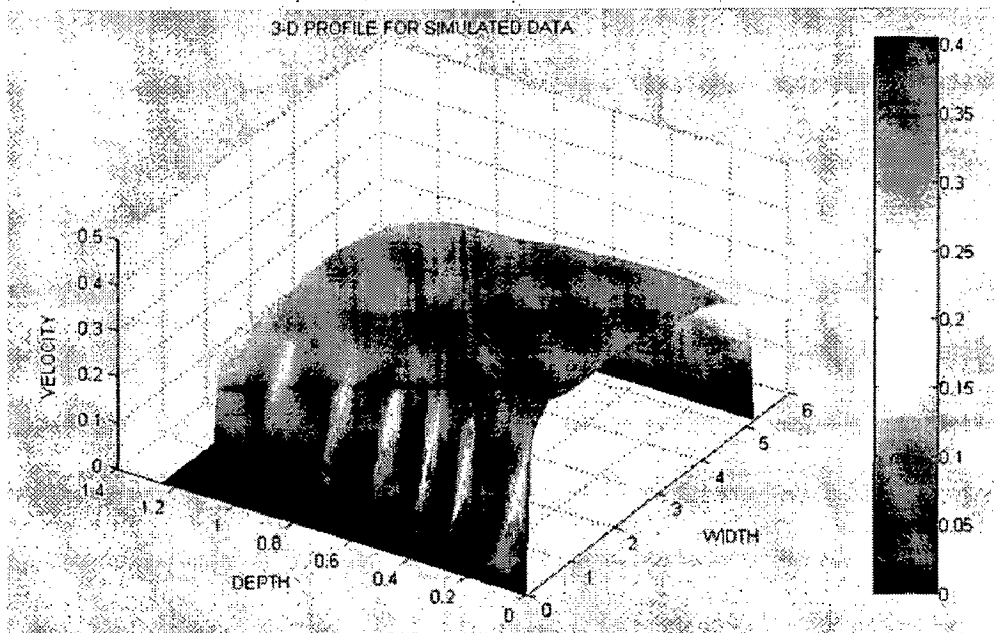
Fig. 4.14 3-D velocity profile plot of simulated data

From the 3-d velocity profile of the CFD simulated data, developed in Matlab (Fig 4.14), it is evident that flow is more in upper tapered region. Further analysis by comparison with ADCP data is done in the next section.

33

4.3.5 GENERATING 3-D PROFILE FROM PROFILER DATA

The real time data acquisition from the site is done using ADCP. Here the entire channel width is divided into a cell size of 10 cm and the average velocity in each cell is obtained and is stored in PC with the help of communication software Win-HADCP and serial port RS-232. The data acquisition procedure is discussed in section 4.2. The obtained data is then used to develop a 3-D profile of the channel. A Matlab code is developed for obtaining the 3-D profile from ADCP data. The profile generated is shown in Fig. 4.15.
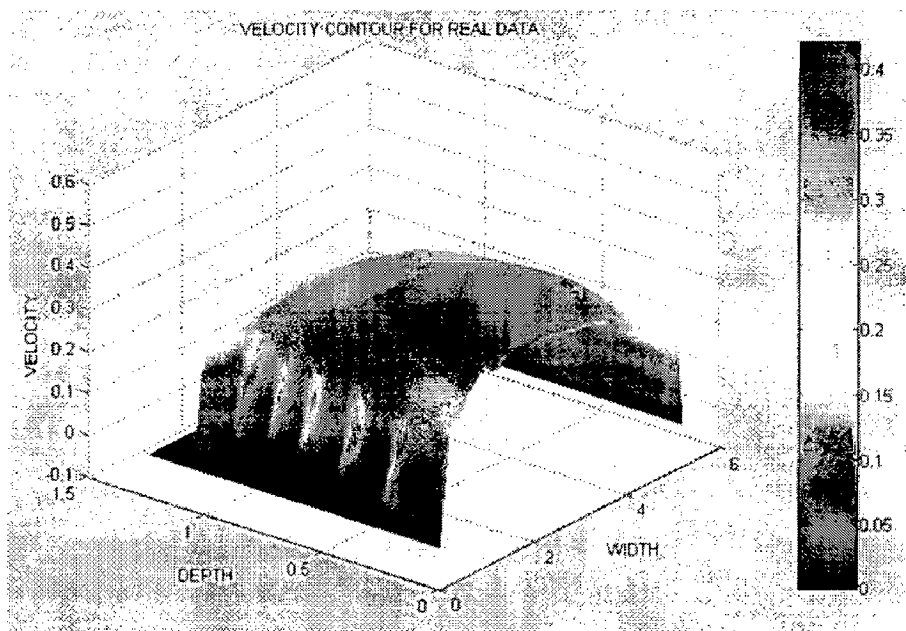
Fig. 4.15 3-D profile for ADCP data

4.4 RESULTS OF VALIDATION

Validation is done by comparing the simulation result and the site data. The average velocity profile along the width of the channel is compared for both datas. The comparison of the velocity contours is also done and the observations are discussed in this section. A comparison of discharge for both the profiles is also presented here:

Real data (ADCP Measurement): Total discharge in the channel is 1.620769 m^3/s

CFD Simulated data: Total discharge in the channel is 1.603693 m^3/s

% Error between two discharges: -1.053574 %

34
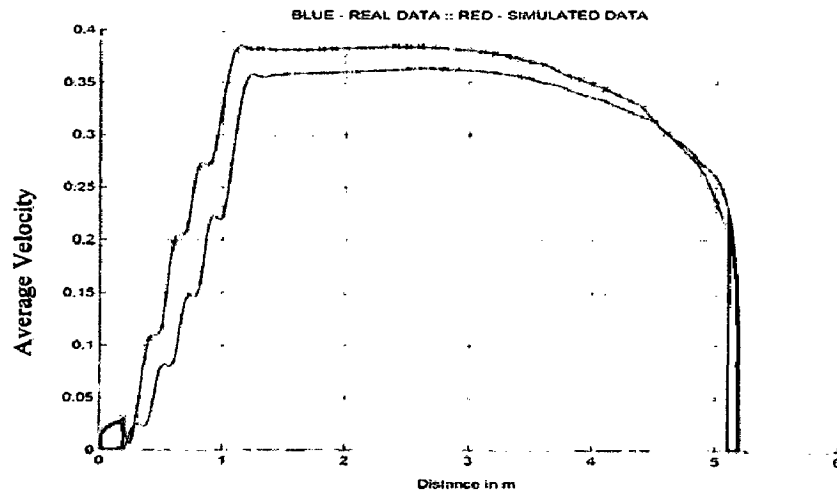
Figure 4.16 Comparison of average horizontal profile
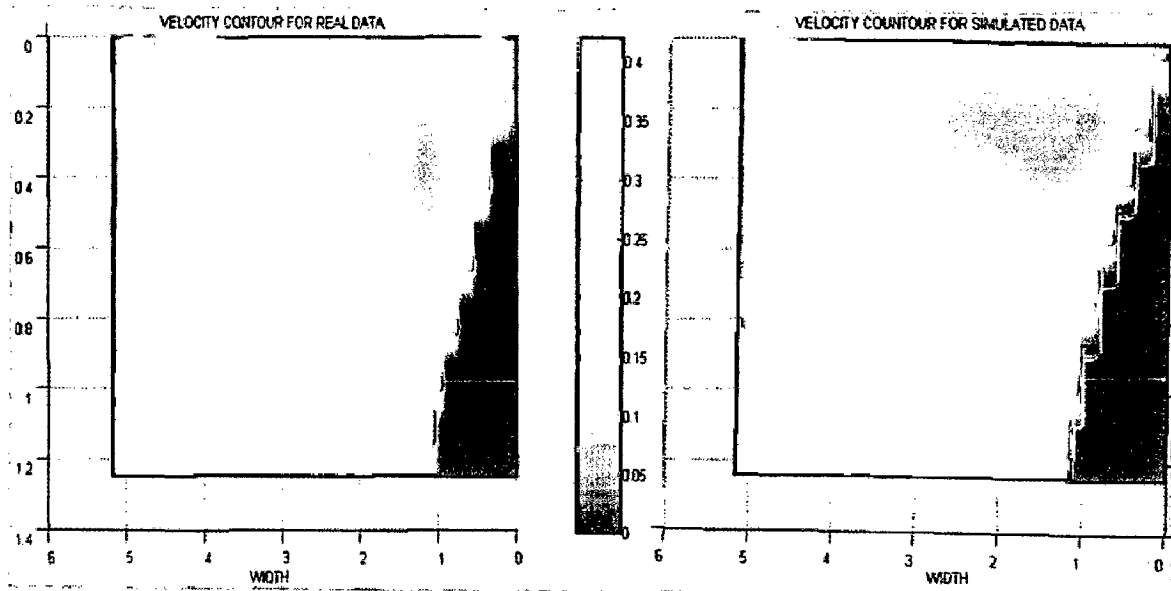
Fig. 4.17 Comparison of the velocity contours (a) Real (b) Simulated

Observations:

1) The velocity contours for the two datas is found to be almost same, with the highest flow component in the top right position of the tapering section.

2) The discharge evaluated for the two datas is only varying by 1% . This variation in magnitude and slight difference of the two profiles may be due to the approximation of average velocity at inlet in CFD simulation and due to discretization in CFD procedure. The measurement errors of the real data may also contribute for this slight discrepancy.

Inspite of this slight variation in magnitude the profiles is observed to be almost identical, means the CFD simulations can be rely upon for further open channel analysis.

CHAPTER 5
MATHEMATICAL MODELING OF FLOW PROFILES

Modeling the distribution of velocity across the cross-section of an open channel is a challenging process. The proposed model should be able to track the variations in every small portion of the cross-section. As the complexity of channel geometry increases the profile developed will also be complex making this procedure extremely difficult. In this work a mathematical model has been developed which is capable of tracking the variation in both horizontal and vertical profiles, with several control parameters, which accounts for various real situations and the 3-D velocity profile can be developed from this model [10].

5.1   DEVELOPMENT OF MATHEMATICAL MODEL

The velocity profile in an open channel is controlled by many parameters of the site. Some of the major factors that affect the profile are given below:

1) The roughness of the two side walls of the channel which affects the horizontal velocity distribution near the walls.

2) The roughness of the channel bed which affects the vertical profile at its lower end.

3) The irregularity in the geometry of the channel due to unlined walls and bed, due to bends, suspended sediments in the flow etc also add to the complexity of the profiles.

4) The turbulence of the flow which is reflected in the Reynolds Number of flow is another major factor.

5) The air friction at the free surface between the top water layer and air affects the vertical flow profile at the top and a little below the surface.

All these factors add to the complexity of open channel flow in real situations, makes it extremely difficult to model these profiles using simple mathematical formulas. The proposed mathematical model with 10 control parameters is capable of incorporating all these major factors. A single control parameter or combination of 2 or 3 parameters accounts for the above mentioned factors in the developed profile.

The three dimensional modeling is done by the combination of two two-dimensional profile equations. Separate models are developed for horizontal as well as vertical profiles. The model developed for horizontal profile gives the variation of velocity along the width of the channel (x-direction) while the vertical profile model gives the distribution of velocity along the depth of the channel (y- direction). The model is defined for normalized width and depth (0 – 1). Matlab code is developed which combine these two models to obtain a 3-D velocity profile with width and depth along x and y axis and velocity along the z-axis. The profile can be obtained for different values of the control parameters.

5.2   ANALYSIS OF HORIZONTAL PROFILE

The horizontal profile can be expressed by a general mathematical equation given below:

$$V_h(x) = \{[1 - w(x)] \cdot \log[\, m_1 \cdot k_1 \cdot w(x) + 1]\} + \{\log[\, m_2 . k_2 . w(x) \cdot \{1 - w(x)\}]\}$$

$$\pm \left\{ \frac{\Gamma(\alpha + \beta)}{\Gamma\alpha + \Gamma\beta} \cdot w(x)^{\alpha-1} \cdot [1 - w(x)]^{\beta-1} \right\} \qquad (5.1)$$

$V_h(x)$ = Velocity magnitude at the point x;

$w(x)$ = Normalized distance of the channel at the point x (from the left bank);

$\alpha \,\&\, \beta$ = constants which accounts for the skewness of the horizontal profile
          due to various channel geometries;

$m_1 \,\&\, m_2$ = constants which accounts for the roughness of the wall in the left and
          right bank;

$k_1 \,\&\, k_2$ = constants which accounts for the turbulence of water in the channel;
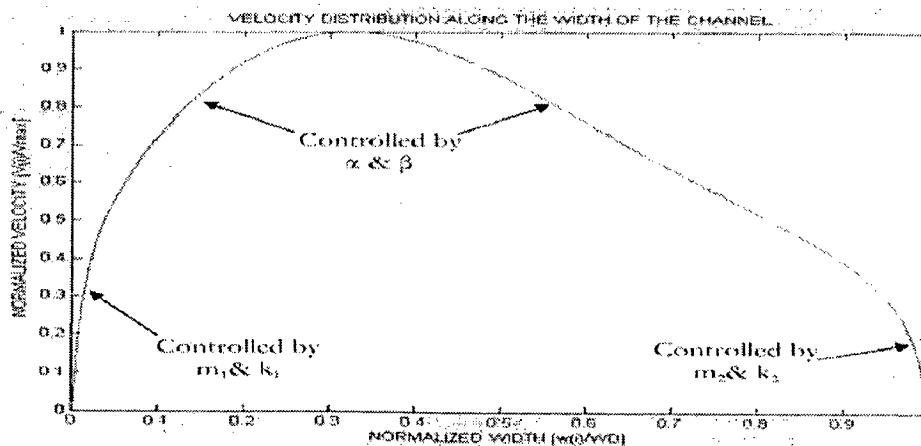
Fig 5.1 Horizontal profile developed from the model and controlling parameters

The horizontal profile can be viewed as the combination or summation of three equations. As observed in equation 5.1, the first two summing factors are logarithmic profiles which control the horizontal profile variations near the left and right wall respectively. The third summing factor of the profile is called the Beta function, which controls the profile variations through out the width of the channel other than the portions near the walls. The six control parameters of the equation can be varied and different horizontal profiles can be obtained for varieties of channel geometries. The effect of these parameters on the horizontal profile is separately discussed in the coming sections. Figure 5.1 shows a horizontal profile developed from the model for normalized width and the parameters which affects each part of the horizontal profile.

5.2.1 EFFECT OF BETA FUNCTION AND PHYSICAL SIGNIFICANCE

An open channel with simple rectangular geometry and lined walls exhibit a normal semi-elliptical horizontal profile with no skewness and single peak. As the geometry varies from this ideal open channel geometry, the horizontal profile becomes irregular by the introduction of skewness or multiple peaks in the profile. Convergence, divergence, bends, trapezoidal channels, obstruction in the flow etc adds to the irregularity of the horizontal profiles. These irregularities in the profile can be modeled using Beta function. The Beta function can represent a complete spectrum of the properties of the transverse velocity distribution for an open channel. This function can produce the velocity profile with symmetrical and skewed distributions and further it can produce both flattened and sharp-peaked velocity profiles. The general form of beta function is as follows [11]:

$$f(x) = \frac{\Gamma(\alpha + \beta)}{\Gamma(\alpha) \cdot \Gamma(\beta)} x^{\alpha-1}(1-x)^{\beta-1}, \quad 0 < x < 1 \tag{5.2}$$

Where α and β are real number parameters and $\Gamma(\alpha)$ and $\Gamma(\beta)$ are the values of gamma function which is defined as

$$\Gamma(\alpha) = \int_0^\infty x^{\alpha-1} e^{-x} dx, \quad \alpha > 0 \tag{5.3a}$$

$$\Gamma(\beta) = \int_0^\infty x^{\beta-1} e^{-x} dx, \quad \beta > 0 \tag{5.3b}$$
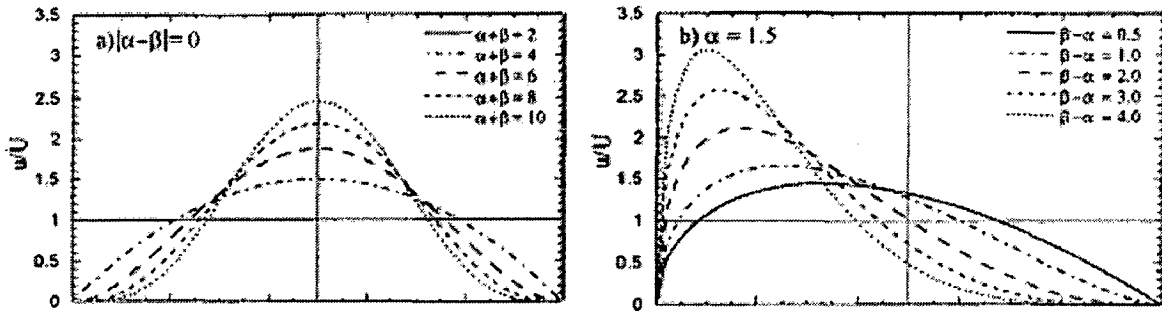
Fig. 5.2 Effects of α and β on beta velocity distribution [11]

The effects of parameters α and β on the velocity profile are plotted in Fig. 5.2. As shown in the figure, the distributions are symmetrical when α = β and skewed when α ≠ β. In the case of symmetrical distributions, shown in Fig. 5.2a, the velocity profile becomes more sharply peaked when both α and β becomes large. For asymmetrical distributions shown in Fig. 5.2b, the velocity profile becomes more skewed when the difference between α and β is larger. Further more it is found that if α is less than β; the profile skews towards the left and vice versa.

Beta function can also be used to model the effect of multiple peaks in the profile. The proposed mathematical model is capable of producing upto 2 peaks. The function can be added or subtracted in the horizontal profile equation as given by ± in equation 5.1. The subtraction of Beta function in the profile equation produces single peaks, while addition causes double peaks. The effect of α and β for both single and double peaked profiles are shown below.
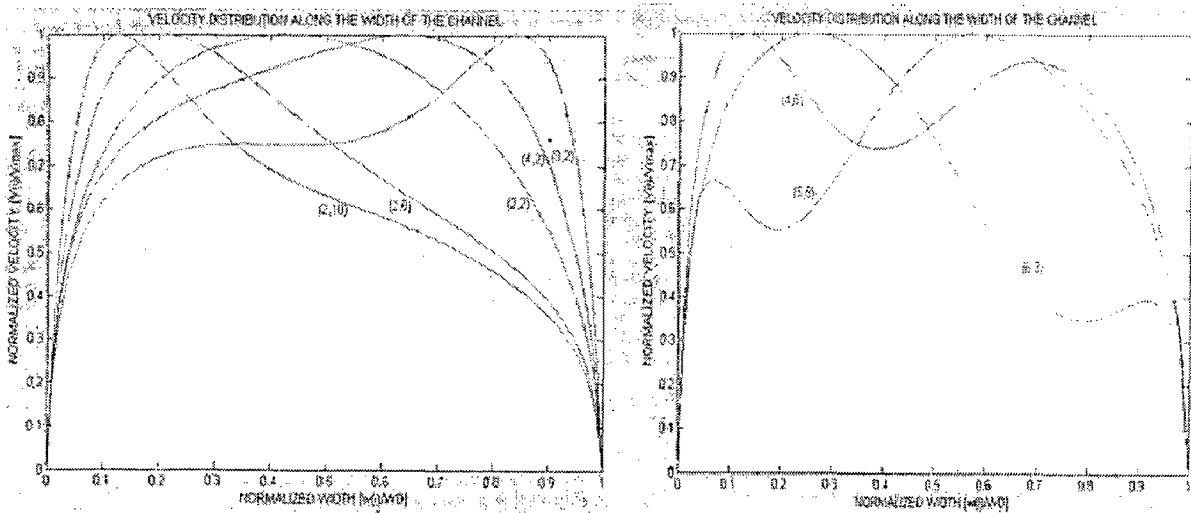
Fig 5.3 (a) Single peak profiles   (b) Double peak profiles

5.2.2 EFFECT OF WALL SURFACE ROUGHNESS AND TURBULENCE

At the two ends of the channel the velocities will have a drastic reduction and the velocity of water layer near the wall will be zero. This steep variation of the horizontal profiles near the walls is modeled using the sum of two logarithmic equations in the profile given by $\{[1 - w(x)] \cdot \log[m_1 \cdot k_1 \cdot w(x) + 1]\}$ *and* $\{\log[m_2.k_2.w(x) \cdot \{1 - w(x)\}]\}$ for left and right side respectively. The constants m_1 and m_2 are called the friction coefficients and can be used to model the effect of wall roughness [13].
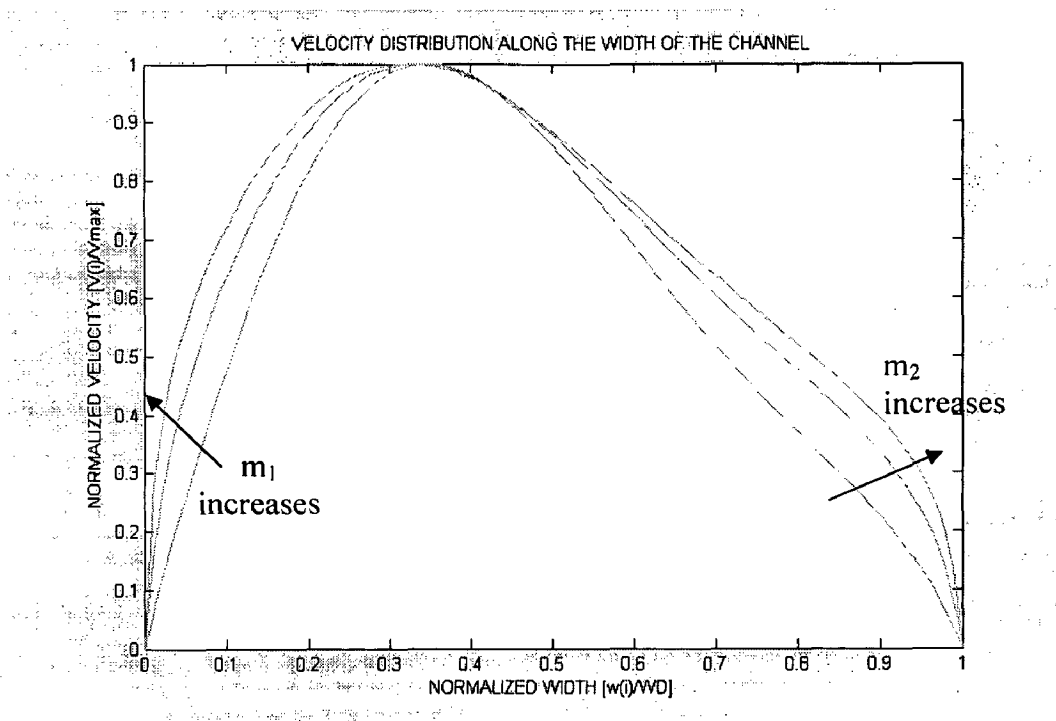
Fig. 5.4 Effect of m_1 and m_2 on horizontal profiles

The effects of parameters m_1 and m_2 are plotted above. It can be seen that as m_1 and m_2 increases, the profile will be more curved and the variation near the wall will be more steeper. The larger values of m_1 and m_2 indicates more smoother walls. As the wall smoothness increases, this will reduces friction between the wall and the water which will cause higher velocities near the wall. The velocity variation nearer to the wall will exhibit a logarithmic variation.The velocity of layer nearer to the wall will always be zero.

Turbulence of the flow is another factor which affects the velocity profiles. Turbulence will affect both horizontal and vertical profile and therefore should be taken into account in both. Turbulence is a function of Reynolds number. Turbulence of flow is increased by the Reynolds number and its effect in horizontal profile is modeled by k_1 and k_2, the variation is same as that of m_1 and m_2. As the whole horizontal profile is generated by the summation of these three equations, each parameters will slightly affect the whole profile and this should be taken care while modeling the 3-D profile by choosing appropriate parameters.

5.3 ANALYSIS OF VERTICAL PROFILE

The horizontal profile can be expressed by a general mathematical equation given below:

$$V_v(y) = \frac{1}{K_V} \cdot \log[m_3 \cdot k_3 \cdot d(y) + 1] + d(y) \cdot \left[1 - p_1 \cdot d(y)^{p_2}\right] \qquad (5.4)$$

$V_v(y)$ = Velocity magnitude at the point y;

$d(y)$ = Normalized distance of the channel at the point y(from the bed);

$m_3 \& k_3$ = constants which accounts for the roughness of the bed and turbulence;

$p_1 \& p_2$ = constants which accounts for the air friction at the free surface and the maximum velocity point;

K_V = Von-Karman Constant
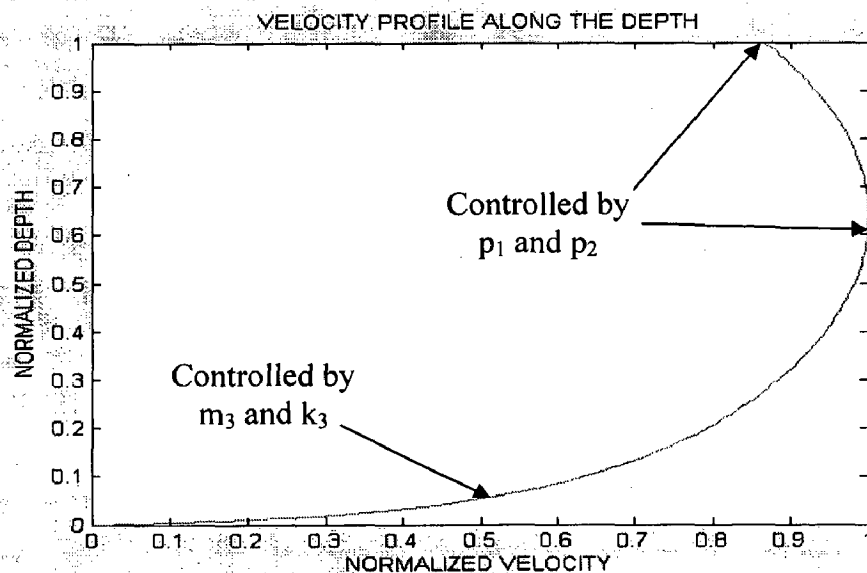
Fig 5.5 Vertical profile developed and controlling parameters

The proposed mathematical model for the vertical profile can be viewed as the sum of two equations. The velocity distribution in the inner zone of a boundary layer can be described by the log law, and that of the outer zone can be described by the parabolic law. This can be termed as binary law [12]. The binary law i.e., the combination of the log law for the inner region and parabolic law for the outer region - is generalized to include cases of flow with maximum velocity occurring below the free surface. The four control parameters of the equation can be varied and different vertical profiles can be obtained for varieties of channel geometries. The effect of these parameters on the vertical profile is separately discussed in the coming sections. Figure 5.5 shows a vertical profile developed from the model for normalized width and the parameters which affects each part of the vertical profile.

5.3.1 EFFECT OF AIR FRICTION

In an open channel it is observed that the maximum velocity does not occur at the free surface. Instead ideally the maximum velocity component will occur at some depth from the free surface. This dip in the surface velocity is due to the air friction between the surface water layer and the atmospheric air. The maximum velocity component in an ideal case will occur at a depth of 40% from the free surface. But this maximum velocity point may vary according to the channel geometries. The major factors which directly affect the surface velocity are air friction and slope of the channel.

The proposed mathematical model is capable of accounting this surface velocity dip and maximum velocity point. The second part of the equation 5.4, the parabolic profile at the outer zone accounts for this air friction effect.

$$d(y) \cdot \left| 1 - p_1 \cdot d(y)^{p_2} \right|$$

The parameters p_1 and p_2 affects both surface velocity and maximum velocity point. Closer analysis revealed that surface velocity is reduced by increase in the value of p_1. It can be observed that the maximum velocity point will be shifted towards bottom as the ratio of p_1/p_2 increases. Variation in vertical profile with different values of p_1 and p_2 is plotted below in Fig. 5.6.

42
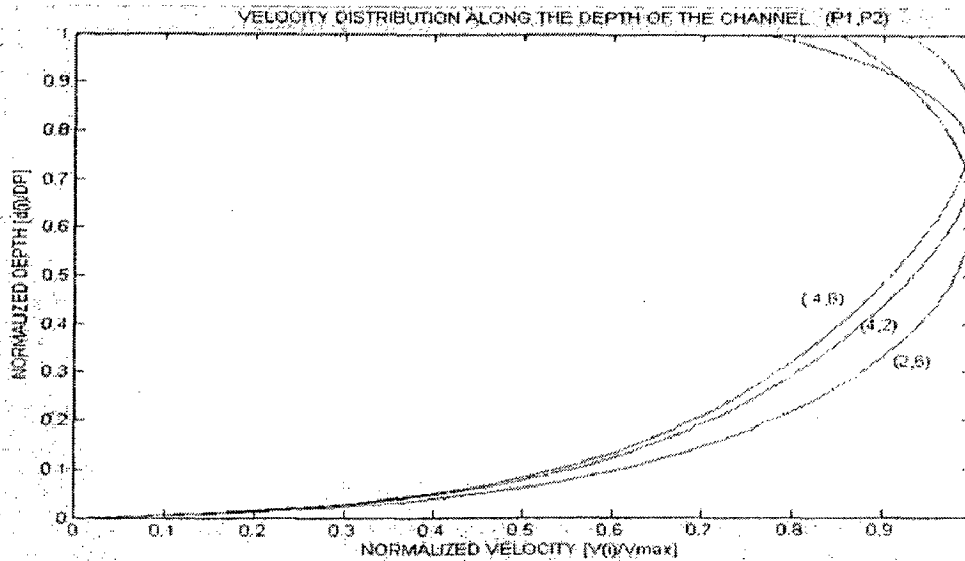
Fig. 5.6 Vertical profile developed for different values of p_1 and p_2

5.3.2 EFFECT OF BED SURFACE ROUGNESS AND TURBULENCE

The vertical velocity distribution in the inner region of the channel is expressed by the logarithmic profile given by: $\dfrac{1}{K_V} \cdot \log[m_3 \cdot k_3 \cdot d(y)+1]$. This logarithmic profile at the bottom is affected by the roughness of the bed and this effect can be modeled by varying the friction parameter m_3 in the equation [13]. The variation in the profile for different values of m_3 is given in figure 5.7
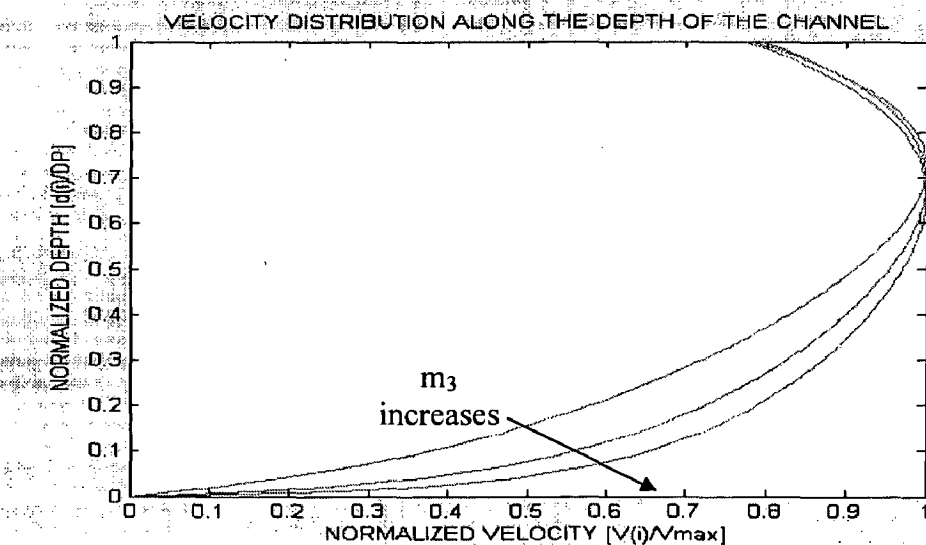
Fig. 5.7 Effect of m_3 on vertical profile

43

As the value of friction coefficient m_3 increases the profile becomes more curvy in nature which shows large flow velocities near the walls. A large value of m_3 indicates a smooth lined bed and the velocity drop near the bed will be very steeper. The turbulence effect can be modeled by the parameter k_3 which shows a similar effect as m_3. As the whole vertical profile is generated by the summation of both logarithmic as well as parabolic profile, each parameter will slightly affect the whole profile and this should be taken care while modeling the 3-D profile by choosing appropriate parameters.

5.4 MODELING OF THE 3-D PROFILE

Modeling of the 3-D profile is done by the combination of both the horizontal and vertical profile equations. A Matlab code is develop which combines these two mathematical models to produce a 3-D dimensional normalized velocity plots with width, height and velocity along x, y and z- axis respectively. Velocity profiles for different values of parameters can be developed. Provision is made in the software to produce a mathematical model with control parameters of user's choice. The code developed is also capable of obtaining the discharge of developed profile by surface integration. Velocity contours can also be produced from generated profiles. The following figures show some of the horizontal and vertical profiles and 3-D profiles generated from that.

Modeling Parameters (Single Peak profile): $(\alpha, \beta) = (2,5)$; $(m_1, m_2, k_1, k_2) = (5, 5, 15,15)$;

$(m_3, k_3) = (5, 15)$; $(p_1, p_2) = (3, 4)$

(a) Horizontal Profile   (b) Vertical Profile

44
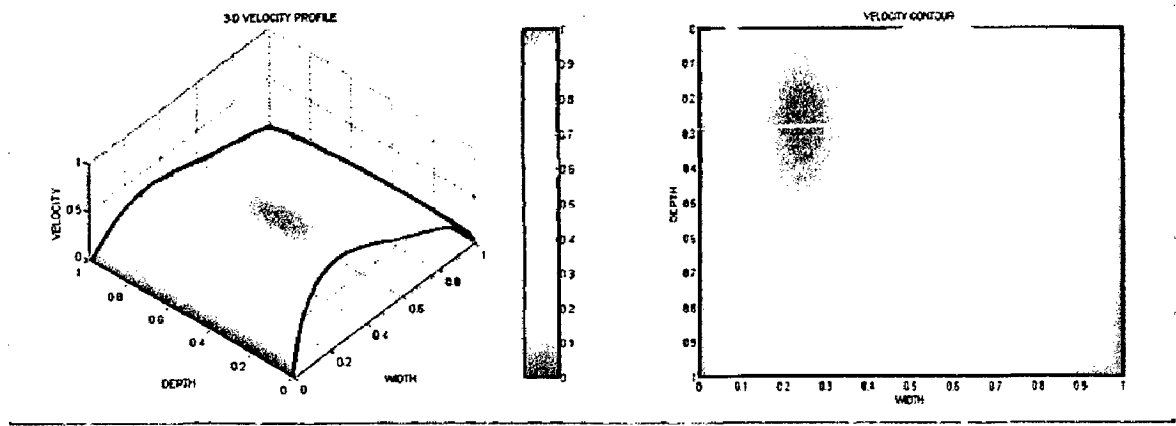
(c) 3-D Velocity Profile   (d) Velocity Contour

Fig. 5.8: 3-D Profile formation in Matlab (Single Peak profile)

Modeling Parameters (Double Peak profile): $(\alpha, \beta)=(6,5)$; $(m_1, m_2, k_1, k_2)=(5, 5, 15,15)$;

$(m_3, k_3)=(5, 15)$; $(p_1, p_2)=(6, 3)$
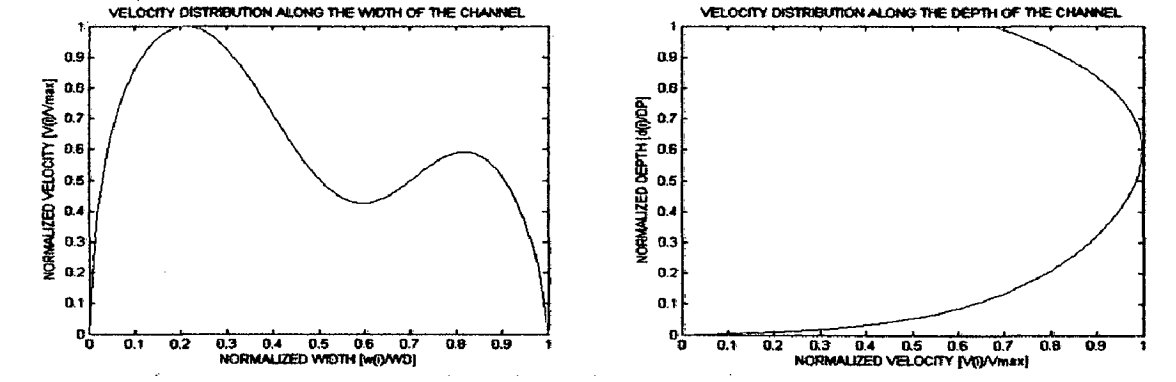
(a) Horizontal Profile   (b) Vertical Profile
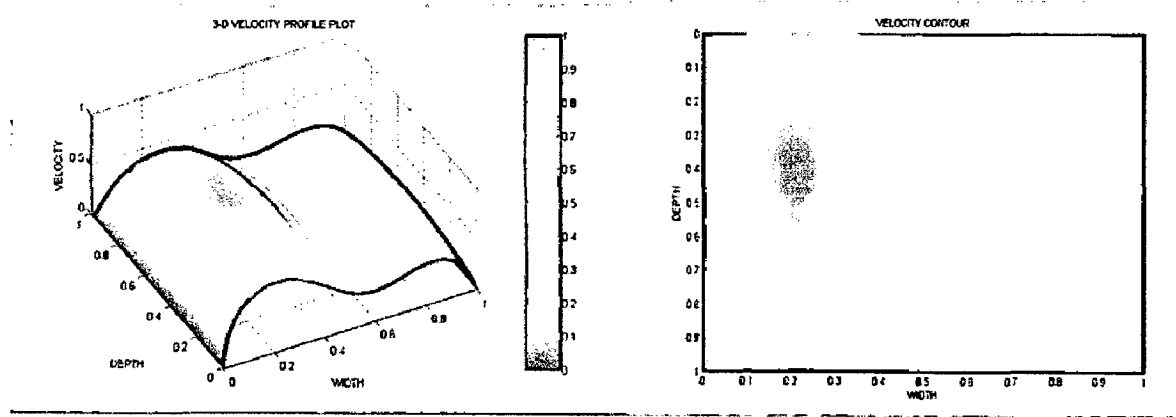
(c) 3-D Velocity Profile   (d) Velocity Contour

Fig. 5.9: 3-D Profile formation in Matlab (Double Peak profile)

45

CHAPTER 6

PROFILE SIMULATION

Accurate discharge measurement requires an open channel with simple straight rectangular geometry and lined walls. But these ideal conditions may not be always present in real situations especially in small hydro power plants. If a measurement has to be done in undesirable conditions, this may lead to large measurement errors. The irregularity of the open channel is one of the major factor which adds to the measurement uncertainty. The velocity profiles developed in various geometries of open channel is found to be very complex, that the accurate measurement of these profiles is a tedious and challenging job [21].

In this work an effort has been made to investigate the velocity profiles of various open channel geometries and to develop a mathematical model for these profiles. CFD analysis is used for simulating the flow [14]. The proposed mathematical model discussed in the previous chapter is used to replicate the simulated profile by the choice of appropriate values for the control parameters. Thus the profiles developed in various open channel geometries are quantified using the mathematical model. Analysis is done for as many as six different geometries and the results are discussed in this chapter. All the geometries are modeled with similar operating and boundary conditions, same as that used for the validation site. Therefore these conditions are not repetitively mentioned here, but are referred to section 4.3, where parameters of CFD modeling are discussed in detail

6.1   RECTANGULAR OPEN CHANNEL (PROFILE – P1)

An open channel rectangular geometry with lined walls and very small slope is developed and the meshing is done in Gambit. The details of site modeling- meshing schemes used and mesh node spacing is similar as that for the site model discussed in validation process, the details of which is given in section 4.3.2. The developed model is straight enough to produce a fully developed flow. In CFD modeling, unlike the real situation the conditions are set to be ideal to produce a steady flow.

Depth – 2m, Width – 4m, Length – 15m, Slope – 0.2m (in 15 m)
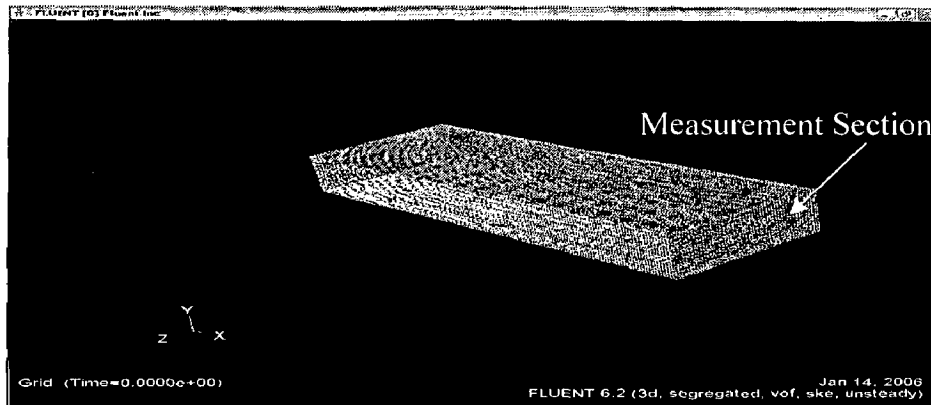
Fig. 6.1 Rectangular site modeled in Gambit

6.1.1 PROFILE SIMULATION IN CFD

Open channel modeling is done by using multi phase VOF model. The boundary types specified are PRESSURE_INLET for free surface and inlet, WALL for side walls and bed, PRESSURE_OUTLET for outlet. The boundary parameters are same as that discussed for validation site discussed in detail in section 4.3.3 except for the average velocity magnitude in inlet, which is given as 0.75 m/s. After the parameters are set, the solver is initialized with inlet conditions and the iteration is done. 500 iterations where given inside which the solution has converged. The simulation result of the flow in the channel is shown in fig. 6.2
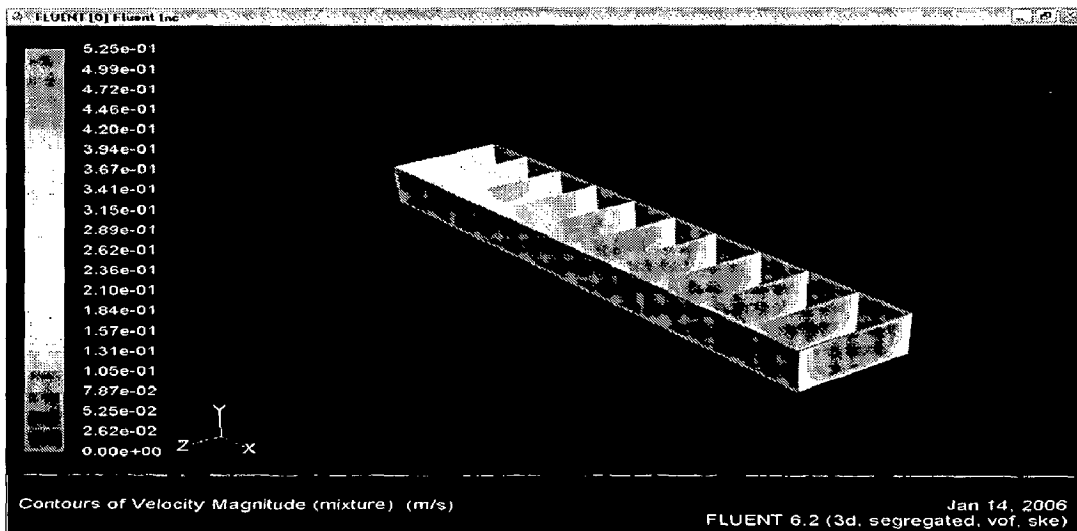
Fig 6.2 Development of flow in a rectangular channel (Simulated in CFD)

47
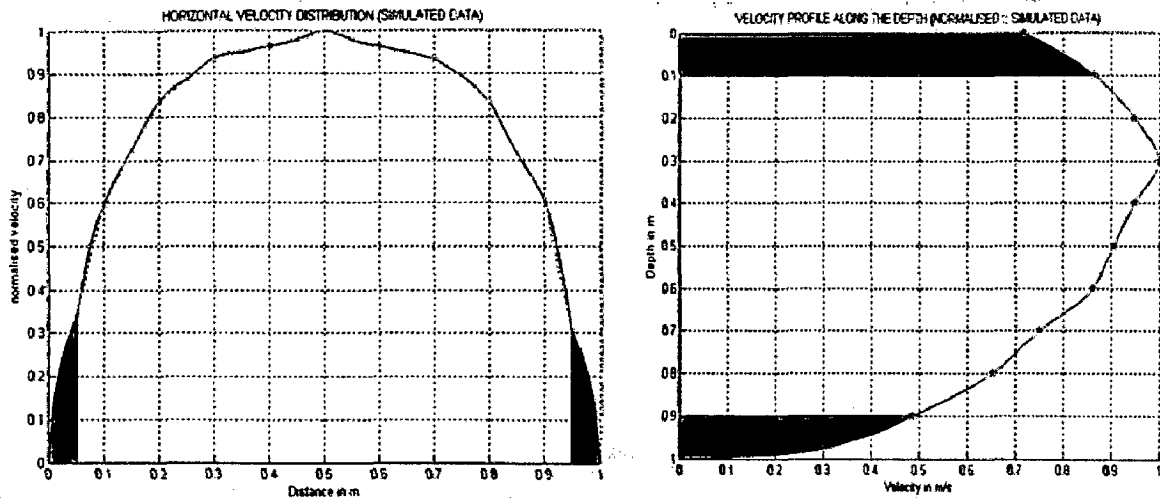
Fig. 6.3 (a) Horizontal and (b) Vertical velocity distribution for CFD simulated data

6.1.2   MATHEMATICAL MODELING OF THE PROFILE

The above simulated profile can be quantified by using the mathematical model. Mathematical model is developed by the comparison of the average horizontal and vertical velocity distribution (in figure 6.3) with profiles created by horizontal and vertical profile equations (discussed in 5.1 and 5.2). The control parameters of these equations are selected in such a way that almost similar profiles are developed.
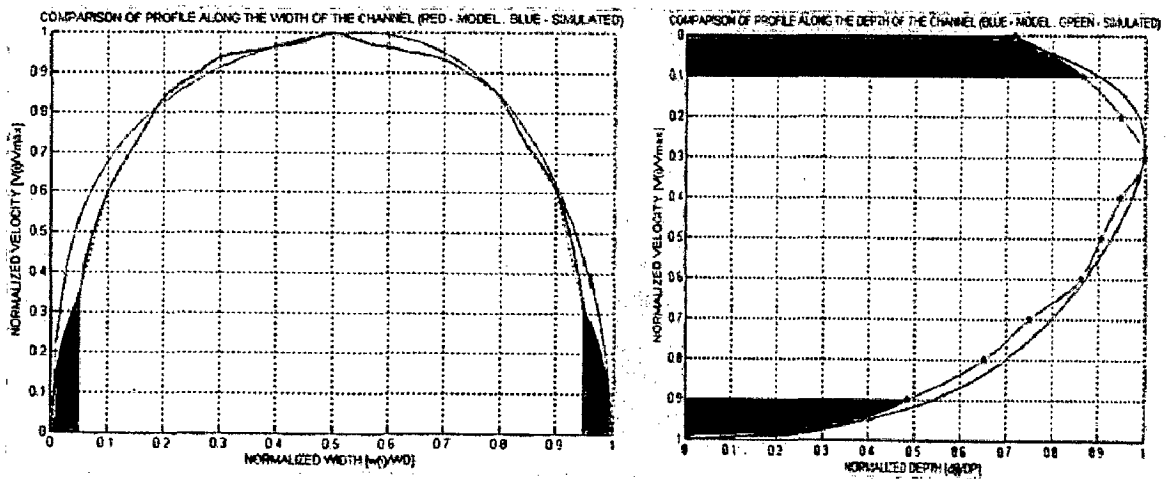
Fig 6.4 Comparison of (a) Horizontal & (b) Vertical profiles (Simulated v/s Model- P1)

These horizontal and vertical profiles developed from mathematical model are used to create the 3-D velocity profile. The parameters used for modeling are given in table 6.1.

48

CONTROL PARAMETERS FOR HORIZONTAL PROFILE		
BETA FUNCTION (SKEWNESS) PARAMETERS	$\alpha = 3$	$\beta = 3$
FRICTION PARAMETERS (FOR SIDE WALLS)	$m_1 = 5$ (LEFT WALL)	$m_2 = 5$ (RIGHT WALL)
TURBULENCE PARAMETERS	$k_1 = 15$	$k_2 = 30$
CONTROL PARAMETERS FOR VERTICAL PROFILE		
AIR FRICTION PARAMETERS	$P_1 = 5$	$P_2 = 7$
FRICTION PARAMETER (FOR BED)	$m_3 = 5$	
TURBULENCE PARAMETER	$k_3 = 30$	

Table 6.1 Mathematical model parameters used for modeling P1

6.1.3   RESULTS AND DISCUSSION

The mathematical model developed (both horizontal and vertical) is combined to obtain the 3-D velocity profile and the results are shown in the figure 6.5

(a) Simulated 3-D profile   (b) 3-D profile from mathematical model
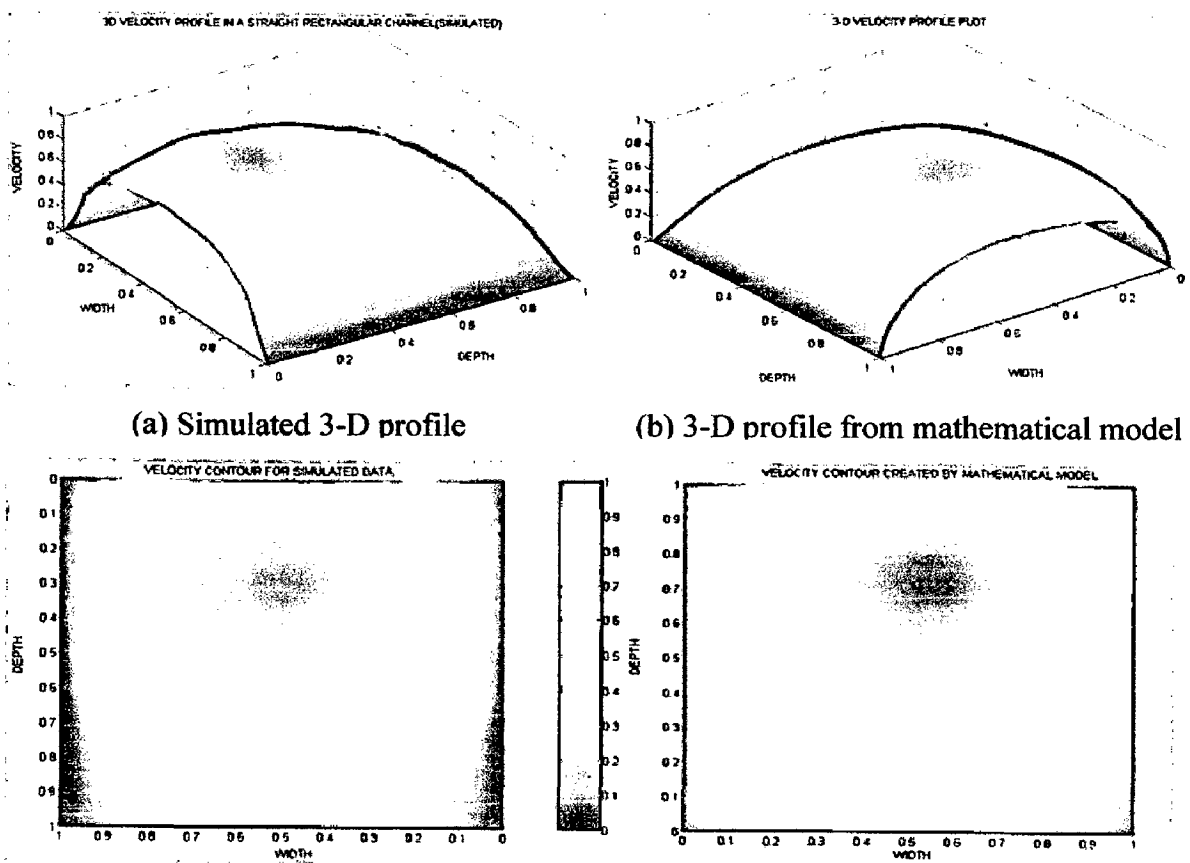
Fig 6.5 Velocity contour for (c) Simulated data   (d) Mathematical model

- The mathematical model and the simulated profile is developed for normalized width, depth and velocity. Turbulence ratio $k_1/k_2 = 0.5$

- The mathematical model developed with the above mentioned values for the 10 control parameters showed excellent coincidence with simulated profiles. Thus the generated profiles is being quantified using the mathematical model and this is can be further used for uncertainty analysis

The discharge of the two profiles is also calculated by the integration of the surface produced. Simulated profile $- 0.603276 \ m^3/s$

Mathematical model $- 0.607356 \ m^3/s$

6.2 RECTANGULAR OPEN CHANNEL WITH MEDIUM SLOPE (PROFILE P2)

Slope of the channel is one of the major factors that affect the velocity profiles. Here the effect of slope on open channel is studied by simulating the flow in regular rectangular geometries with various slopes. A rectangular open channel with medium slope (0.5 in 15 m) is modeled in Gambit. The details of site modeling- meshing schemes used and mesh node spacing is similar as that for the site model discussed in validation process, the details of which is given in section 4.3.2.

Site specifications:

Depth – 2m, Width – 4m, Length – 15m, Slope – 0.5m (in 15 m)

Fig. 6.6 Rectangular geometry with medium slope

6.2.1   PROFILE SIMULATION IN CFD

The operating and boundary conditions are same as that for the rectangular open channel except for the free surface level and bottom level in the outlet. Free surface level -1.5m and the bottom level - -0.5 is set in the outlet (to account for the slope of the channel). After the parameters are set, the solver is initialized with inlet conditions and the iteration is done. 500 iterations where given inside which the solution has converged. The simulation result of the flow in the channel is shown in fig. 6.7
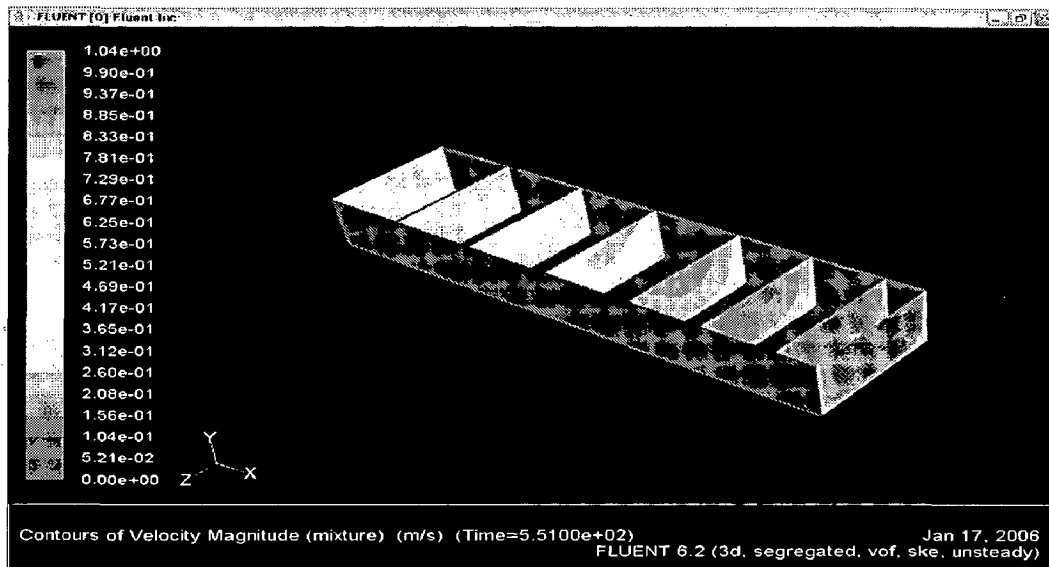
Fig 6.7 Development of flow in a rectangular channel with medium slope
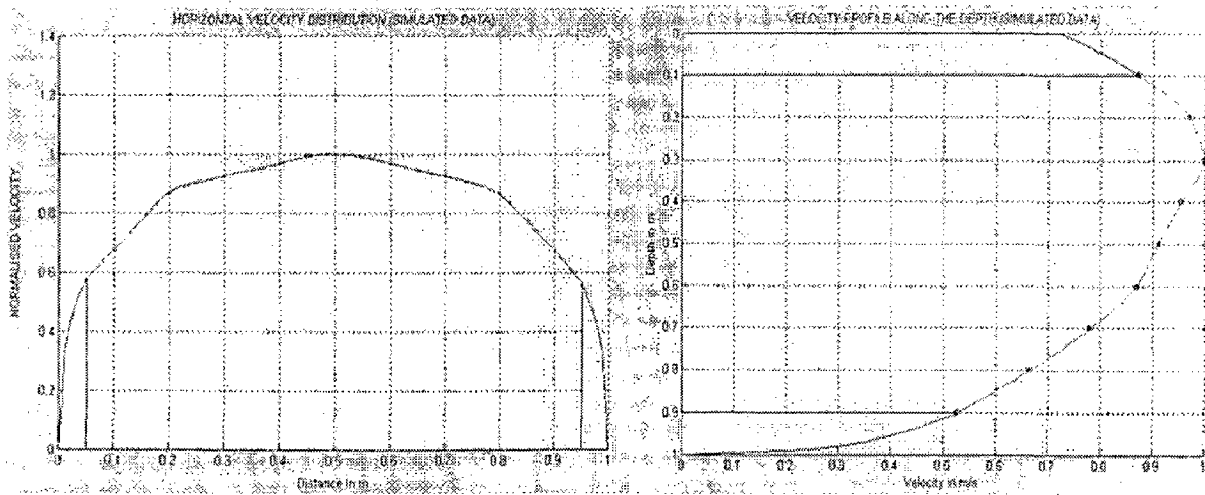
Fig. 6.8 (a) Horizontal and (b) Vertical velocity profile for P2 (Simulated data)

51

The quantification of the simulated profile is done using the mathematical model by the comparison of horizontal and vertical profiles. Appropriate values for control parameters are selected for modeling the flow and are given in the table 6.2. The profiles developed from mathematical model is compared with simulated profiles (figure 6.9)

Fig 6.9 Comparison of (a) Horizontal & (b) Vertical profiles (Simulated v/s Model P2)

CONTROL PARAMETERS FOR HORIZONTAL PROFILE		
BETA FUNCTION (SKEWNESS) PARAMETERS	$\alpha = 2$	$\beta = 2$
FRICTION PARAMETERS (FOR SIDE WALLS)	$m_1 = 5$ (LEFT WALL)	$m_2 = 5$ (RIGHT WALL)
TURBULENCE PARAMETERS	$k_1 = 15$	$k_2 = 45$
CONTROL PARAMETERS FOR VERTICAL PROFILE		
AIR FRICTION PARAMETERS	$P_1 = 5$	$P_2 = 5$
FRICTION PARAMETER (FOR BED)	$m_3 = 5$	
TURBULENCE PARAMETER	$k_3 = 15$	

Table 6.2 Mathematical model parameters used for modeling P2

These horizontal and vertical profiles developed from mathematical model are used to create the 3-D velocity profile.

The mathematical model developed (both horizontal and vertical) is combined to obtain the 3-D velocity profile and the results are shown in the figure 6.10
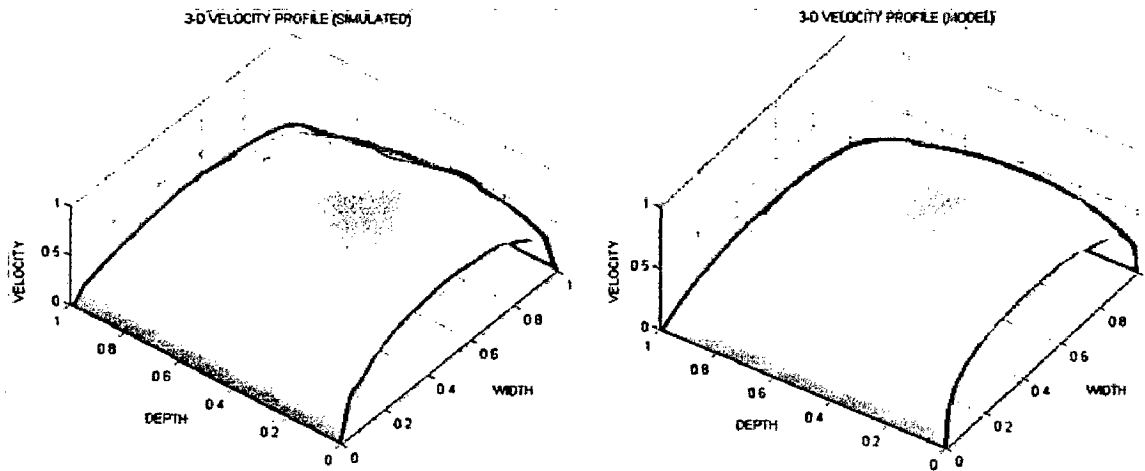
(a) Simulated 3-D profile   (b) 3-D profile from mathematical model

Fig 6.10 Velocity contour for (c) Simulated data   (d) Mathematical model

- The mathematical model developed with the above mentioned values for the 10 control parameters showed excellent coincidence with simulated profiles.

- As the slope increased the horizontal profile became more flat and is reflected in the model by the smaller value of α & β (2,2) compared to earlier case(P1).

- The ratio of k1/k2 decreased from 0.5 (in earlier case) to 0.33 which shows a slight increase in the turbulence of the channel due to the slope.

- Discharge Values: Simulated profile   – 0.654752 m³/s

    Mathematical model – 0.658510 m³/s

6.3 RECTANGULAR OPEN CHANNEL WITH LARGE SLOPE (PROFILE P3)

The effect of slope on the velocity profile can be further analyzed by simulating the flow through a rectangular channel with large slope. A rectangular channel with slope 1.5m in 15 m is modeled and the flow is simulated. The channel geometry is given in figure 6.11.

Site specifications:

Depth – 2m, Width – 4m, Length – 15m, Slope – 1.5m (in 15 m)
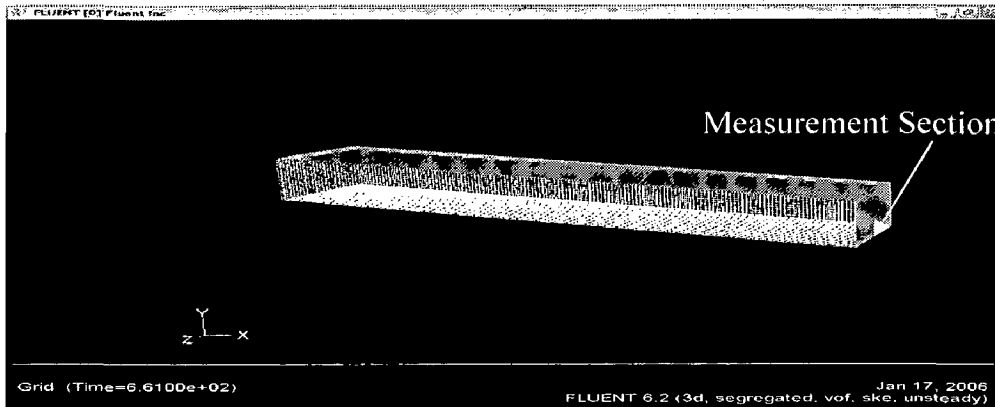
Fig. 6.11 Rectangular channel with large slope

6.2.1 PROFILE SIMULATION IN CFD

The operating and boundary conditions are same as that for the rectangular open channel. Free surface level is 0.5m and the bottom level is -1.5 in the outlet. After the parameters are set, the solver is initialized with inlet conditions and the 500 iteration is done. The simulation result of the flow in the channel is shown in fig. 6.12

Fig 6.12 Development of flow in rectangular channel with large slope

Fig. 6.13 (a) Horizontal and (b) Vertical velocity profile for P3 (Simulated data)

6.3.2 MATHEMATICAL MODELING OF THE PROFILE

Appropriate values for control parameters are selected for modeling the flow and are given in the table 6.3. The profiles developed from mathematical model is compared with simulated profiles (figure 6.14)

Fig 6.14 Comparison of (a) Horizontal & (b) Vertical profiles (Simulated v/s Model- P3)

CONTROL PARAMETERS FOR HORIZONTAL PROFILE		
BETA FUNCTION (SKEWNESS) PARAMETERS	$\alpha = 1$	$\beta = 1$
FRICTION PARAMETERS (FOR SIDE WALLS)	$m_1 = 5$ (LEFT WALL)	$m_2 = 5$ (RIGHT WALL)
TURBULENCE PARAMETERS	$k_1 = 30$	$k_2 = 150$

CONTROL PARAMETERS FOR VERTICAL PROFILE		
AIR FRICTION PARAMETERS	$P_1 = 14$	$P_2 = 2$
FRICTION PARAMETER (FOR BED)	$m_3 = 5$	
TURBULENCE PARAMETER	$k_3 = 300$	

Table 6.3 Mathematical model parameters used for modeling P3

These horizontal and vertical profiles developed from mathematical model are used to create the 3-D velocity profile.

6.3.3 RESULTS AND DISCUSSION

The mathematical model developed (both horizontal and vertical) is combined to obtain the 3-D velocity profile and the results are shown in the figure 6.15

(a) Simulated 3-D profile   (b) 3-D profile from mathematical model

Fig 6.15 Velocity contour for (c) Simulated data   (d) Mathematical model

- The mathematical model developed showed excellent coincidence with simulated profile

- As the slope increased further the horizontal profile became more flat & is reflected in the model by the smaller value of α & β (1,1) compared to the rectangular channel with small & medium slope

- The ratio of k_1/k_2 decreased from 0.5 (in earlier case) to 0.2 which shows an increase in the turbulence of the channel due to the slope

- The surface velocity is reduced drastically (reflected in higher value of p1=14) & the maximum velocity point is shifted towards bottom (reflected in high ratio of p1/p2 =7)

- Discharge Values: Simulated profile   – 0.677592 m^3/s

                     Mathematical model – 0.675875 m^3/s

6.4 RECTANGULAR OPEN CHANNEL WITH 90° BEND (PROFILE B1)

Bend in the channel is one of the major factors which affect the velocity profile. Here the variation in the velocity profile caused due to a 90° bend is studied by modeling the geometry and simulating the flow. A plane immediately after the bend is selected as the measuring section and velocity profile developed in the measuring section is analyzed.

Site specifications:

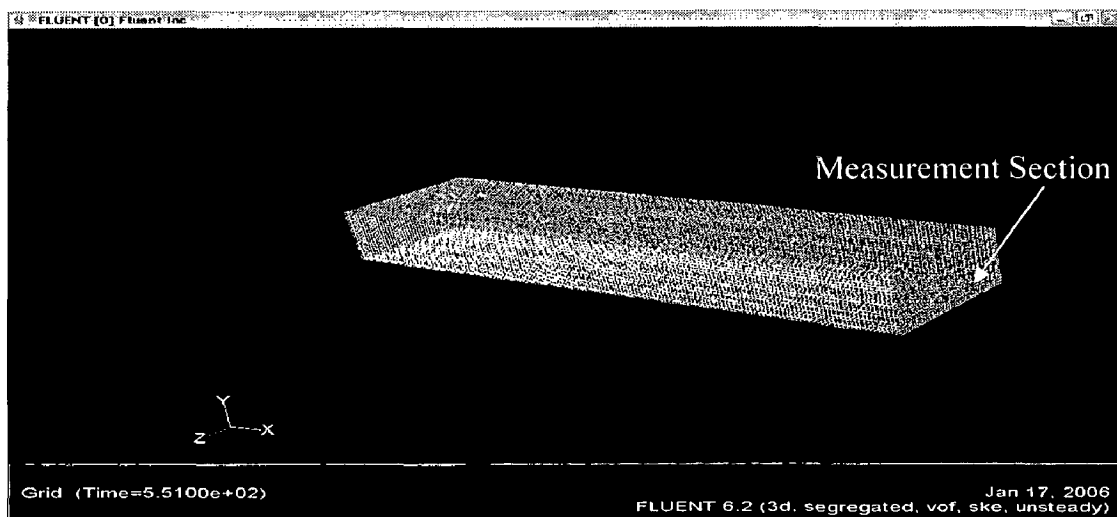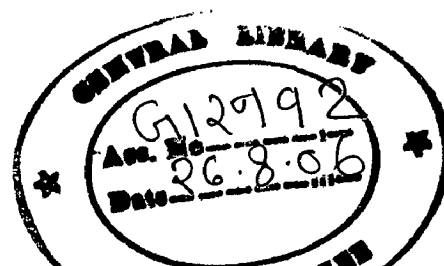Depth – 2m, Width – 4m, Length – 15m, Slope – 0.2m (in 15 m), Bend 90°

Fig. 6.16 Rectangular channel with 90° bend

6.4.1 PROFILE SIMULATION IN CFD

The operating and boundary conditions are same as that for the rectangular open channel. Here the flow is set to x-direction in the inlet and z-direction in the outlet (to account for 90° bend). After the parameters are set, the solver is initialized with inlet conditions and the 500 iteration is done. The simulation result of the flow is shown in fig. 6.17


Fig 6.17 Development of flow in rectangular channel with 90° bend
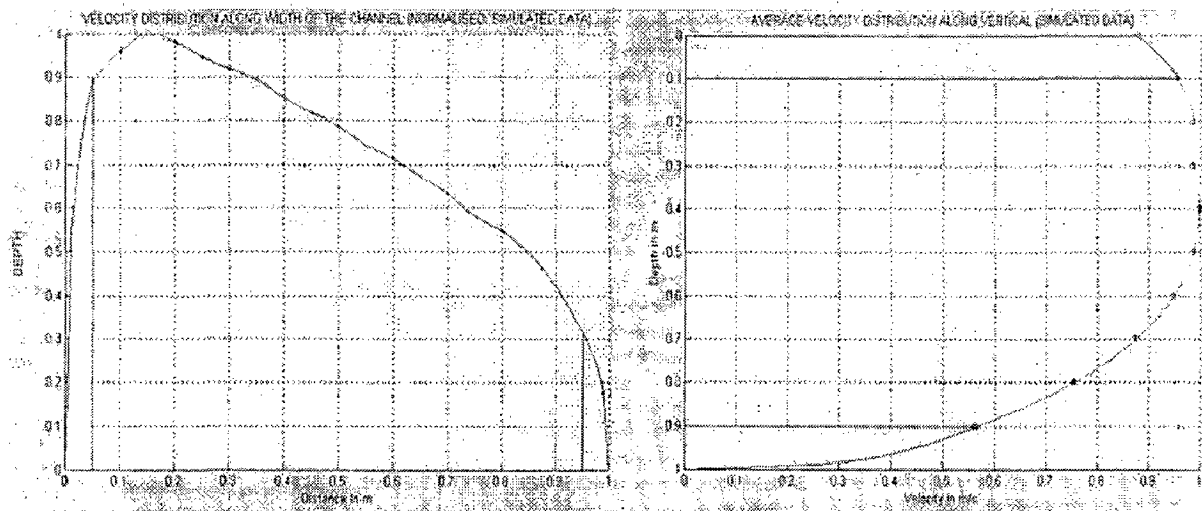
Fig. 6.18 (a) Horizontal and (b) Vertical velocity profile for P3 (Simulated data)

6.4.2 MATHEMATICAL MODELING OF THE PROFILE

Appropriate values for control parameters are selected for modeling the flow and are given in the table 6.4. The profiles developed from mathematical model is compared with simulated profiles (figure 6.19)
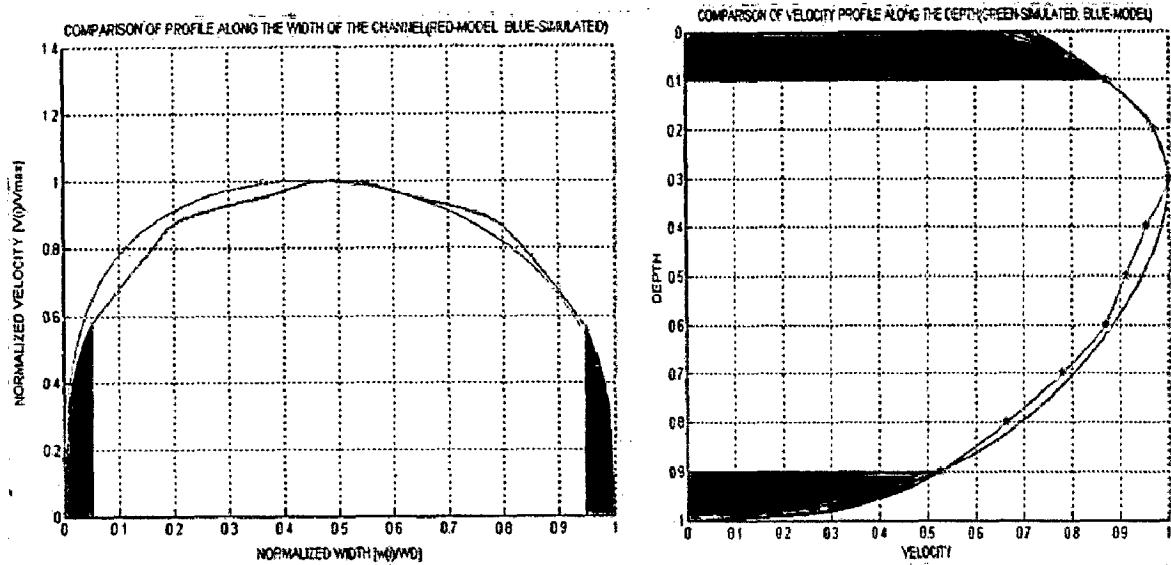
58

Fig 6.19 Comparison of (a) Horizontal & (b) Vertical profiles (Simulated v/s Model- B1)

CONTROL PARAMETERS FOR HORIZONTAL PROFILE		
BETA FUNCTION (SKEWNESS) PARAMETERS	$\alpha = 1$	$\beta = 4$
FRICTION PARAMETERS (FOR SIDE WALLS)	$m_1 = 5$ (LEFT WALL)	$m_2 = 5$ (RIGHT WALL)
TURBULENCE PARAMETERS	$k_1 = 15$	$k_2 = 60$
CONTROL PARAMETERS FOR VERTICAL PROFILE		
AIR FRICTION PARAMETERS	$P_1 = 4$	$P_2 = 2$
FRICTION PARAMETER (FOR BED)	$m_3 = 5$	
TURBULENCE PARAMETER	$k_3 = 30$	

Table 6.4 Mathematical model parameters used for modeling B1

These horizontal and vertical profiles developed from mathematical model are used to create the 3-D velocity profile.

6.4.3 RESULTS AND DISCUSSION

The average horizontal velocity profile is skewed towards the left side of the channel and is explainable due to the 90° bend towards the left side of the channel. The mathematical model developed (both horizontal and vertical) is combined to obtain the 3-D velocity profile and the results are shown in the figure 6.20. Discharge in the channel can be obtained by the surface integration of the generated profile surfaces.
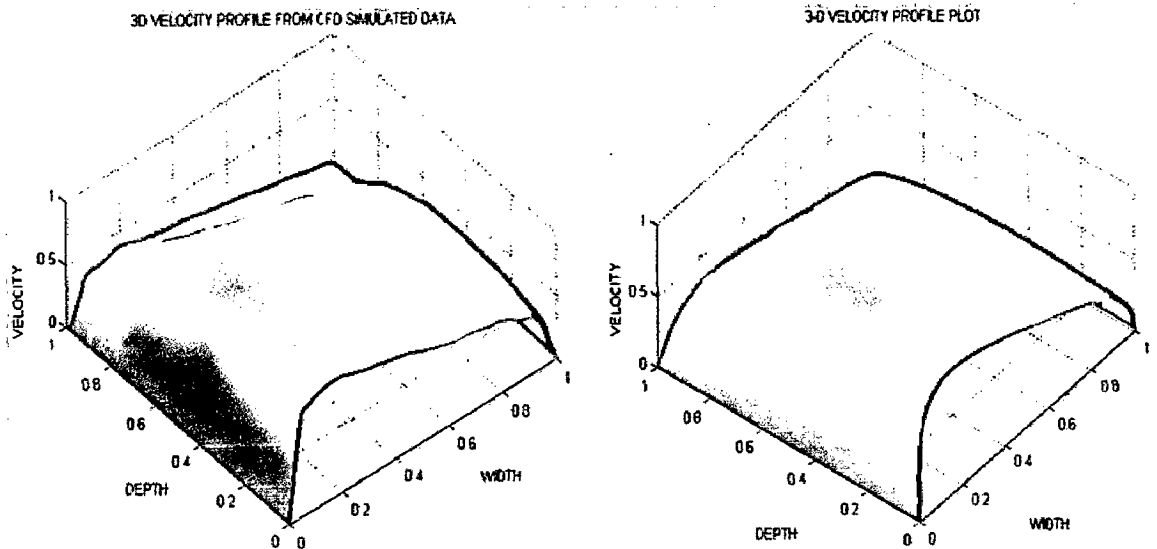
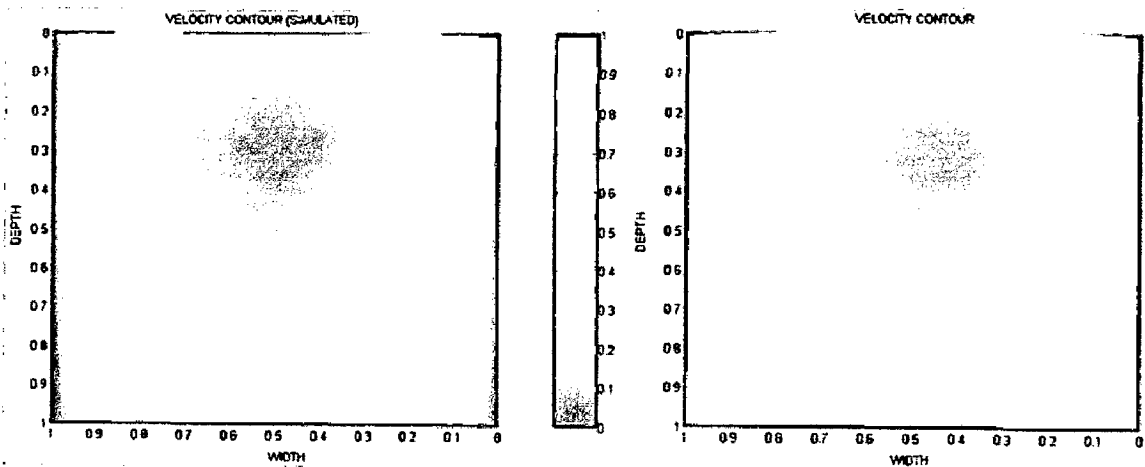(a) Simulated 3-D profile   (b) 3-D profile from mathematical model
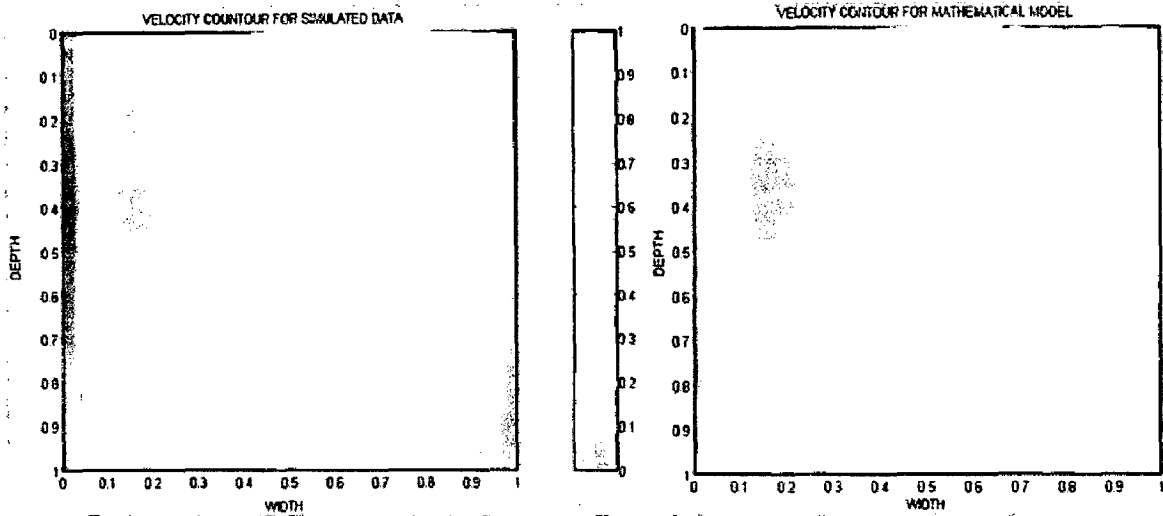
Fig 6.20 Velocity contour for (c) Simulated data   (d) Mathematical model

- The mathematical model developed with the above mentioned values for the 10 control parameters showed excellent coincidence with simulated profiles

- The skewness in the horizontal profile is due to the bend in the channel and is reflected in the difference between values of α (1) and β (4).

- The ratio of k_1/k_2 is reduced to 0.25 which shows an increase in the turbulence of the channel due to bend compared to profile P1

- Discharge Values: Simulated profile   – 0.62140 m^3/s

  Mathematical model – 0.62021 m^3/s

6.5 RECTANGULAR OPEN CHANNEL WITH DIVERGENCE (PROFILE D1)

Velocity profile will be largely affected by the deviation of channel from the normal rectangular geometry. In this section the effect of divergence on velocity profile is analyzed. A rectangular open channel with a divergence is modeled (figure 6.21) and the flow is simulated by CFD analysis.

Site specifications:

Depth – 2m, Width – 3m (before divergence) & 6m (after divergence), Divergence length- 4m, Angle- 20.56°, Length – 15m, Slope – 0.2m (in 15 m)
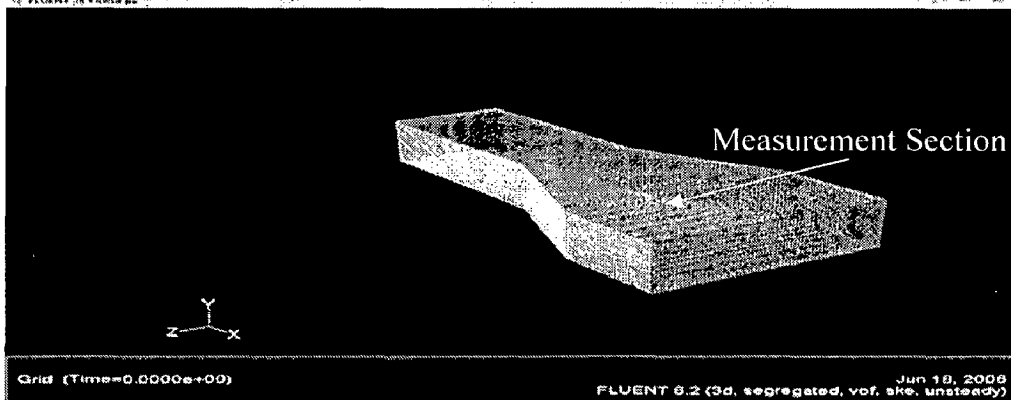
Fig. 6.21 Rectangular channel with divergence

6.5.1   PROFILE SIMULATION IN CFD

The operating and boundary conditions are same as that for the rectangular open channel. Free surface level is 1.8 m and the bottom level is -0.2 in the outlet. After the parameters are set, the solver is initialized with inlet conditions and the 500 iteration is done. The simulation result of the flow is shown in fig. 6.22
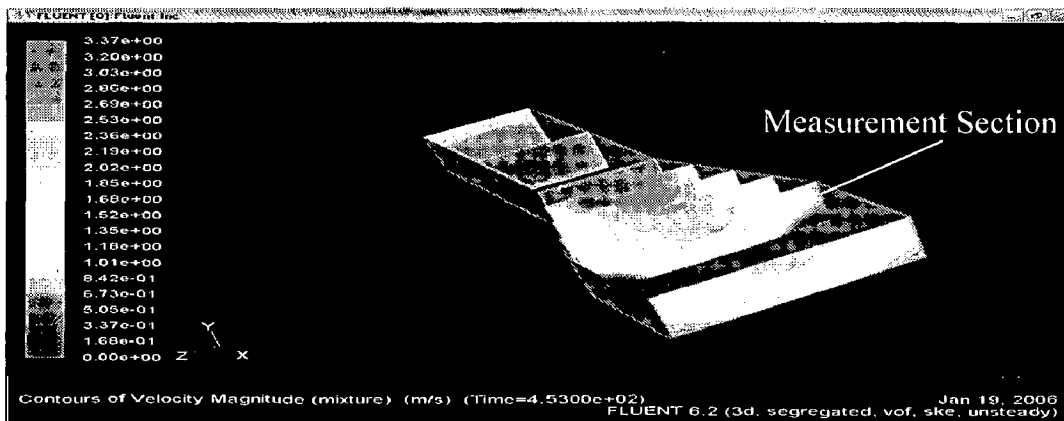
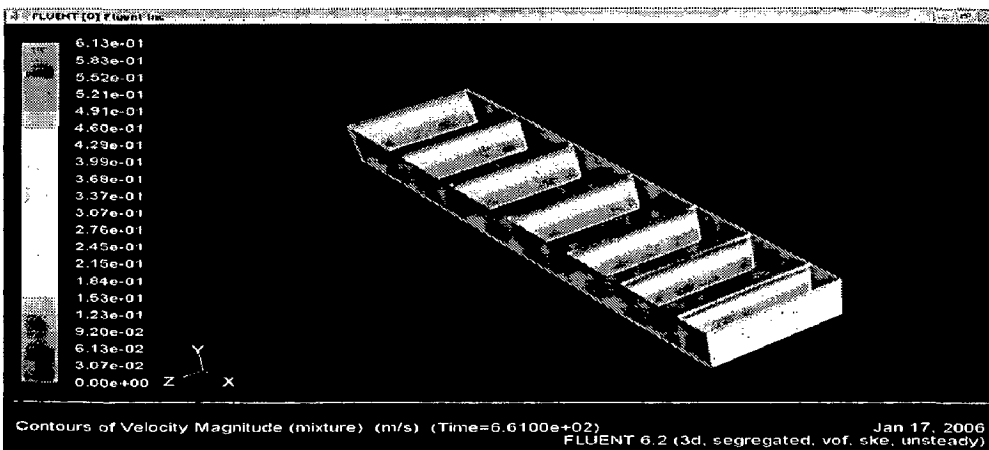Fig. 6.22 Development of flow in rectangular channel with divergence
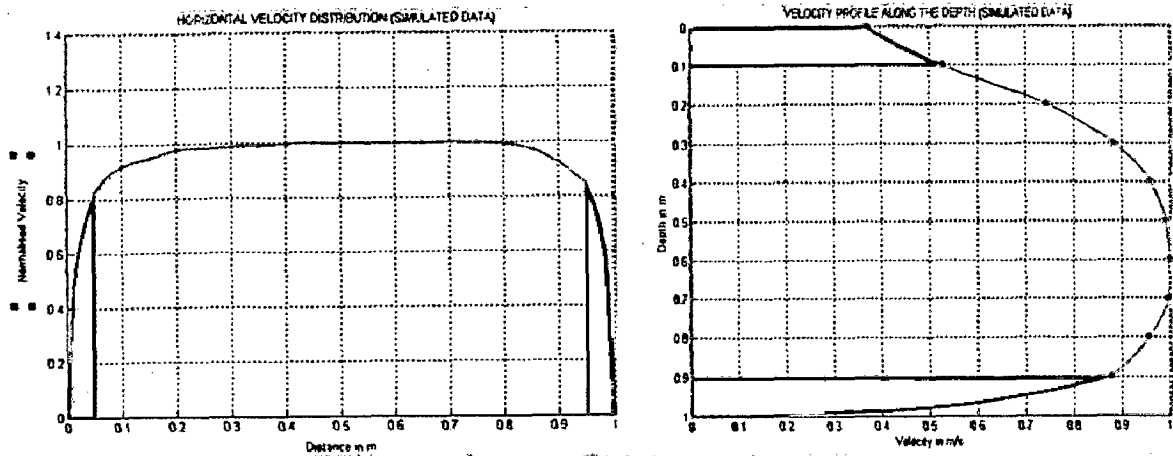
61
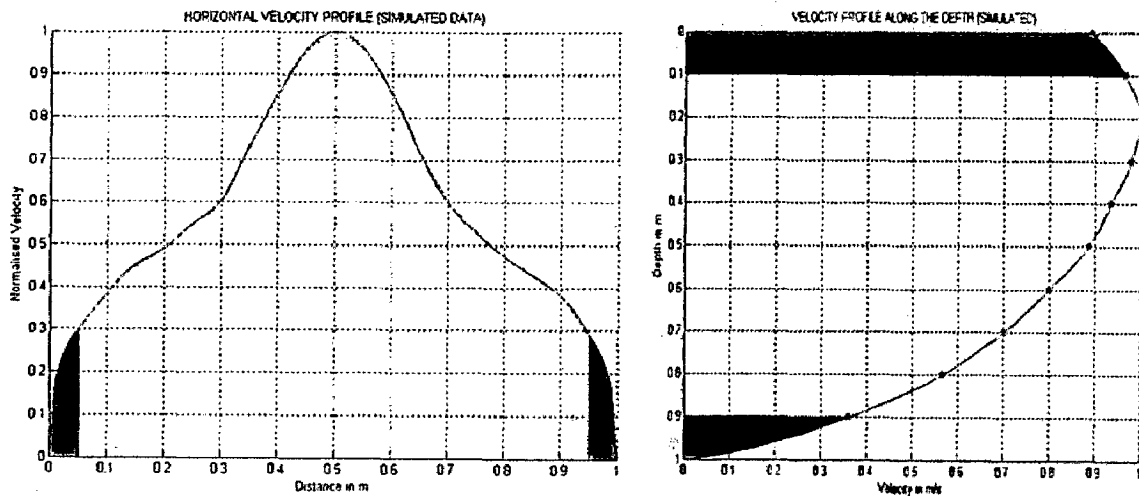
Fig. 6.23 (a) Horizontal and (b) Vertical velocity profile for D1 (Simulated data)

6.5.2 MATHEMATICAL MODELING OF THE PROFILE

Appropriate values for control parameters are selected for modeling the flow and are given in the table 6.5. The profiles developed from mathematical model is compared with simulated profiles (figure 6.24)
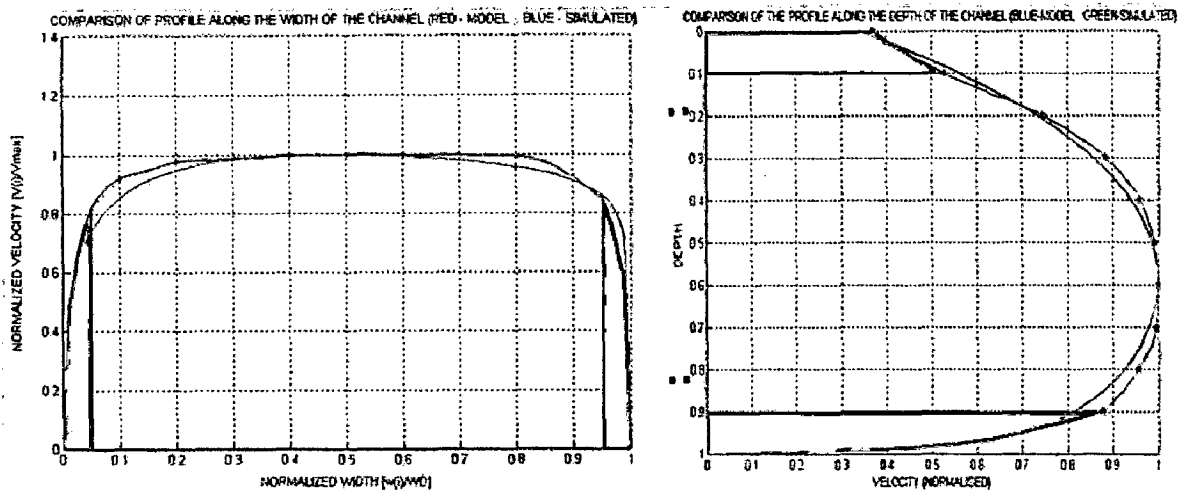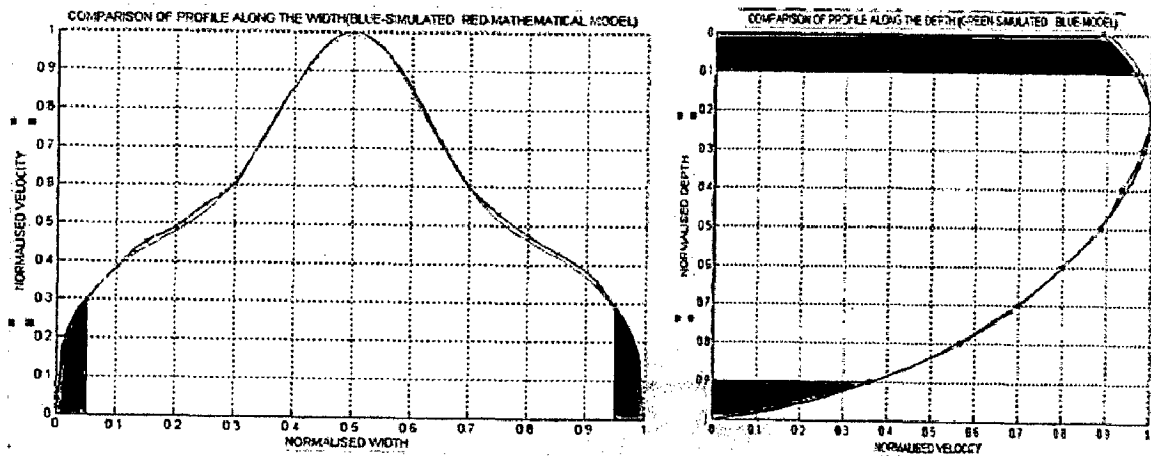

Fig 6.24 Comparison of (a) Horizontal & (b) Vertical profiles (Simulated v/s Model- D1)

CONTROL PARAMETERS FOR HORIZONTAL PROFILE		
BETA FUNCTION (SKEWNESS) PARAMETERS	$\alpha = 10$	$\beta = 10$
FRICTION PARAMETERS (FOR SIDE WALLS)	$m_1 = 5$ (LEFT WALL)	$m_2 = 5$ (RIGHT WALL)
TURBULENCE PARAMETERS	$k_1 = 3$	$k_2 = 45$

CONTROL PARAMETERS FOR VERTICAL PROFILE		
AIR FRICTION PARAMETERS	$P_1 = 2$	$P_2 = 4$
FRICTION PARAMETER (FOR BED)	$m_3 = 5$	
TURBULENCE PARAMETER	$k_3 = 3$	

Table 6.5 Mathematical model parameters used for modeling D1

These horizontal and vertical profiles developed from mathematical model are used to create the 3-D velocity profile.

6.5.3 RESULTS AND DISCUSSION

The mathematical model developed (both horizontal and vertical) is combined to obtain the 3-D velocity profile and the results are shown in the figure 6.25. Here due to the divergence the developed profile is too much peaky at the centre.

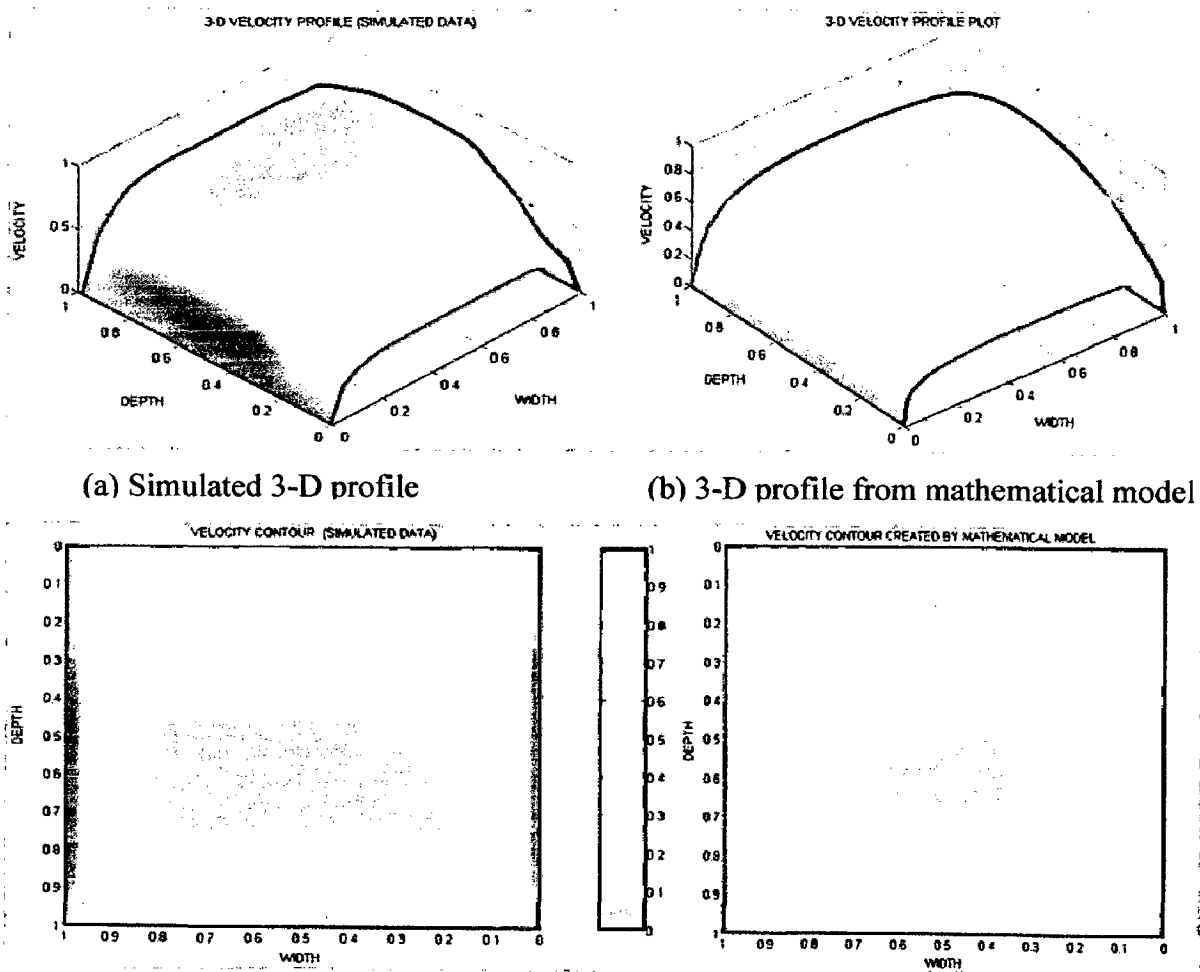(a) Simulated 3-D profile   (b) 3-D profile from mathematical model
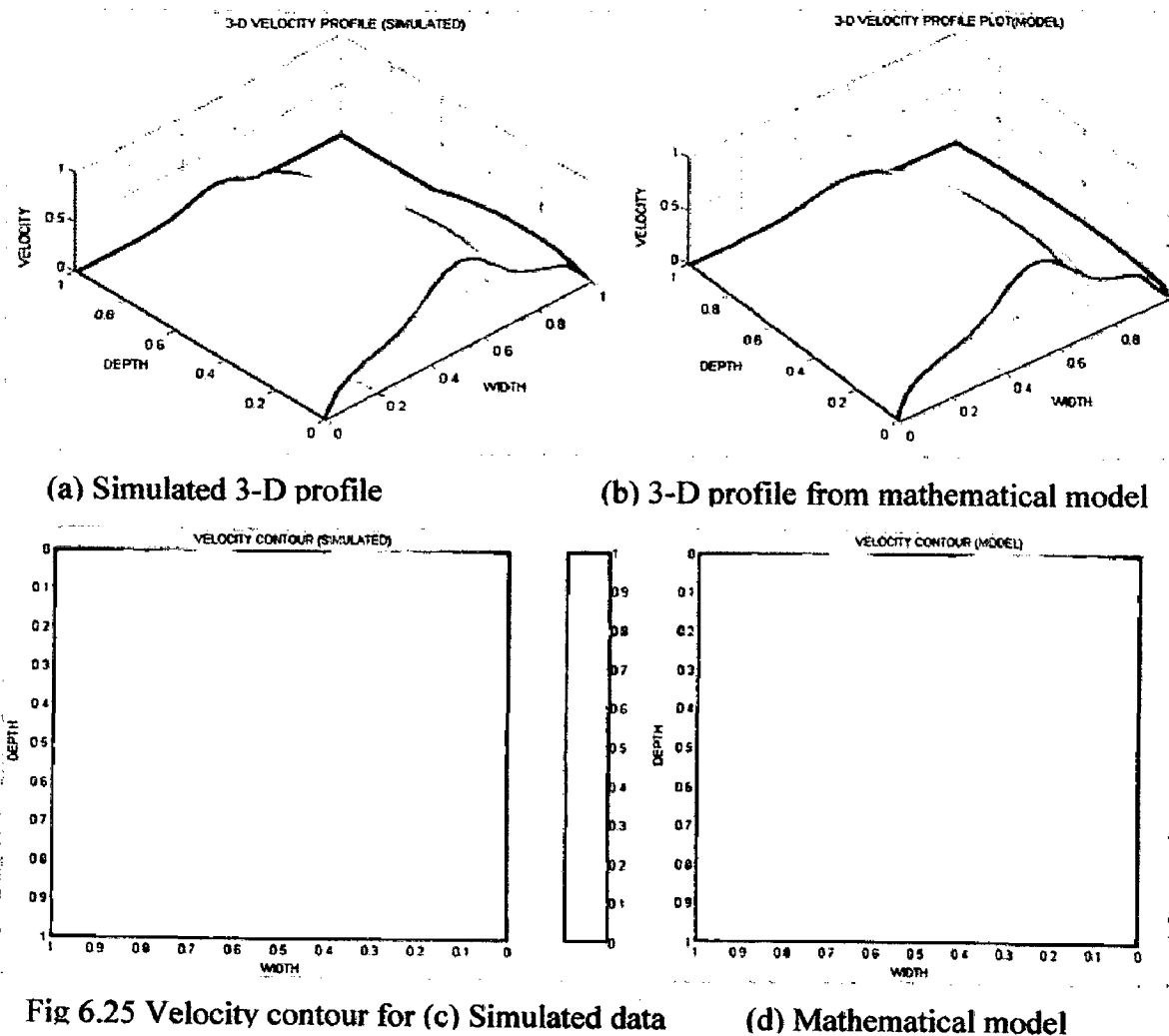
Fig 6.25 Velocity contour for (c) Simulated data   (d) Mathematical model

- The mathematical model developed showed excellent coincidence with simulated profile

- Due to the divergence the profile is very peaky in the centre & is reflected in the model by the higher value of α & β (10,10)

- The ratio of k_1/ k_2 has a very low value (0.067) which shows an increase in the turbulence of the channel due to the divergence

- The surface velocity is only slightly reduced (reflected in lower value of $p_1=2$) & the maximum velocity point is shifted towards the top (reflected in lower ratio of $p_1/ o_1 =0.5$)

- Discharge Values: Simulated profile $- 0.42614 \ m^3/s$

            Mathematical model $- 0.42890 \ m/s$

6.6 RECTANGULAR OPEN CHANNEL WITH CONVERGENCE (PROFILE C1)

In this section the effect of convergence on velocity profile is analyzed. A rectangular open channel with a convergence is modeled (figure 6.26) and the flow is simulated by CFD analysis.

Site specifications:

Depth – 2m, Width – 6m (before convergence) & 3m (after convergence), Convergence length- 4m, Angle- 20.56°, Length – 15m, Slope – 0.2m (in 15 m)
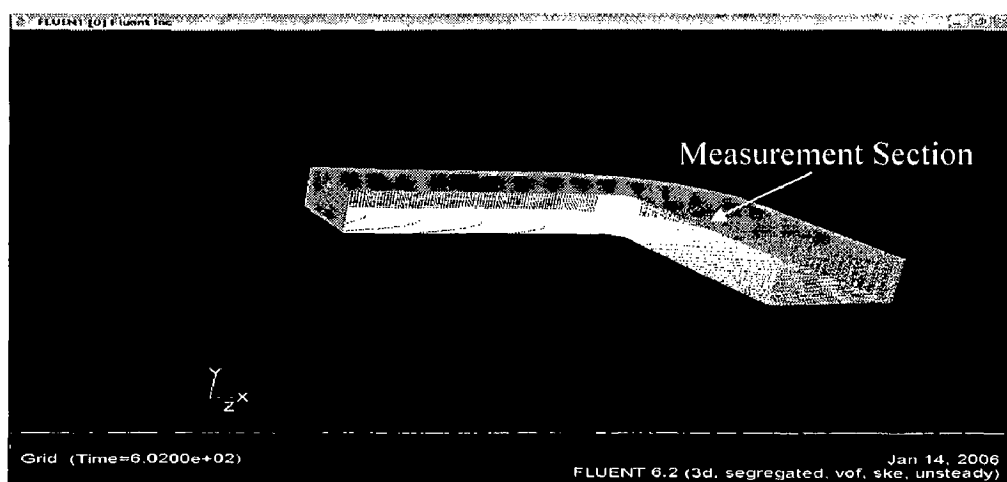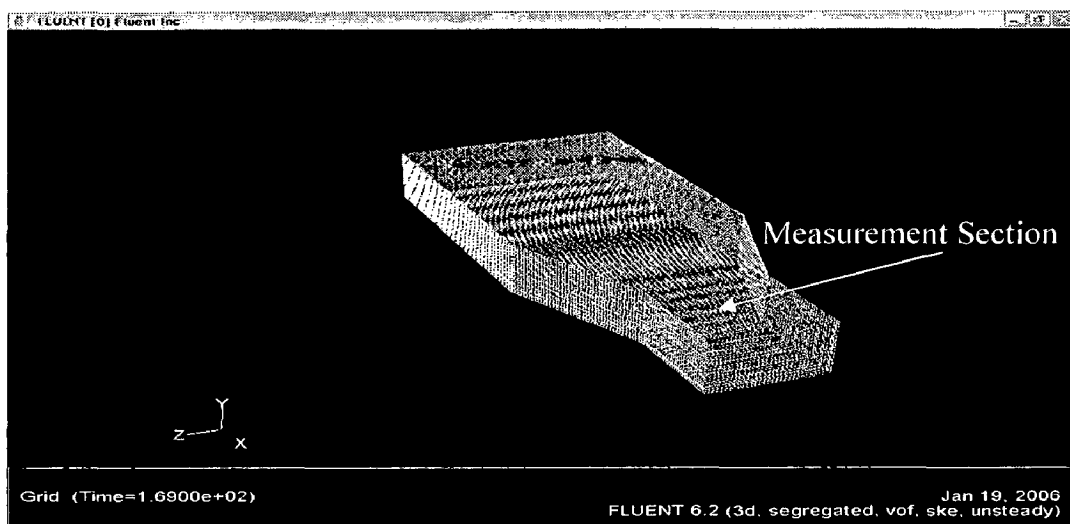

Fig. 6.26. Rectangular channel with convergence

64

6.6.1 PROFILE SIMULATION IN CFD

The operating and boundary conditions are same as that for the rectangular open channel. Free surface level is 1.8 m and the bottom level is -0.2 in the outlet. After the parameters are set, the solver is initialized with inlet conditions and the 500 iteration is done. The simulation result of the flow is shown in fig. 6.27
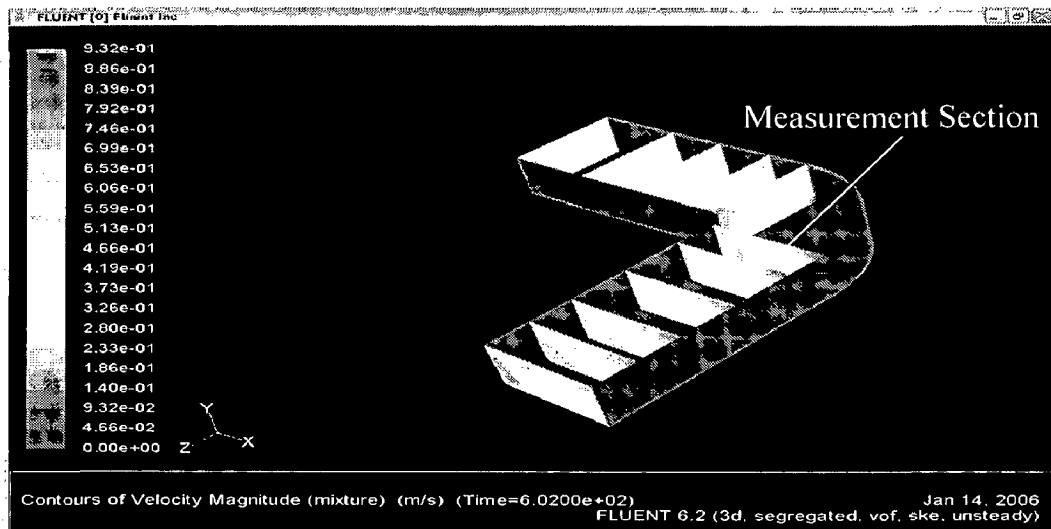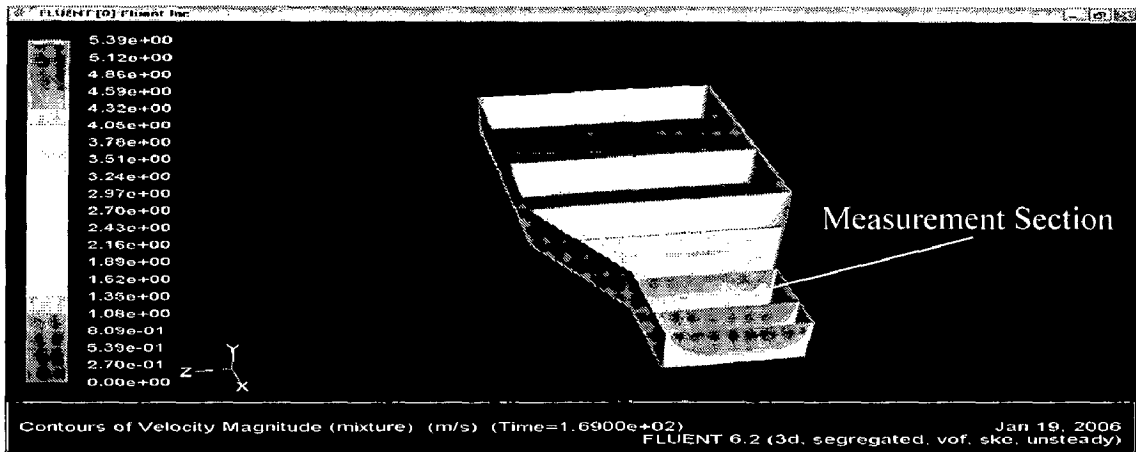

Fig. 6.27 Development of flow in rectangular channel with convergence
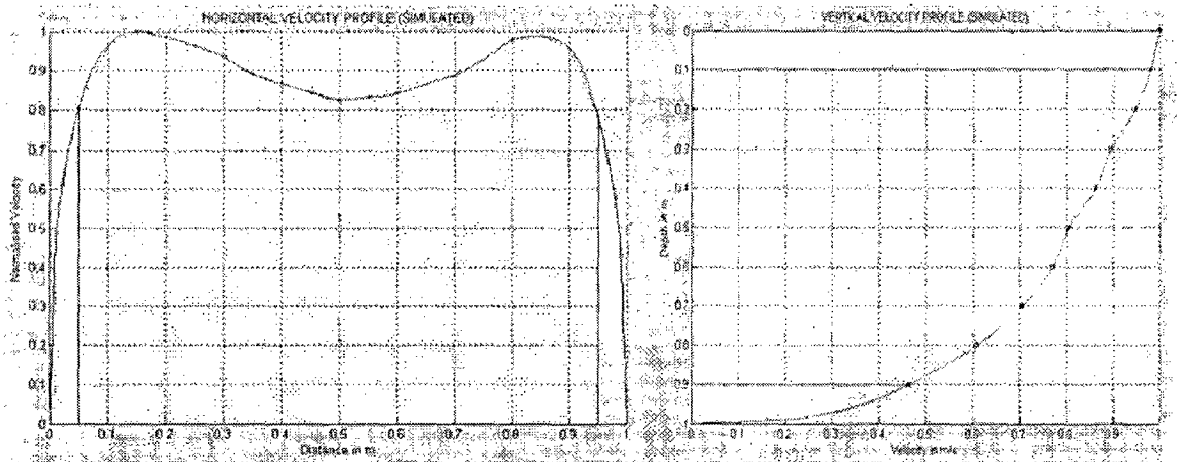
Fig. 6.28 (a) Horizontal and (b) Vertical velocity profile for C1 (Simulated data)

6.6.2 MATHEMATICAL MODELING OF THE PROFILE

In this analysis, since the horizontal velocity distribution of the simulated data is a double peak profile, the double peak profile equation of the mathematical model is selected for modeling. Appropriate values for control parameters are selected for modeling the flow and are given in the table 6.6. The profiles developed from mathematical model is compared with simulated profiles (figure 6.29)
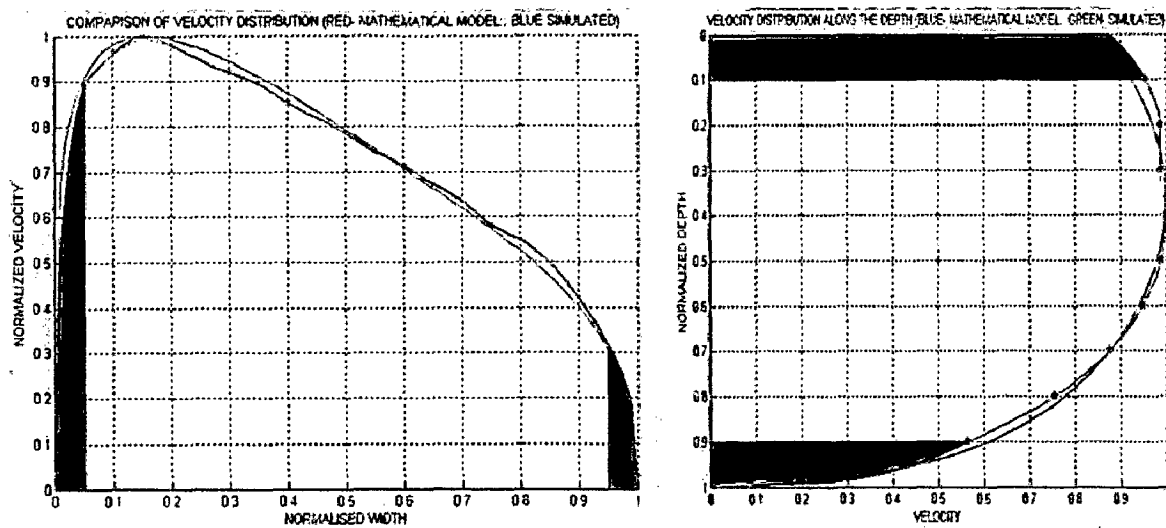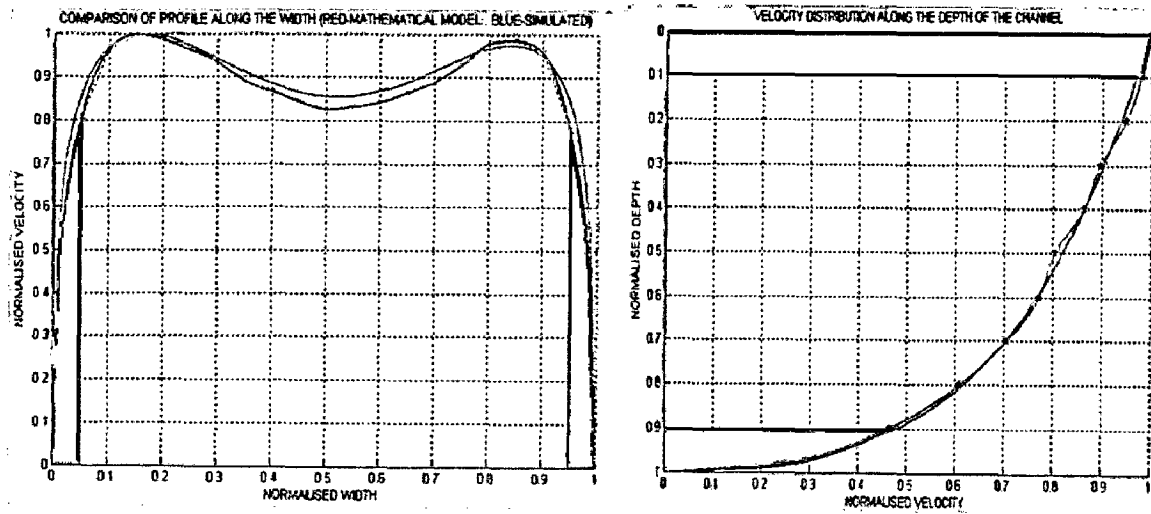
Fig 6.29 Comparison of (a) Horizontal & (b) Vertical profiles (Simulated v/s Model- C1)

CONTROL PARAMETERS FOR HORIZONTAL PROFILE		
BETA FUNCTION (SKEWNESS) PARAMETERS	$\alpha = 3$	$\beta = 3$
FRICTION PARAMETERS (FOR SIDE WALLS)	$m_1 = 5$ (LEFT WALL)	$m_2 = 5$ (RIGHT WALL)
TURBULENCE PARAMETERS	$k_1 = 5$	$k_2 = 500$
CONTROL PARAMETERS FOR VERTICAL PROFILE		
AIR FRICTION PARAMETERS	$P_1 = 0$	$P_2 = 3$
FRICTION PARAMETER (FOR BED)	$m_3 = 5$	
TURBULENCE PARAMETER	$k_3 = 18$	

Table 6.6 Mathematical model parameters used for modeling C1

These horizontal and vertical profiles developed from mathematical model are used to create the 3-D velocity profile.

6.6.3   RESULTS AND DISCUSSION

The mathematical model developed (both horizontal and vertical) is combined to obtain the 3-D velocity profile and the results are shown in the figure 6.30. Here due to the convergence the developed profile is a double peaked profile and the mathematical modeling is done using the double peaked profile (i.e. the beta function is summed in the horizontal profile model).
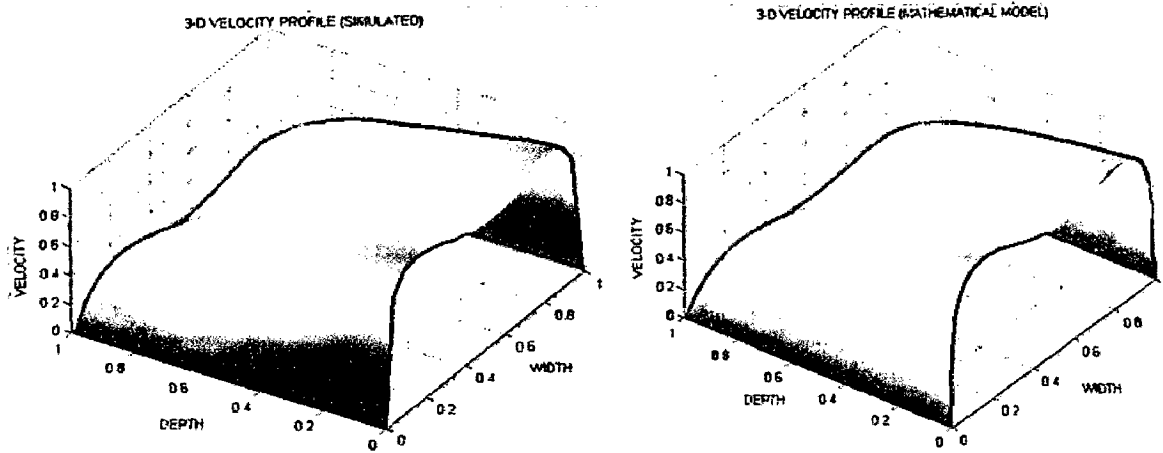
(a) Simulated 3-D profile   (b) 3-D profile from mathematical model
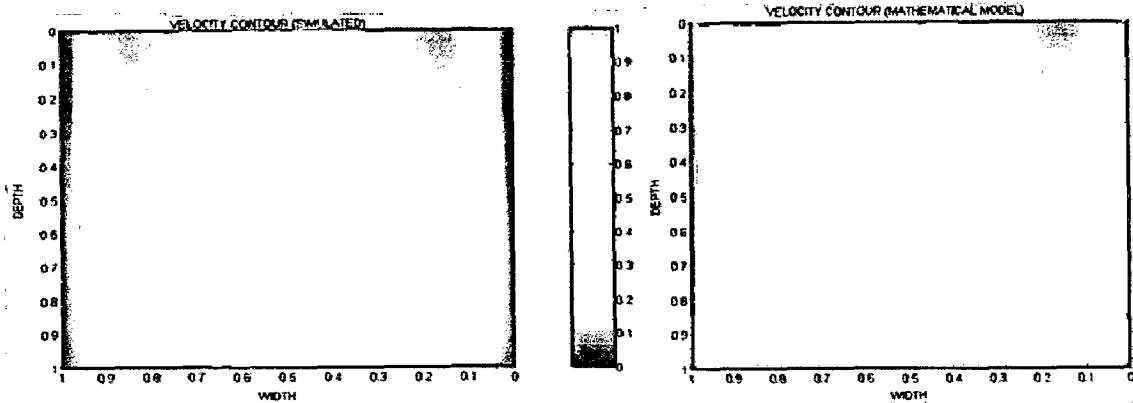
Fig 6.30 Velocity contour for (c) Simulated data   (d) Mathematical model

- The mathematical model shows excellent coincidence with simulated profile

- Due to the convergence the profile exhibited a double peak nature & so double peak horizontal profile equation is used for modeling with α & β = (3,3)

- The ratio of k_1/k_2 has a very low value (0.01) which shows an increase in the turbulence of the channel due to the convergence

- The velocity is maximum at the surface (reflected in value of $p_1=0$)

- Discharge Values: Simulated profile $- 0.67490 \ m^3/s$

        Mathematical model $- 0.67710 \ m^3/s$

Velocity profiles developed in different geometries of open channel is developed and is quantified using the mathematical model. Six different profiles with different properties have been developed. This developed mathematical model is further used in uncertainty analysis to compute the actual discharge.

UNCERTAINTY ANALYSIS OF CURRENT METER MEASUREMENTS

No measurement is free from error, so was the discharge measurement with Propeller Current meter and UTTF. Discharge measurement with a matrix of Current meters or an eight-path UTTF is an application that has to account for many factors related to the fields of fluid mechanics, civil engineering, electrical, electronics and instrumentation. IEC 60041 specifies certain instrument errors and systematic errors which are prone to occur during the measurement. Among these, few errors were identified to largely influence accuracy of both of these flow meters and is discussed in this and the succeeding chapter. Those errors give scope to correct the "as obtained" accuracy.

The first step to deal with the errors is to establish a relationship between the parameter responsible for the error and the error in discharge measurement. The next step is to account for them through 'compensation' or with an error correction factor, so that the accuracy of is improved. The errors are discussed in brief in the following sections. Later an improved scheme for area velocity integration is suggested and the effect of number of current meters in measurement is also analysed

7.1 ERROR SOURCES IN MEASUREMENT USING CURRENT METERS

Major sources of error which are likely to occur while using propeller current meters are listed below [15]

7.1.1   OBSTRUCTION ERROR

As the size of the current meter matrix increases, it gives more information about the velocity profile in the channel. But this will increase the obstruction to the flow, which will effect the accuracy of measured discharge. So there should be a trade off between these two and the number of current meter used for the measurement should be determined in such a way that it gives good accuracy without causing much obstruction to the flow.

IEC-41 provides the guide line for the number of current meters for a particular size of the channel, size of current meters and the speed at which they should be moved in the channel, so that the error is minimized. At least 25 measuring points shall be used in a rectangular or trapezoidal section. [1] If the velocity distribution is likely to be non-uniform, the number of measuring points, Z, shall be determined from:

$$24\sqrt[3]{A} < Z < 36\sqrt[3]{A}$$

Where A is the area of measuring section in square meters. If the conduit or channel is divided into several sections, measurement shall be made simultaneously in all sections.

Current-meter propeller shall not be less than 100mm diameter except for measurements in the peripheral zone where propellers as small as 50mm may be used. The distance from trailing edge of the propeller to the leading edge of the mounting rod shall be at least 150mm. The angle between the local velocity vector and the axis of the current meter should not exceed 5 degrees. When larger angles are unavoidable, self-compensating propellers which measure directly the axial component of the velocity shall be used, but only at angles for which they have been designed and calibrated.

7.1.2 INTEGRATION ERROR

Regardless of a number of current meters used in the measuring section, these will never be able to provide full information about the flow. The missing informations has to be interpolated and extrapolated using various integration techniques to obtain the velocity profile and hence the discharge. This interpolation and extrapolation will introduce some errors to discharge calculations and will depend upon the schemes used.

The integration errors can be reduced by increasing the matrix size of the current meters, but can't be increased beyond a limit (provided by IEC-41), as this will increase the obstruction errors. The interpolation scheme which gives the best accurate result as per IEC-41 is Cubic spline. This scheme is also used for surface velocity calculation by extrapolation. At the left and right bank and the bed of the channel, the flow can be more accurately extrapolated by power law, by its coefficient is determined by the roughness of the material of the wall [1].

7.1.3 ROUGHNESS ERROR

Flow along Open channels and pipes encounter resistance that is proportional to the roughness of the bounding wall. This will affect the profile near the boundary walls. The influence of roughness has been cataloged in the form of roughness coefficient. In flow measurement using propeller current meters the roughness effect is influenced by the power law coefficient 'm'. The roughness error can be reduced by the proper selection of this coefficient. It may vary from 2 for rough walls to 10 for smooth walls.

7.1.4 INSTALLATION AND SURVEY ERROR

The accuracy of measurement also largely depends on the selection of the measuring points and also the precise placement of current meters on the selected points. Human errors are always bound to occur in these cases. These errors can be reduced by using accurate instruments for the precise measurement for width and depth and also careful installation of the current meters.

7.2 INTEGRATION ERROR: AN IMPROVED SCHEME

The basic principle behind Area-velocity Integration is discussed in the section 2.2.3 [1,16]. In this section an improved scheme using Cubic spline interpolation and Power law extrapolation proposed by ISO-748 is described, which gives more accurate discharge measurement. The proposed scheme is implemented in MATLAB.
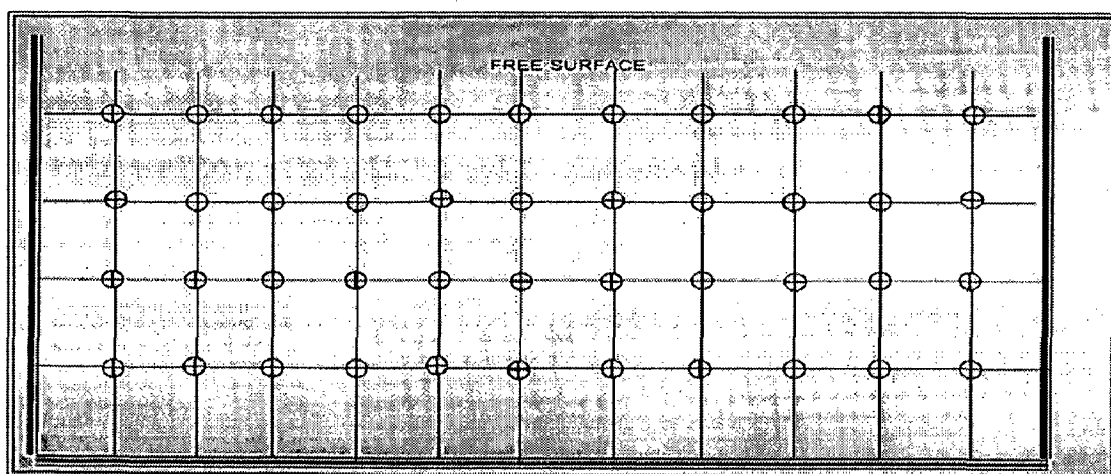
Fig. 7.1 Matrix of Current Meters in the measuring section

70

The velocities readings are taken at number of points on the vertical transect. A matrix of current meters is installed across the cross-section of the measuring section to obtain the point velocities as shown in the figure 7.1. The velocity readings recorded for each vertical are plotted against depth as shown in Fig. 7.2(a). *Cubic spline interpolation* scheme is used for the interpolation between the point velocities [17]. The area contained by the velocity curve produced for each vertical gives the discharge for unit width or known as unit-width discharge of the corresponding section. Where necessary, velocity curves can be extrapolated to the surface by cubic spline and to bed using *power law* and the coefficient of power law depends on the roughness of the channel (as per IEC 41 & ISO-748 standards) .The values of unit-width discharges (v. d) are then plotted for each vertical cross-section and joined to form a continuous curve as shown in figure. Cubic spline interpolation is used for this and the right bed and left bed are extrapolated using the power law (figure 7.2 b). The area under this curve will give the discharge in the channel. The accuracy of the measurement depends on the size of matrix used, which is analysed later in this chapter.
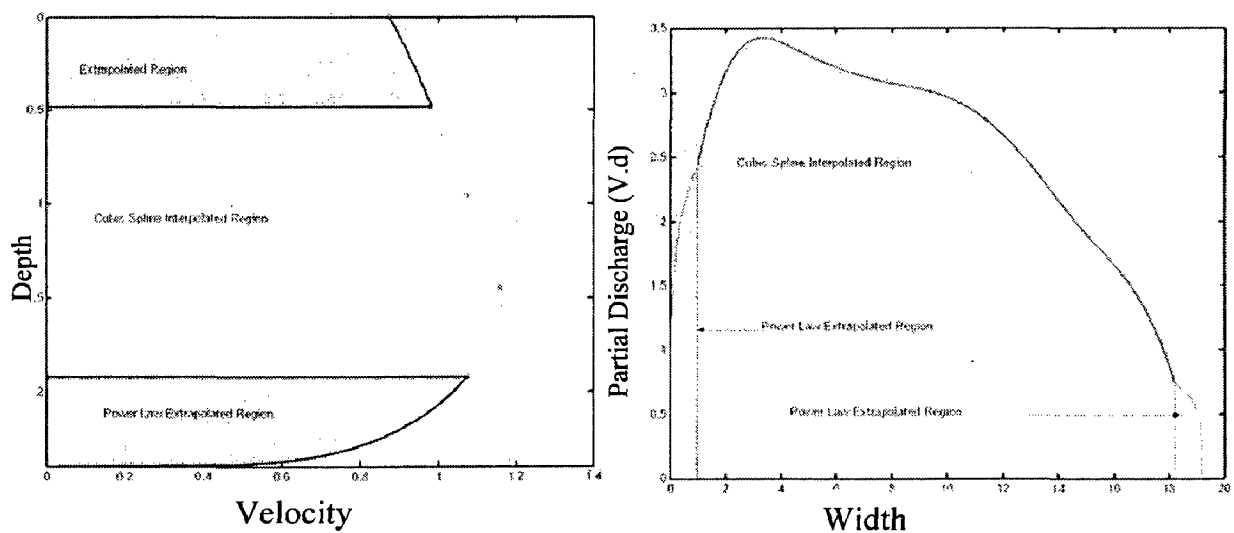
Fig. 7.2(a) Velocity profile along the depth   (b) Along the width

7.2.1   CUBIC SPLINE INTERPOLATION SCHEME

In this approach, a set of cubic spline functions is used for velocity distribution approximation. Spline functions are partial polynomial functions that are connected in measuring points and have the same second derivative in this point. The algorithm using a set of cubic spline functions is very stable for unlimited number of measuring points

and for any distance distribution of measuring points throughout the cross-section (unlike other polynomials of higher power, e.g. Newton's interpolation polynomial for non-equidistant spacing etc.). Here, the same procedure is carried out for average velocity measurement, described in section (7.1), but instead of higher degree polynomial function, the data is interpolated in the interpolating range and extrapolation can be done to find the surface velocity of the channel if the current meter is not placed very close to surface. This method of cubic spline interpolation is considered to be most commonly used for finding the velocity distribution in the vertical transect and horizontal velocity profile along the width of the channel [17].

7.2.2   POWER LAW EXTRAPOLATION SCHEME

When the turbulent flow condition exists, the velocity curve can be extrapolated from the last measuring point to the bed or wall by calculating v_x from the equation

$$v_x = v_a \left(\frac{x}{a} \right)^{\frac{1}{m}}$$
(7.1)

where;

v_x is the open point velocity in the extrapolated zone at a distance x from the bed or wall.

v_a is the velocity at the last measuring point at a distance a, from the bed or wall. Generally m lies between 3 and 7 but it may vary over a wider range depending on the hydraulic resistance. The value m=3 applies to coarse beds or walls while m=10 is characteristic of smooth beds or walls [1].

7.2.3   COMPUTATION OF OPEN-CHANNEL DISCHARGE

A generalized MATLAB program was written for calculating the absolute discharge, which can take any number of point velocities from the excel data sheet in a pre-specified format. As per ISO-748, an **improved scheme using Cubic Spline Interpolation and Power Law Extrapolation** was introduced for the computation of the discharge. The entire program is divided into four modules.

Module 1 : Data Entry from excel sheet, *Module 2:* Surface velocity calculation by Cubic spline extrapolation, *Module 3:* Plotting vertical profiles for different values of 'm', *Module 4:* Selection of 'm' and discharge evaluation.

7.2.4 FLOW-CHART OF THE ENTIRE SCHEME

Fig. 7.3 (Contd.)

73

```
                    ┌───┐
                    │ 1 │
                    └───┘
                      │
                      ▼
        ┌──────────────────────────────────┐
        │  Calculate the Partial Discharge, m²/s  │
        │                 &                │
        │   Average Velocity in Transect, m/s  │
        └──────────────────────────────────┘
                      │
                      ▼
     No          ◇─────────────◇
   ┌───┐   ◄──── │ All Vertical │
   │ 2 │         │ Transect taken│
   └───┘         ◇─────────────◇
                      │ Yes
                      ▼
        ┌──────────────────────────────┐        ┌────────────────────┐
        │ Perform Cubic Spline Interpolation, │   │ Find area under    │
        │  (C.S.I) for Horizontal Plane │ ─────►│ curve, m³/s        │
        └──────────────────────────────┘        └────────────────────┘
                      │
                      ▼
        ┌──────────────────────────────┐
        │ Plot Horizontal Velocity Profile in │
        │    an Interpolated Region     │
        └──────────────────────────────┘
                      │
                      ▼
          ╱─────────────────────╲
         ╱  Input the value of 'm' ╲
        ╱   for left & right side of ╲
        ╲        the channel         ╱
         ╲─────────────────────────╱
                      │
                      ▼
        ┌──────────────────────────────┐
        │ Plot the Power Law Eq. for the two ends │
        │  of Channel & Find area under curve │
        └──────────────────────────────┘
                      │
                      ▼
                    ⊗ ◄────────────────────┐
                      │          ┌────────────────────────┐
                      │          │ Plot partial discharge v/s │
                      │          │  width of the channel  │
                      ▼          └────────────────────────┘
        ┌──────────────────────────────┐
        │ Calculate the Total Discharge (m³/s) │
        │                &               │
        │      Mean Velocity (m/s)       │
        └──────────────────────────────┘
                      │
                      ▼
   Yes          ◇─────────────◇
  ┌──── ◄────── │   Re-check   │
  │             │   for 'm'?   │
  │             ◇─────────────◇
  │                   │ No
  │                   ▼
  │               ┌────────┐
  │               │  Stop  │
  │               └────────┘
  └──────────(loops back to Input)
```

74

7.3 UNCERTAINTY ANALYSIS

The error sources involved in measurement using current meters is discussed in the beginning of this chapter. Accuracy demands of discharge measurement in hydro-plants are very high and constant effort has been made to keep these errors to the minimum thereby reducing the uncertainty of measurement [15]. The standards ISO-748 and IEC-41 provides the proper guidelines which has to be precisely followed while conducting the measurements. An improved scheme of Velocity-Area Integration method using cubic spline interpolation and power-law extrapolation was implemented in MATLAB for discharge calculation, which gave excellent results with minimum error. Here the percentage of error depends on the number of current meters (matrix of current meters) used for the measurement, a close analysis is done in the following section

7.3.1 EFFECT OF MATRIX SIZE ON DISCHARGE MEASUREMENT: AN ANALYSIS

In Velocity-Area Integration method a matrix of current meters is introduced into the flow channel and point velocities are obtained. As we increase the number of current meters in the matrix, more point velocities can be obtained from the channel. That is, as the number of current meter increases, more information about the velocity profile in the channel is obtained. From this it is evident that as the current meters in the channel is increased, the uncertainty in the discharge calculation can be reduced.

It should be noticed that as the number of current meters in the channel is increased, the obstruction to the flow will be large, which will in turn leads to false discharge indication. So there should be trade of between these two factors and an optimum number of current meters is selected, so that the error in discharge calculation is minimum. The following section gives the results of the effect of various matrix size of current meters on discharge measurement. The 6 profiles which is used for analysis here are created by CFD simulations, which is already been presented in previous chapter. The measured discharge (Q_{MEAS}) is calculated for various matrix size using Area-Velocity Integration method and is compared with actual discharge (Q_{ACT})

7.3.2 ACTUAL DISCHARGE CALCUALTION BY EXACT INTEGRATION

The mathematical profile expressions are used to find out the "actual" discharge with zero error. Exact surface integration is applied to the mathematical expressions of profiles to find out the actual value of discharge and in turn the mean velocity. Equation (7.2) gives the expression for the surface integration:

$$Q_{ACT} = \oiint_S V_z(x, y) \, dx \, dy \qquad (7.2)$$

where $V_z(x, y)$ is the velocity profile as a function of x and y.

The parameters r and y are varied from 0 to 1. Since the profile is described by two different equation $V(x)$ and $V(y)$ the surface integration is done by the summation of the surface profile matrix (100 X 100) created by both these equation.

$$Q_{ACT} = \sum_{x,y=0}^{1} V(x).V(y) \qquad (7.3)$$

7.3.3 DISCHARGE CALCUALTION BY VELOCITY AREA INTEGRATION

The measured discharge (Q_{MEAS}) is calculated by Velocity Area Integration using the improved scheme discussed in section 7.2. The discharge is calculated for three different size of current meter matrix size; 10 X 10, 5 X 5 and 1 X 5. The variation of these measured discharge with the actual discharge is also calculated. From this study the effect of number of current meters on discharge measurement can be analysed

7.3.4 ERROR CALCULATION

The difference between the "actual" value and the "measured" value obtained from numerical integration is the error ascribed to the numerical integration technique. Thus it is given by

$$\% \, Error = \left[\frac{Q_{MEAS}}{Q_{ACT}} - 1 \right] \times 100 \qquad (7.4)$$

76

7.3.5 FLOWCHART AND RESULTS

Figure 7.4 illustrates the steps followed in calculating Area-Velocity integration error for different matrix sizes (100 X 100, 10 X 10, 5 X 5, 5 X 1). The results are tabulated in table 7.1.

```
                    VELOCITY PROFILE
                       V = f(x, y)
```

CURRENT METER MATRIX SET UP
FOR OBTAINING POINT VELOCITIES

SURFACE INTEGRATION

$$Q_{ACT} = \oiint V_z(x, y).dx.dy$$

Calculation of Q_{MEAS} for different matrix size by Area-Velocity Integration

$$(Q_{MEAS}) = \sum_{I,J=1}^{R,C} V_{I,J}.A$$

MATRIX SIZES (R, C) = 100 X 100, 10 X 10, 5 X 5, 5 X 1

Percentage Error Calculation

$$\%E = \left[\frac{Q_{MEAS}}{Q_{ACT}} - 1\right] \times 100$$

➤ %E
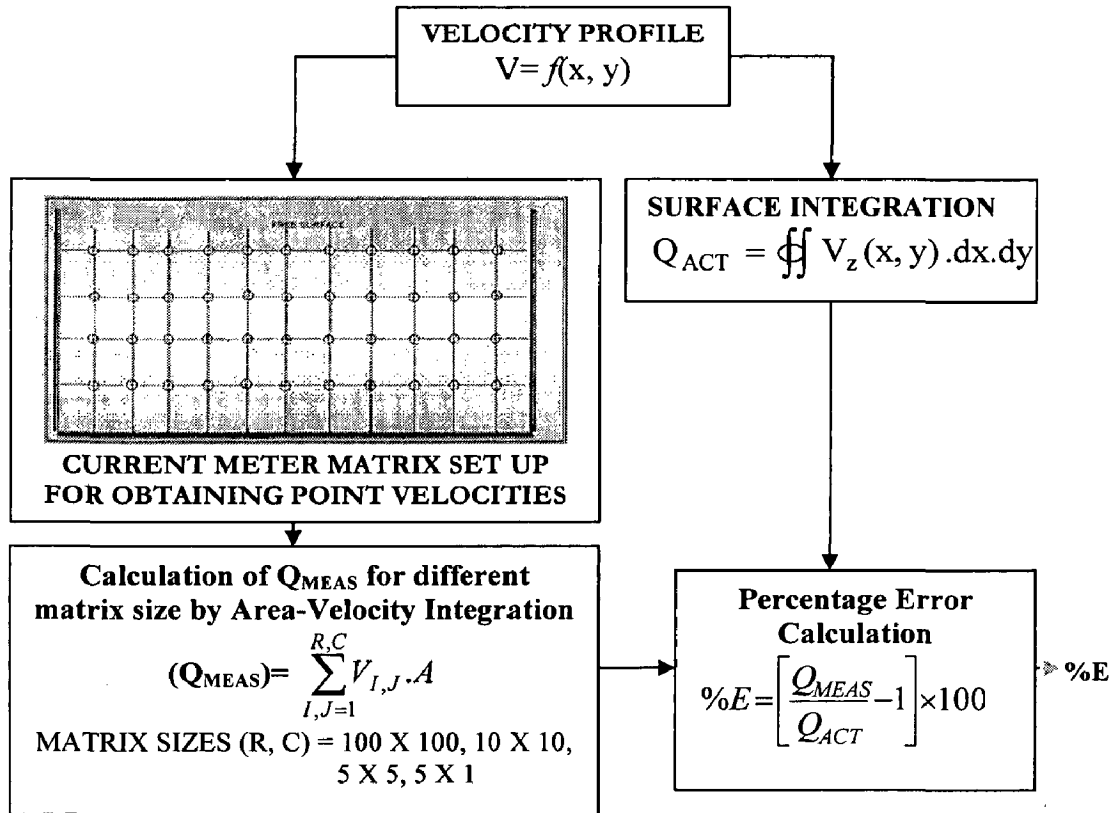
Fig. 7.4 Steps involved in the calculation of Area-Velocity Integration error.

SIMULATED PROFILES	Q_{ACT} (m³/s)	Q_{MEAS} FOR DIFFERENT MATRIX SIZE (m³/s)				PERCENTAGE ERROR			
		1 X 5	5 X 5	10 X 10	100 X 100	$\%E_{1X5}$	$\%E_{5X5}$	$\%E_{10X10}$	$\%E_{100X100}$
P1	0.60736	0.62584	0.60104	0.60366	0.60735	+3.0427	-1.0404	-0.6091	0
P2	0.65851	0.67933	0.65019	0.65389	0.65849	+3.1617	-1.2641	-0.7011	0
P3	0.67588	0.69976	0.66702	0.67029	0.67586	+3.5332	-1.3097	-0.8271	0
B1	0.62021	0.56962	0.62988	0.62592	0.62024	-8.1569	+1.5593	+0.9202	0
D1	0.42614	0.45381	0.43347	0.43019	0.42615	+6.4932	+1.7196	+0.9497	0
C1	0.67710	0.64067	0.68942	0.68446	0.67714	-5.3803	+1.8192	+1.0874	0

Table 7.1 Integration error for different matrix size (Analysis done for identified profiles)

The results for the Area – Velocity Integration error has been analysed and the following points are observed:

1. As the size of the matrix is increased the percentage error is decreased, ie, the measured discharge will be closer to actual discharge.

2. The reduction in matrix size means only less information about the velocity profile is captured from the site. Therefore the interpolation distance between the point velocities increases, which means an increase in integration error.

3. If a matrix size of 100 X 100 is used, it will give approximately the actual discharge, but is practically impossible in real situations.

4. It can be observed from above analysis that if the discharge measurement within the range of ±1% error is allowable, then the matrix size 10 X 10 will serve the purpose.

5. From the table it is also evident that, as the complexity of profile increases, the uncertainty in measurement also increases. The error is maximum for divergence (D1- Peaky profile), convergence (C1-Double peak profile) and for 90° bend (B1- Skewed profile)

UNCERTAINTY ANALYSIS OF UTTF MEASUREMENTS

The approach for uncertainty analysis in UTTF is also the same as that done for current meters, already discussed in the previous chapter. The error sources in UTTF measurement in a correction perspective is discussed in brief in the following sections [18]. The second half of the chapter discusses the numerical integration methods and the cause of numerical integration error is analyzed.

8.1   ERROR SOURCES IN MEASUREMENT USING UTTF

8.1.1 REYNOLDS NUMBER ERROR

The Reynolds number is the basic parameter underlying, which influences the nature of flow profile. Direct consequences of the Reynolds number on flow measurement can be observed in a single path UTTF. Where the flow velocity measured by the single path and the mean flow rate of the whole cross section of the conduit are related through a function in Reynolds number (R_e).

$$\frac{\text{Mean flow measured}}{\text{Path flow measured}} = f(R_e) \tag{8.1}$$

$$\overline{V} = V_{max}(1 + 0.19R_e^{-0.1}) \tag{8.2a}$$

$$\overline{V} = V_{max}(1 + 0.01\sqrt{6.15 + 431R_e^{-0.237}}) \tag{8.2b}$$

$\overline{V}$ is the flow velocity measured by the ultrasonic path and

V_{max} is the maximum velocity of the turbulent flow profile.

Empirical relations for the error correction are given in Eqns. (8.2a) and (8.2b) [25]. The error was understood more as an influence of Reynolds number on the measurement path than on the flow profile. The correction of the Reynolds number is significant, due to the reason that the flow is no more of single kind and is a mixture of 3 different kinds of flow corresponding to different ranges of Reynolds numbers across the channel cross section. The Reynolds number correction for a multi-path UTTF can be applied separately to each path, individual path velocities can be corrected before the discharge calculation [26].

8.1.2 ROUGHNESS ERROR

The roughness error correction is another challenging task. The influence of roughness can be represented in the form of a roughness coefficient based on data obtained from wide range of field and laboratory observations [13]. The experimental analysis of influence of roughness parameter on mean flow rate in open channels can be found by the roughness coefficient . Roughness coefficients are typically defined in one of two ways:

(1) Chezy's resistance coefficient, or (2) Manning's n.

Flow losses are defined in terms of a uniform flow state defined as steady flow with a fixed discharge and flow depth. In practice this usually means the flow in a channel of uniform cross section and having a constant slope such that the gravitational acceleration down the slope is balanced by frictional resistance at the boundaries of the channel. Chezy derived a simple formula to describe this uniform state,

$$V = C\sqrt{R_h S},$$

(8.3)

where V is the mean flow velocity in ft/s, R_h is the hydraulic radius in ft (i.e., flow cross sectional area divided by wetted perimeter), and S is the channel slope. C is called Chezy's coefficient of flow resistance, or simply Chezy's C. (A more general expression in which C would be dimensionless is obtained by inserting a factor of the acceleration of gravity under the square root.)

The Manning formula, which is meant to do the same thing as Chezy's but from a more empirical point of view, is

$$V = \frac{1.49}{n} R_h^{2/3} S^{1/2},$$

(8.4)

in which n is a parameter called Manning's n. The relationship between Chezy's C and Manning's n is easily shown to be

$$C = \frac{1.49}{n} R_h^{1/6}.$$

(8.5)

The values for Manning's n that covers a wide range of artificial and natural channels are available, which is experimently determined and verified. These values can be used for roughness error correction.

8.1.3 INSTALLATION AND SURVEY ERRORS

The accuracy of the mounting transducers is largely dependent on the measurement of depth, path length and installation angle. The measurement of width is an important factor in deciding the path lengths of the UTTF, path angle, etc. IEC 60041 suggests the measurement of width as an average from five points evenly distributed across the measuring section. But the lateral distances at which the ultrasonic paths have to be mounted is of six digit precision after the decimal point (Table 8.1). A surveying instrument called 3D Theodalite is capable of measuring distances with such a precision is used while installing ultrasonic paths [26].

8.1.4 PROTRUSION EFFECT

The UTTF can be applied to measure discharge using two kinds of transducers, namely wet and clamp-on transducers. Wet type transducers are used for measurement in open channels. But the one immune effect of wet transducers is that, it induces distortion in the sensitive region (transition region) of the flow profile. The major issues that are to be discussed with respect to the protrusion of the transducer into the flow conduit are as follows:

> ▶ Sampling error – some part of the flow profile is left un-sampled by the ultrasonic flow path which results in 'high' reading.

> ▶ Disturbance around the transducer may make the path read 'low' or 'high'.

> ▶ Dead water in the transducer pocket, if any will lead the path to read 'low'
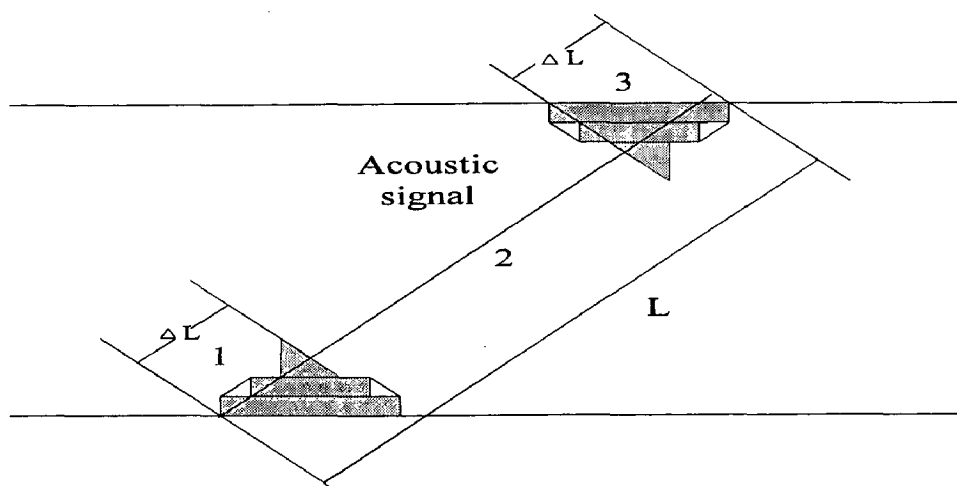
Fig. 8.1. Protrusion effect (top view of the channel) (Source: [26])

CFD simulation of the transducer protrusion puts forth a method of correction against the protrusion effect for discharge measurement [22]. The effective path length for each of the UTTF paths is length of the line joining the two transducer ends, where the ultrasonic wave emanates. Each UTTF path can be divided into 3 sections proceeding from one transducer along the path to the other transducer. Section 2 (Fig. 8.1) is free from the influence of the protrusion. Sections 1 and 3 are influenced by protrusion and needs correction for the same. The influence of the protrusion is ratio between flow velocity with and without protrusion, which is called the protrusion coefficient, f.

$$f = \left[\frac{\int_0^{l_{oD}} V'_{Proj}(s)ds}{\int_0^{l_{oD}} V_{Proj}(s)ds} \right] \quad (8.6a)$$

$$\overline{V}_i = \left[\frac{f_i \int_0^{l'_{iD}} V_{Turb}(s)ds + \int_{l'_{iD}}^{l_i - l'_{iD}} V_{Turb}(s)ds + f_i \int_{l_i - l'_{iD}}^{l_i} V_{Turb}(s)ds}{l_i} \right] \quad (8.6b)$$

where

$V'_{Proj}(s)$ is the projected velocity with protrusion,

$V_{Proj}(s)$ is the projected velocity without protrusion,

f_i is the protrusion coefficient of the transducers installed along the inner UTTF paths,

$V_{Turb}(s)$ is the velocity in a fully developed turbulent flow,

L_i is the effective length and

V_i is the mean flow velocity in regard to protrusion effect.

Equations (8.6a) and (8.6b) provide with expressions for the flow velocity calculation incase of protrusion. Important conclusions that can be reached on protrusion are:

▶ The effect of protrusion decreases linearly with the increase in the width of the channel.

▶ The upstream transducer influences the discharge measurement non-linearly compared to the downstream transducer.

8.2 NUMERICAL INTEGRATION METHODS

One important source of error is the error in numerical integration used for discharge measurement from UTTF observations. Integration can be seen as a summation series with the number of sampling points in the given interval as infinity. Numerical integration can be treated as a simplified model of exact integration, owing to the constraints imposed by the complexity of the application and optimization tradeoff. A four point Gaussian integration technique is applied when measuring discharge with multi-path UTTF [23,24].

The eight-path UTTF uses four-point Gaussian quadrature technique. The two abscissae (n=4) are the lateral distances above and below the vertical center point. IEC 60041 ascertains that each of the paths in a plane (at an angle to the flow propagation) should be complimented by an axis-symmetric path in order that the transverse component of the low velocity cancels out. Thus the UTTF in the discussion comprises of eight paths.

8.2.1 GAUSS-JACOBI (GJ) NUMERICAL INTEGRATION METHOD

Also called as the Tchebychev numerical integration method, this is one of the gaussian quadrature techniques used for the application of eight-path UTTF. From Table 8.1 it is clear that the shape factor for GJ, k, is equal to 1.000 for closed conduits and 0.994 for rectangular channels, indirectly suggesting that GJ is method that suits for closed pipes.

8.2.2 GAUSS-LEGENDRE (GL) NUMERICAL INTEGRATION METHOD

GL is no different from GJ, except that the abscissae and the weight are different. The shape factor from Table 8.1 can be seen as 1.0 for rectangular sections and 1.034 for closed pipes. So GJ can be a suggestive method for rectangular channels. The abscissae and the corresponding weights are listed in Table 8.1.

The normalized lateral distances, as specified by IEC 60041, which have a six-digit resolution. This implies that it is very important to measure parameters like diameter, path length and angle with a similar resolution and accuracy. The calculation of flow rate (discharge) from the average velocities measured by UTTF along the eight paths should also have a matching accuracy.

8.2.3 ROLE OF NUMERICAL INTEGRATION IN DISCHARGE MEASUREMENT

Integration can be seen as a summation series with the number of sampling points in the given interval as infinity. Numerical integration can be treated as a simplified model of exact integration, owing to the constraints imposed by the complexity of the application and optimization tradeoff. A four point Gaussian integration technique is applied when measuring discharge with multi-path UTTF. The eight-path UTTF uses four-point Gaussian quadrature technique. The two abscissae $(n=4)$ are the lateral distances above and below the (horizontal) diameter. IEC 60041 ascertains that each of the paths in a plane (at an angle to the flow propagation) should be complimented by an axis-symmetric path in order that the transverse component of the low velocity cancels out. Thus the UTTF in the discussion comprises of eight paths.

The first step in flow rate measurement using multi-path UTTF is the installation of ultrasonic transducers at certain lateral distance from the diametrical path and at a certain angle with respect to the flow direction. The normalized lateral distances, as specified by IEC 60041, which have a six-digit resolution. This implies that it is very important to measure parameters like diameter, path length and angle with a similar resolution and accuracy. The calculation of flow rate (discharge) from the average velocities measured by UTTF along the eight paths should also have a matching accuracy.

			Gauss-Legendre method		Gauss-Jacobi method	
			Paths 1 and 4	Paths 2 and 3	Paths 1 and 4	Paths 2 and 3
	d/(D/2)		± 0.861136	± 0. 339981	± 0.809017	± 0.309017
	W		0.347855	0.652145	0.369317	0.597667
k	Circular section		0.994		1	
	Rectangular section		1		1.034	

Table 8.1 Abscissae and weights of GJ and GL methods

Then the original equation used for discharge measurement will be as follows: (described in detail in section 2.3.2)

$$Q = k \frac{D}{2} \sum_{1}^{n} W_i \overline{V}_{ai} L_{wi} \sin \varphi \tag{8.7}$$

8.3 UNCERTAINTY ANALYSIS

8.3.1 NUMERICAL INTEGRATION ERROR AND WHY ?

In the first place, it is to be remembered that the numerical integration treats the output required (discharge) as a polynomial of *fixed order*. But flow analysis in open channel reveals that the flow distribution is not static, but dynamic in nature. The flow profile is very sensitive to the discontinuities and the roughness of the bed which cannot be easily quantified. The assumption that flow profile is static contributes to error in discharge measurement. The flow profile varies with the various parameters of the open-channel flow. The variation in the flow profile is directly reflected in the degree of the flow polynomial. Thus change in the degree to a higher value demands a higher-point quadrature method to be used to preserve the accuracy [26].

While rapid variation in the flow profile is an important source for the numerical integration error, another cause that significantly effects numerical integration error is the near-wall flow. The reason that hampers the performance of quadrature techniques is that the flow distributions near the wall cuts deep along the wall with a steep descent, till the flow velocity near the bed and the two banks is nearly zero.

The quadrature techniques are best suited for smooth flow distributions with no singularities at any point of the flow profile. Singularity is an abrupt zero which changes the flow profile so much that it gets distorted. Obviously the numerical integration is not going to probe into that rapid variation in the profile, and takes it for granted that the profile is smooth with no singularities unless other wise the UTTF path cuts through such an abrupt variation. Whether there is a singularity in the flow profile function or not, but there exists always singularity near the pipe wall which is going to affect the accuracy of numerical integration, thus the numerical integration error is always in the place.

The near-wall flow pattern comprises of a steeply descending function. Such a steep function in the flow profile is responsible for a poor performance of numerical integration techniques and holds them back from being 'exact', especially in case of distorted flow.

8.3.2 NUMERICAL INTEGRATION ERROR: FLOWCHART AND RESULTS

The mathematical profile expressions developed for simulated profiles (discussed in Chapter 6) are used to find out the "actual" discharge with zero-error. Exact surface integration is applied to the mathematical expressions of profiles to find out the actual value of discharge and in turn the mean velocity. (described in Chapter 7.3.2) Since the profile is described by two different equation V(x) and V(y) the surface integration is done by the summation of the surface profile matrix (500 X 500) created by both these equation (step size 1/500).

The error analysis is done for two numerical integration technique GL and GJ method. The measured discharge is obtained from the 4 mean path velocities obtained from an eight path UTTF by using the equation 8.7. The abscissae, weights and the shape factor for each of this method is substituted from the table 8.1.

VELOCITY PROFILE
$V = f(x, y)$

V_{PATH_1}, V_{PATH_2}, V_{PATH_3}, V_{PATH_4}

Are the four mean path velocities obtained from 8-path UTTF measurement. The placement of UTTF for measurement for GJ and GL method is as per IEC-41 guideline.

SURFACE INTEGRATION
$$Q_{ACT} = \oiint V_z(x, y) \, dx.dy$$

Calculation of Q_{MEAS} by Gauss-Jacobi and Gauss-Legendre method

$$[Q_{MEAS}]_{GJ} = \sum_{i=1}^{n} W_{GJ\_i} . V_{PATH\_i}$$

$$[Q_{MEAS}]_{GL} = \sum_{i=1}^{n} W_{GL\_i} . V_{PATH\_i}$$

Percentage Error Calculation

$$\%E = \left[\frac{Q_{MEAS}}{Q_{ACT}} - 1 \right] \times 100$$
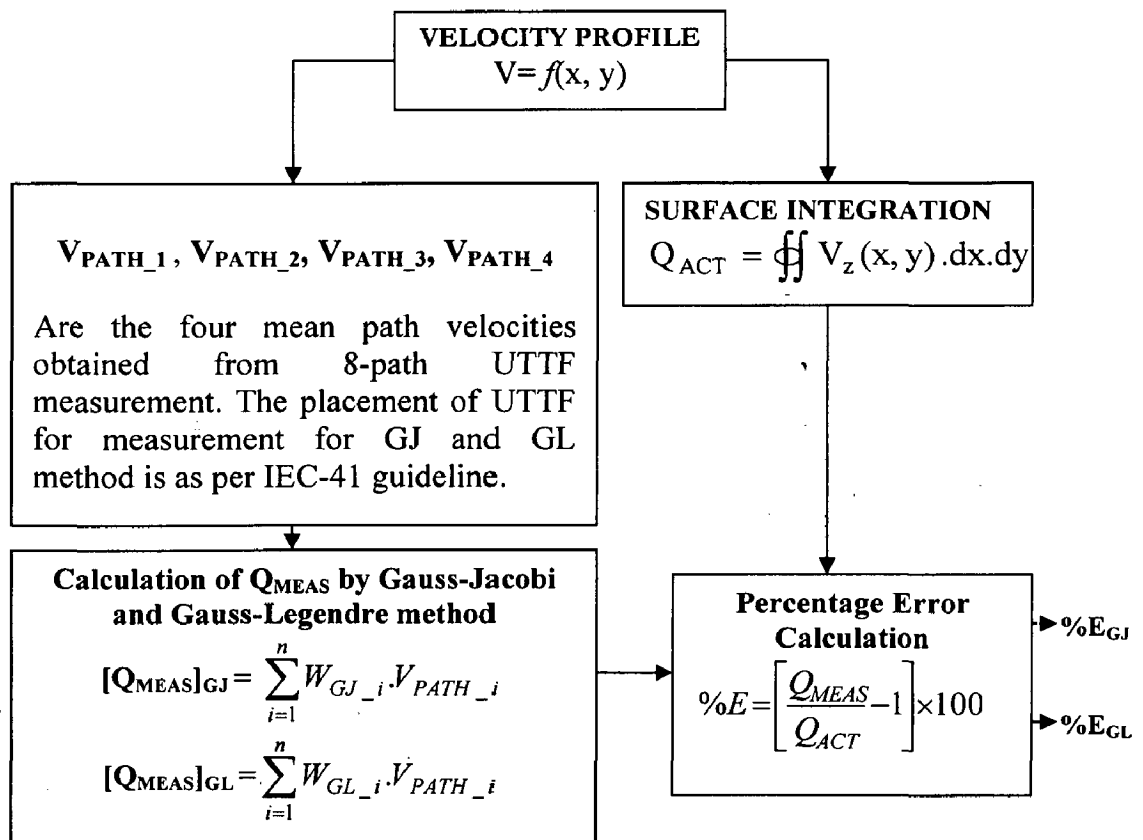
→ %E_{GJ}

→ %E_{GL}

Fig. 8.2 Steps involved in the calculation of numerical integration error.

SIMULATED PROFILES	INTEGRATION TECHNIQUE	MEAN PATH VELOCITIES FROM 8-PATH UTTF				Q_{MEAS} (m^3/s)
		V_{PATH_1} (m/s)	V_{PATH_2} (m/s)	V_{PATH_3} (m/s)	V_{PATH_4} (m/s)	
P1	GL	0.611237	0.801532	0.594316	0.281478	0.610415
	GJ	0.676132	0.793586	0.566538	0.341281	0.614532
P2	GL	0.641856	0.826765	0.669853	0.365185	0.663158
	GJ	0.691463	0.821461	0.670328	0.400432	0.669436
P3	GL	0.351265	0.758737	0.870121	0.508256	0.680619
	GJ	0.401523	0.752616	0.865825	0.628572	0.696772
B1	GL	0.672316	0.740185	0.664215	0.285461	0.624519
	GJ	0.688543	0.739282	0.661438	0.342179	0.628617
D1	GL	0.501865	0.542187	0.417866	0.085731	0.415246
	GJ	0.533162	0.538194	0.421655	0.100162	0.417518
C1	GL	0.865327	0.770421	0.629658	0.347875	0.667536
	GJ	0.860252	0.765824	0.637681	0.387711	0.649861

Table 8.2 Mean path velocities and measured discharge for GJ and GL method

SIMULATED PROFILES	Q_{ACT} (m^3/s)	Q_{MEAS} (m^3/s)		PERCENTAGE ERROR	
		Q_{GJ}	Q_{GL}	$\%E_{GJ}$	$\%E_{GL}$
P1	0.607356	0.614532	0.610415	+1.181450	+0.503683
P2	0.658510	0.669436	0.663158	+1.659268	+0.710174
P3	0.675875	0.696772	0.680619	+3.091791	+0.702023
B1	0.620210	0.629617	0.624519	+1.516683	+0.694923
D1	0.426141	0.4175176	0.415246	-2.024875	-2.556669
C1	0.677102	0.649861	0.667536	-4.023133	-1.412792

Table 8.3 Percentage error for GJ and GL methods for identified profiles

The results for numerical integration error by Gauss-Jacobi (GJ) and Gauss-Legendre (GL) methods are analyzed and the following interesting points are observed:

1. GL in almost all the cases performs better than GJ method, the reason being that GL method is exactly meant for rectangular channels as it is evident from the shape factor k (1 for GL method and 1.034 for GJ method)

2. It can be observed from the table that as the profile become complex the percentage error increases, which clearly suggests the performance of these numerical integration techniques will be largely affected as the channel geometry deviates from rectangular structure

CHAPTER 9

CONCLUSION

9.1 SUMMARY

In spite of the fact that ultrasonic transit time flow meter and propeller current meters use the state of art technologies, the discharge measurement is not free from error. From the uncertainty analysis it is observed the integration error in both cases influences the accuracy of discharge measurement significantly. An accurate discharge measurement with propeller current meter requires the precise placement and number as demanded by IEC-41 and ISO-748. Likewise accuracy of measurement with UTTF is significantly influenced by the number and accuracy of placement of transducers.

CFD analysis gave an insight to various aspects of the problem. The complex velocity profiles in open channels of different geometries, as many as 6 profiles, have been modeled and simulated. Two generalized mathematical models for normalized width and depth are developed which is capable of modeling the velocity profiles in open channels with 10 control parameters. A MATLAB code is developed which combines these models to obtain the 3-D velocity profiles. All the six CFD simulated profiles are then quantified using the mathematical model by varying the ten control parameters. The correlation of these profile parameters with the site conditions is also analyzed. The mathematical model for the six profiles is further used for the actual discharge evaluation and uncertainty analysis.

9.2 FUTURE SCOPE

Scope of research as an extension to the work done here is very wide. A few suggestions are given below:

(i) CFD analysis of 6 geometries is done in this work. The work can be extended to develop and analyze the profiles for various other geometries of open channel and combinations of geometries presented here.

(ii) The mathematical model developed here is capable of modeling upto double peak profiles only. The real site conditions may demand more flexibility in the model which is capable of incorporating any number of peaks. This can be taken as a further advancement in this work.

(iii) The integration error corresponding to GL and GJ numerical integration techniques is analyzed here. An improvement over this technique known as OWICS (Optimal Weighted Integration for Circular Section) has been formulated for circular sections [27]. A similar improvement can be investigated for open channels such as to reduce the numerical integration errors.

(iv) The work done here is confined to only rectangular open channels and similar sort of analysis can be done for trapezoidal open channels.

REFERENCES

[1] IEC-60041, Field acceptance tests to determine the hydraulic performance of hydraulic turbines, storage pumps and pump turbines, 1991.

[2] "Introduction to CFD analysis", Introductory Fluent notes, Fluent User Services Centre, January 2002.

[3] "Measurement of liquid flow in open channels - Velocity-area methods", Third edition, 1997, ISO-748.

[4] Spitzer D W, "Flow Measurement, The instrumentation, systems, and Automation Society", chap. 20.

[5] H. K. Versteeg and W. Malalasekera, "An introduction to CFD- The finite volume method", Longman Group Ltd. 1995.

[6] Michael R Simpson, "Discharge Measurement Using a Broad-band Acoustic Doppler Current Profiler", US Geological survey, Sacramento, California 2001.

[7] M J Franca and U. Lemmin, "Eliminating Velocity Aliasing in Acoustic Doppler Velocity profiler data", Institute of Physics Publishing, January 2006.

[8] Wang F and Huang H, "Horizontal Acoustic Doppler current profiler (H-ADCP) for real time open channel flow measurement: Flow calculation model and field validation", Submitted to 31st IAHR Congress 2005.

[9] WinH-ADCP Users Guide, RD Instruments, June 2005

[10] Derek G. Goring, Jeremy M. Walsh, "Modeling the distribution of Velocity in a River Cross-section", New Zealand Journal of Marine and Freshwater Research, 1997, Vol. 31, 155-162.

[11] Won Seo and Kyong Oh Baek, "Estimation of the Longitudinal Dispersion Coefficient Using the Velocity Profiles in Natural Streams", Journal of Hydraulic Engineering, Vol. 130, No. 3, March 2004.

[12] Kandula V. N. Sarma, B .V. Ramana Prasad and A. K. Sarma, "Detailed Study of Binary Law for Open Channels", Journal of Hydraulic Engineering, Vol. 126, No. 3, March 2000.

[13] D. T. Souders and C. W. Hirt, "Modeling Roughness Effects in Open Channels", Flow Science Inc. 2002

[14] Thomas Zwinger, " Fluent – Fluid Dynamic Software", CSC, February 2006

[15] R.W. Herschy, "The Uncertainty in a Current Meter Measurement", Elsevier-Flow Measurement and Instrumentation 13 (2002) 281–284.

[16] "Liquid Flow Measurement in open-channels-velocity area methods-Collection and processing and processing of data for determination of errors in measurement", Second edition - 1985-01-15, ISO-1088.

[17] Randolph J. Taylor, "Interpolation Using the Cubic Spline Function", Pi Mu Epsilon Journal, Vol. 6, No. 7, (1977), pp. 387-393.

[18] "The Measurement, Instrument and Sensors", CRC press, John G Webster, 1999, pp (28-74) – (28-89).

[19] Spitzer D W, "Flow Measurement", The instrumentation, systems, and Automation Society, chap. 20.

[20] Technical data sheets of Ryttimeyer for Risonic 2000.

[21] Salami L A, "On velocity-area methods for asymmetric profiles", University of Southampton Interim Report V, 1972.

[22] Alex Voser, "CFD-Calculations of the Protrusion effect and Impact on the acoustic discharge measurement accuracy", IGHEM, Montreal, 1996.

[23] Rajeshekaran S (1999), "Numerical Integration Methods in Science and Engineering", Wheeler publishing, pp 375-430.

[24] Gordan K. Smyth, "Numerical Integration", May 1997.

[25] Kritz, J, "An Ultrasonic Flowmeter for liquids", Proc. ISA, 1955.

[26] Prem V. K. Mandimala, "Transit Time Flow Meter Application to Closed Pipes Demanding High Accuracy", M.Tech Dissertation Report, Dept. of Electrical Engg. Indian Institute of Technology Roorkee, June 2005

[27] Alexandre Voser and Staubli T, "Integration Error of Multipath Acoustic Discharge Measurements in Closed Conduits", IGHEM, Reno, 1998.